Barker, P. F., Kennett, J. P., et al., 1990
Proceedings of the Ocean Drilling Program, Scientific Results, Vol. 113

21. CENOZOIC MAGNETOSTRATIGRAPHY OF LEG 113 DRILL SITES, MAUD RISE, WEDDELL SEA, ANTARCTICA[1]

Volkhard Spieß[2]

ABSTRACT

A detailed paleomagnetic study was carried out on biosiliceous and calcareous sediments drilled on Maud Rise, Antarctica, during ODP Leg 113. High-quality APC sections were retrieved in the upper 220 m of Holes 689B and 690B. Average deposition rates range from 3 to 15 m/m.y. A close (25 cm) paleomagnetic sample spacing provided a medium-resolution magnetostratigraphic sequence for the Paleogene and Neogene. Paleomagnetic samples were demagnetized stepwise by alternating fields, and characteristic remanent magnetization directions were derived from detailed vector and difference vector component analysis.

A magnetochronologic framework has been established for the first time for the Southern Ocean sedimentary sequences spanning Paleocene to Oligocene and middle Miocene to early Pliocene times. Biosiliceous and calcareous microfossil stratigraphies were used to constrain magnetostratigraphic age assignments. Although average sedimentation rates were rather low, nearly complete sections of the geomagnetic polarity time scale (e.g., Chrons C5 and C5A) could be correlated with the inferred polarity pattern. Miocene and Pliocene records are marked by a high number of hiatuses mainly identified by diatom biostratigraphy. Good paleomagnetic correlation between the two holes is afforded in particular in the middle to upper Miocene. Oligocene magnetostratigraphy reveals a high-quality paleomagnetic record with a mostly complete Oligocene section in Hole 689B at ~5 m/m.y. deposition rate. Hole 690B exhibits higher deposition rates (7–12 m/m.y.), although two hiatuses are present. Early and late Eocene sedimentary sequences could be analyzed in both holes, but in Hole 689B middle Eocene chrons were disrupted by hiatuses and only incomplete polarity intervals C21 and C24 were encountered. Highest resolution (14 m/m.y.) was achieved in Hole 690B in a complete early Eocene and late Paleocene sequence from Chrons C23 to C26, with a number of short polarity intervals detected within Chrons C24 and C25.

INTRODUCTION

During Ocean Drilling Program (ODP) Leg 113 in the Weddell Sea, a depth transect of nine sites was drilled for studies of different water masses and paleoclimatic and paleoceanographic history of the Southern Ocean. They included locations on the Maud Rise, the Antarctic Continental Margin, the central Weddell Basin, and the South Orkney microcontinent (Fig. 1). High-latitude drilling is crucial for understanding global climatic changes, glaciation of the polar regions, and climatic feedback mechanisms. In this context, the Weddell Sea plays a key role in global climate control and bottom water mass production. The Maud Rise, an aseismic ridge that is isolated from the Antarctic continent by more than 600 km, was expected to be at an ideal position to recover complete, predominantly biosiliceous and calcareous sediment sequences of Cenozoic and late Mesozoic ages. Magnetostratigraphic data together with biostratigraphic analyses and the study of stable isotopes provide a promising basic chronostratigraphy for future, more detailed stratigraphic studies and reconstructions of Southern Ocean paleoceanography and paleoclimatology in the Mesozoic and Cenozoic.

The principal objective of this high-resolution paleomagnetic study was to establish a magnetochronostratigraphic framework for Paleogene and Neogene sediments. Important age constraints were provided by different microfossil biostratigraphies such as diatoms and radiolarians in the Neogene as well as nannofossils and foraminifers in the Paleogene. This study covers sediments of Early Paleocene to Pleistocene age, whereas the magnetostratigraphy of the Mesozoic and the Cretaceous/Tertiary boundary

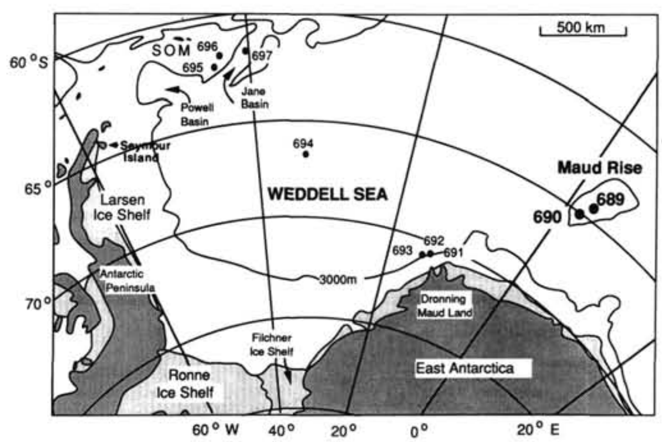

Figure 1. Location map of Leg 113 drill sites on the Maud Rise oceanic plateau.

at Maud Rise Sites 689 and 690 is presented by Hamilton (this volume). Cenozoic sediments were predominantly drilled with the advanced piston coring technique (APC). Recovery within these sections exceeded 90% for Hole 689B and reached 100% for Hole 690B, leading to an overall excellent core quality. The ages represented in the drilled sedimentary series as derived from this study are shown in Figure 2 as vertical bars in comparison to the geomagnetic polarity time scale of Berggren et al. (1985).

MAGNETIC NOMENCLATURE

As the reference scale for the magnetostratigraphic interpretation, the geomagnetic polarity time scale of Berggren et al. (1985) was adopted for this study. It provides a radiometrically calibrated, absolute age assignment of polarity reversals being

[1] Barker, P. F., Kennett, J. P., et al., 1990. *Proc. ODP, Sci. Results,* 113: College Station, TX (Ocean Drilling Program).

[2] Fachbereich Geowissenschaften, Universität Bremen, P.O. Box 330 440, D-2800 Bremen 33, Federal Republic of Germany.

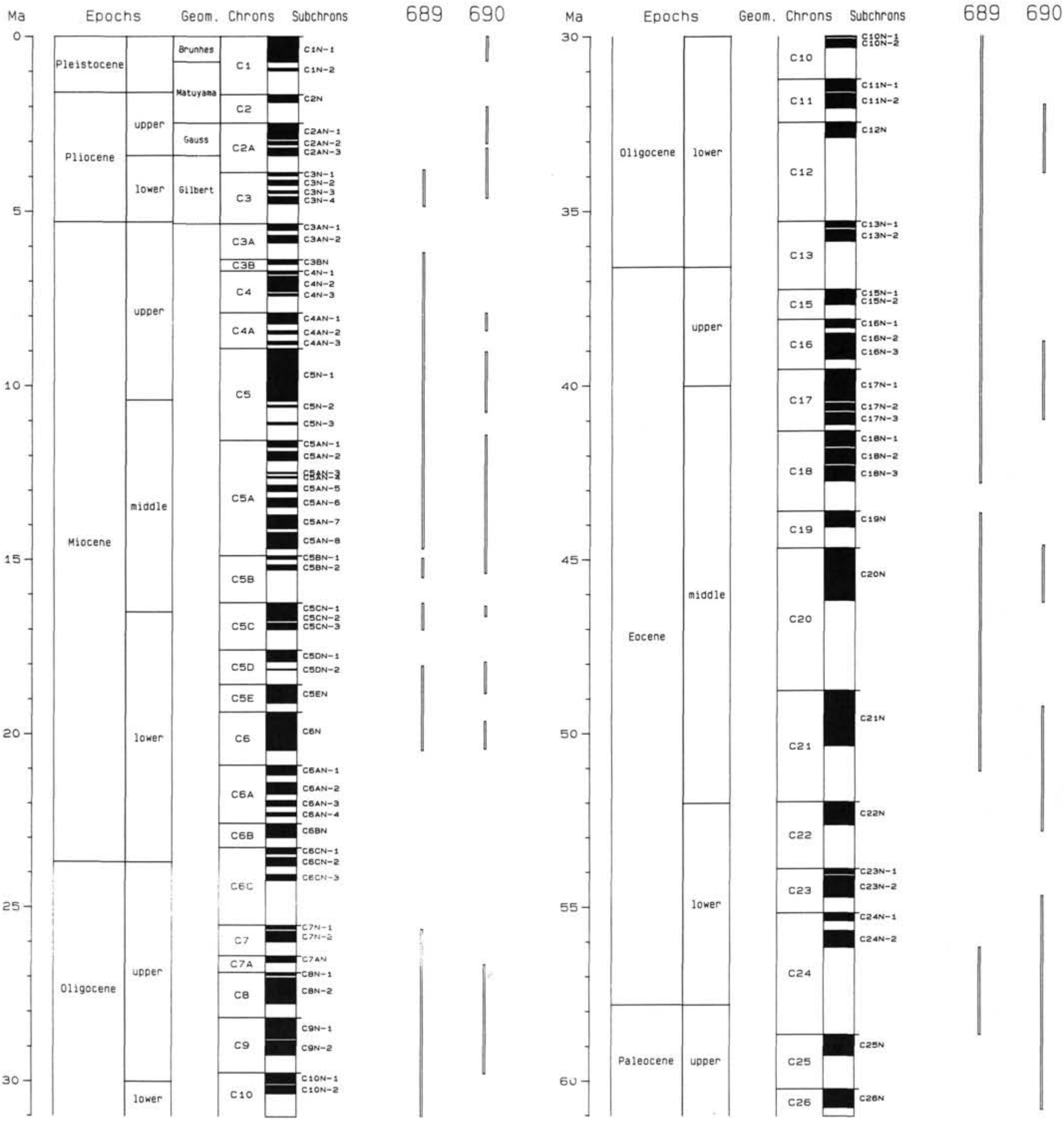

Figure 2. Geomagnetic polarity time scale of Berggren et al. (1985) used in this study. Intervals of normal polarities are plotted in black, reversed polarities in white. The Chron nomenclature was basically adopted from LaBrecque et al. (1983) with a modification of numbering in the middle Miocene Chron C5A, where the second level of anomaly lettering (Chron C5A, C5AA, C5AB, C5AC) was replaced by a continuous numbering (Chrons C5A-1 to -8). Geologic boundaries are adopted from Berggren et al. (1985). Columns on the right show age intervals represented in sediments recovered at Sites 689 and 690.

correlated with Cenozoic marine magnetic anomaly sequences as well as biostratigraphic zonation schemes. The chron nomenclature, which makes use of the numbering and lettering of marine magnetic anomalies, was first described by LaBrecque et al. (1983). For magnetostratigraphic work on Leg 113 (Barker, Kennett, et al., 1988), we decided to allow only one level of subchron numbering. Thus a slight difference in names exists in Chron C5A, where Subchrons C5A, C5AA, C5AB, and C5AC were renamed to C5AN/R-1 to -8 (for details see Fig. 2). For the Pleistocene and Pliocene, the classical description with Brunhes, Matuyama, Gauss, and Gilbert geomagnetic chrons was also used.

METHODS

The onboard long-core magnetometer of the *JOIDES Resolution* was not available during Leg 113 because of a previous breakdown. For this reason and in comparison with many other legs, a dense sample spacing of 25 cm (6 specimens per section) was used for all APC and XCB cores of good quality. For paleomagnetic analyses of discrete samples, standard ODP 2-cm plastic sample boxes were used. The low sedimentation rates found, especially within the Miocene sections, however, would have required an even closer spacing to resolve all polarity intervals of short duration (<50,000 yr) with two or more samples. Although the shipboard stratigraphic data had indicated very low sedimentation rates, an immediate refinement during this leg was not possible because of the large number of paleomagnetic samples (>5000) to be taken and analyzed. On the basis of this study, further analyses will be completed in intervals of special interest.

The magnetization intensities were measured with a three-axis cryogenic magnetometer (Cryogenic Consultants GM 400) at the University of Bremen. The difference of two measurements with and without a sample was used to determine the intensities of all three magnetization vector components. For intensity values below 0.2 mA/m, a stacking scheme of four orientations with separate determinations of the zero level was used to eliminate the additional magnetization of the sample holder. By this procedure the noise level was reduced below 0.03 mA/m, and vector intensities down to a level of 0.05 mA/m could be used for standard paleomagnetic analyses.

Resolution and quality of the shipboard data were totally inadequate to establish a high-quality magnetostratigraphy due to the restriction of NRM (natural remanent magnetization) measurements to a 75-cm sample spacing. Thus a systematic progressive demagnetization was carried out for all 1547 samples taken from Maud Rise Holes 689B and 690B. The demagnetization steps were chosen at 5, 10, 15, 20, 30, 40, and 50 mT (milli-Tesla) peak amplitude for the alternating field. If there was larger change/variability in inclination or if the median destructive field (MDF) was not reached, three steps at 65, 80, and 95 mT were added.

Analysis of magnetization directions makes use of the demagnetization characteristics of each sample and their different graphical representations (Figs. 3, 4, and 5). Directional changes of resultant and difference vectors (Hoffman and Day, 1978) between demagnetization steps reveal different magnetization components and their stability. This approach aims to separate a high-coercivity primary magnetization direction from secondary components of lower stability, which are demagnetized first. Stable directions were determined from those intervals of parallel difference and resultant vectors, where only one remaining magnetization direction is destroyed. Usually mean direction were calculated and compared for the same demagnetization steps for both vectors. In most cases they do not differ by more than 20° in inclination, which allows a reliable determination of polarity. This method has also been successfully applied in previous DSDP and ODP paleomagnetic studies (Weinreich and Theyer, 1985; Bleil, 1985, 1989).

Additional magnetization components may be caused by the drilling process, laboratory handling, or a viscous overprint of the ambient Earth's magnetic field of the last 730,000 yr. Generally these secondary magnetization directions could be eliminated with alternating field (AF) peak values less than 20 mT, and in many cases single-component magnetizations are left. A more complex situation was often, but not exclusively, found near polarity reversal boundaries. Multicomponent systems indicate that both polarities are stored in overlapping similar coercivity spectra and are associated with low NRM intensities and more scattering to chaotic vector paths. Low sedimentation rates and a lock-in process, lasting significantly longer than the polarity reversal itself, may explain this observation. The interpretation of paleomagnetic data of those samples turned out to be more difficult, and sometimes a stable direction and polarity could not be defined.

The demagnetization characteristics observed in Maud Rise sediments can be subdivided into three classes. Figures 3 through 5 show examples of single-, two-, and multicomponent systems as well as the chaotic demagnetization behavior, which do not, however, correlate in general with different lithologies. They can be described following the scheme proposed by Bleil (1989) for Norwegian Sea sediments drilled during ODP Leg 104.

Type A is a single-component remanence with minor overprint (Fig. 3), which could be easily removed by AF values of 10 mT. A large number of samples (~40%) of predominantly normal polarity could be subsumed under this class. These characteristics were not necessarily associated with steep inclination values, but a remarkable number of samples show low directional scatter around shallower inclinations ≤45°.

The two-component system shown in Figure 4 represents Type B remanence found in about 50% of all samples. Antiparallel magnetization components were observed, which approximately follow the orientation of the recent Earth's magnetic dipole field. This type of demagnetization behavior is often found in intervals of reversed polarity, and frequently several tens of mT are required to eliminate these secondary magnetization components. Type B remanences are located in reversed polarity sequences, but to a smaller degree in normal polarity intervals with an overprint of reversed antiparallel direction.

Multicomponent magnetization systems (Type C; Fig. 5; ~10% of all samples) are of variable value for magnetostratigraphic analyses, but still a high percentage can be interpreted in terms of polarity, if they were demagnetized in great detail. Pilot-sample demagnetization, which was widely used in previous studies, would have been absolutely inadequate for these samples and would have produced mostly erroneous results. The high-frequency component of a polarity reversal pattern is carried to a significant portion by Type C samples representing short polarity intervals. Since this information is most important for pattern recognition, the paleomagnetic quality and preservation of primary magnetization must be evaluated separately for each sample by a careful analysis. This is possible only by treating every sample by the same demagnetization procedure.

Because of the availability of demagnetization data, additional information about magnetic stabilities and coercivities can be derived for each sample, usually described by the median destructive field parameter (MDF). But, considering the large number of two-component systems, it does not appear to be adequate to use the standard definition of MDF, which is related to the NRM intensity and which does not account for directional variation. In this study, a new approach was used to get a better approximation of the stability of magnetic carriers and the coercivity spectrum of each sample. Assuming nonoverlapping coercivity spectra of two nonparallel magnetization com-

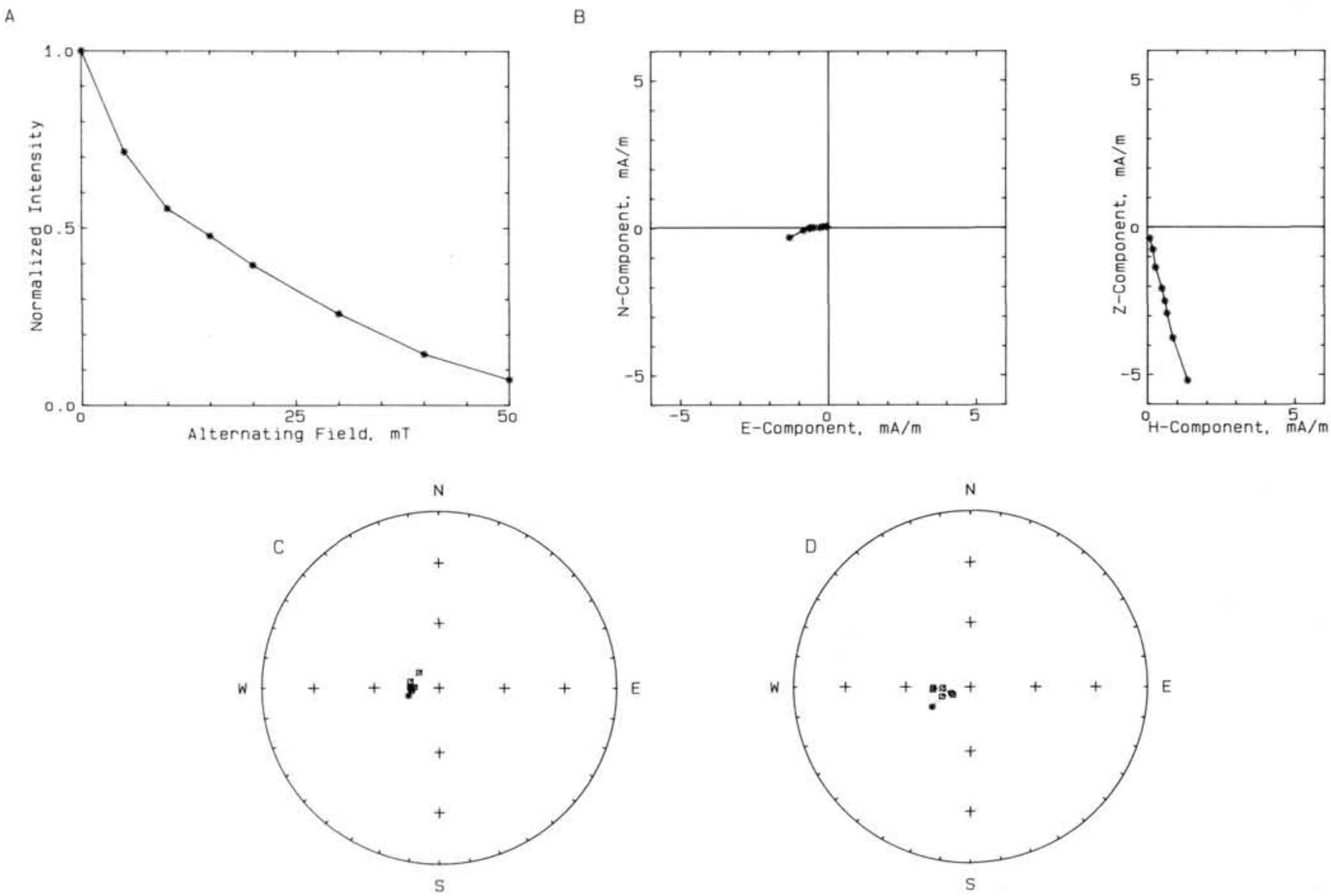

Figure 3. Demagnetization of natural remanent magnetization (NRM) for the single-component remanence (Type A) of Sample 113-689B-10H-2, 75 cm. **A.** Intensity decay curve. NRM normalized magnetization intensity variation as a function of alternating peak field amplitude. **B.** Zijderveld vector diagrams. Magnetization vector components in the horizontal (declination) and vertical (inclination) plane. **C.** Stereographic projection of the resultant magnetization vector. Asterisk = NRM direction. **D.** Stereographic projection of the difference vectors between consecutive demagnetization steps. Asterisk = first demagnetization interval. Closed symbol of the stereographic plot represent positive, open symbols negative inclinations. Subsequent vectors are connected along great circles.

ponents, the best approximation for the intensity decay curve in comparison to a single-component remanence would be the sum of all difference vectors. From this a correct MDF can easily be calculated by interpolating the alternating field value, when the summed intensity drops below 50% of the NRM sum. Despite the fact that different magnetization components usually overlap significantly, this still appears to be an improved approximation and is therefore used in all tables and figures throughout this study. A comparison of the two MDF values as well as the NRM intensity and the NRM sum, which also gives some idea about the degree of overprint and/or directional scatter in a sample, can be drawn from the raw data (Appendices A and B).

The paleomagnetic polarity was determined directly from stable inclinations, if their absolute values were greater than 15°. Shallow inclinations below 30° were used only if the directional scatter was low and the vertical magnetization component showed a characteristic decay with increasing AF field strength. Although in standard magnetostratigraphic work polarity intervals must be based on two or more consecutive samples, in this study single samples were also included in the polarity reversal sequence, because they represent a spacing on the order of 50,000 years. Almost all short intervals were assigned to the geomagnetic polarity time scale, but later resampling of these intervals is necessary to confirm the actual interpretation.

Some statistical parameters were calculated for both holes (Tables 1 and 2) and different time intervals and lithological units. The magnetostratigraphic results and their interpretation are given in Tables 3 and 4 for Holes 689B and 690B. Beside the sample names and the sample mean depth of the polarity reversal boundaries additional parameters are listed. An age derived from the Subchron definition of the polarity time scale of Berggren et al. (1985) is assigned to the mean boundary depth. These values were used to calculate sedimentation rates, which carry the given uncertainties associated with the placement of the mean boundary depth. Hiatuses are denoted by wavy lines. They were exclusively derived from biostratigraphy, but their precise placement within the biostratigraphic uncertainty of each boundary is chosen in combination with the magnetostratigraphic polarity interpretation. In this context it was also considered that there is a high probability that about half of the hiatuses are associated with a polarity boundary. For most of the hiatuses, a crude estimate of age and duration was given. Sedimentation rates, usually taken from adjacent polarity intervals, were extrapolated to calculate ages for the beginning and end of a hiatus and listed in

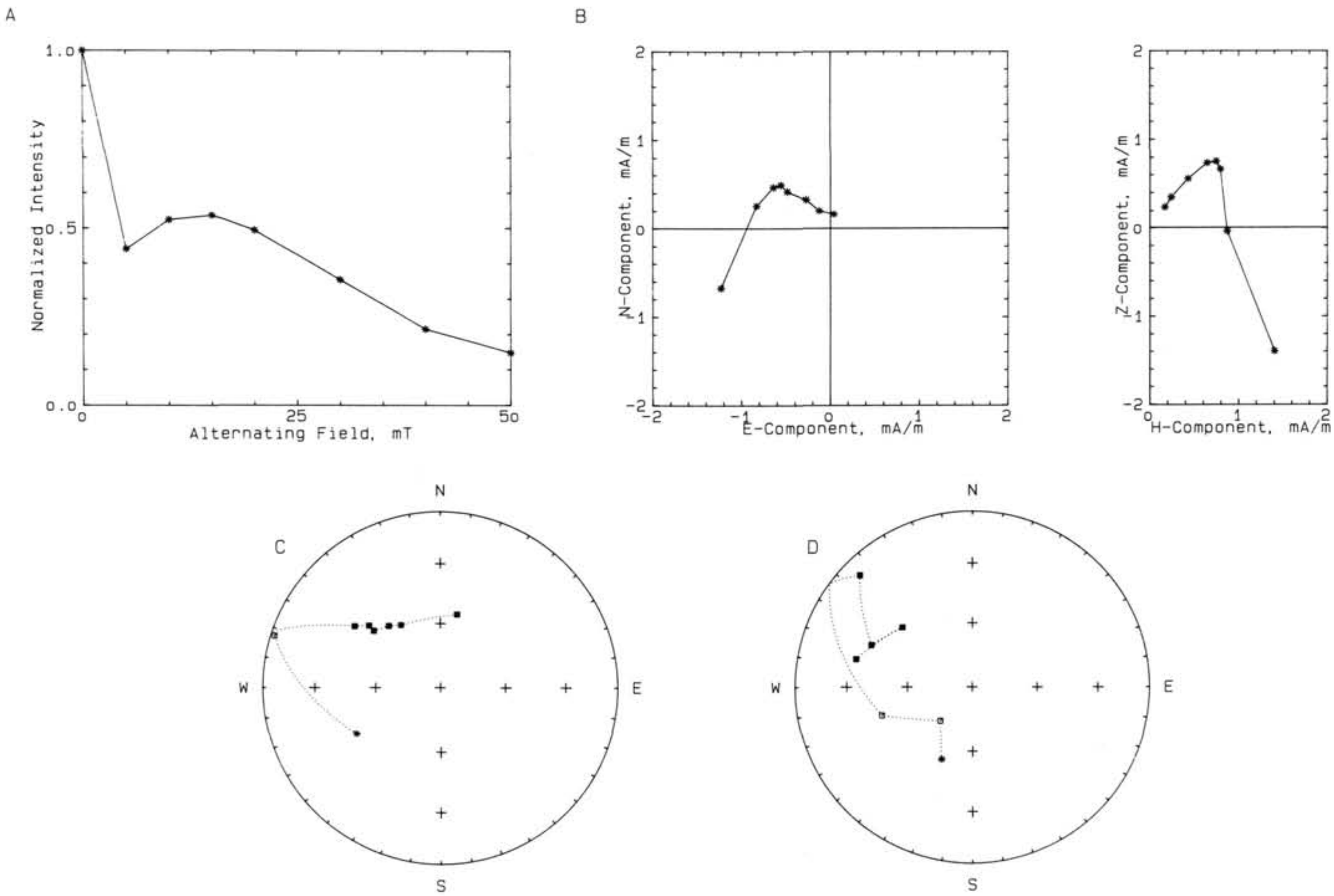

Figure 4. Demagnetization of NRM for a two-component remanence (Type B) of Sample 113-689B-6H-3, 100 cm. See Figure 3 for further explanation.

brackets in Tables 3 and 4. In special cases deposition rates averaged over two or more polarity intervals were used instead. In Paleocene and Eocene Chrons C24 and C25, estimated mean ages for short polarity intervals were added in brackets.

Site 689

Site 689 was located at (64°31.01′S; 3°06.00′W) on top of the Maud Rise oceanic plateau in a pelagic depositional environment in 2080 m water depth. It was expected to provide undisturbed Cenozoic and Mesozoic biosiliceous and calcareous sedimentary sequences. Four holes were drilled at Site 689. In Hole 689A one core of 9.35 m was retrieved without, however, recovering the seafloor. Hole 689B was drilled by the APC/XCB (advanced piston corer/extended core barrel) technique down to 297.3 mbsf into Upper Cretaceous sediments. Holes 689C and 689D duplicate the upper 133.8 m of Hole 689B. Focusing on Cenozoic sediments, the systematic magnetostratigraphic analysis was carried out on 725 samples from Cores 113-689B-1H to -21H and -22X to -24X.

The sediments recovered from Hole 689B were subdivided into three lithologic units. Generally the composition changes with depth from mainly biosiliceous (diatoms, radiolarians) to calcareous components (nannofossils, foraminifers). Other components were of minor importance. Lithologic Unit I (0.0–31.0 mbsf) is composed of biogenic siliceous ooze. Unit II reveals a mixture of variable biosiliceous and calcareous composition with higher biosiliceous content in Subunit IIa (31.0–72.1 mbsf) and dominantly nannofossil oozes in Subunit IIb (72.1–149.1 mbsf). Unit III represents a sedimentary sequence of indurated nannofossil oozes and chalk (149.1–297.3 mbsf).

NRM measurements and progressive AF-demagnetization experiments were completed for all 725 samples. The NRM intensities approximately follow a geometric distribution (Fig. 6A) with a geometric mean value of 1.5 mA/m, which can be AF demagnetized to at least 50 mT peak field. Stabilities of magnetization during the demagnetization process are expressed in the median destructive field (MDF), which shows a broad geometric distribution (Fig. 6B) from extreme values of 2.8–78 mT with a maximum at around 20 mT. Low MDF's typically result from a low coercivity overprint caused by the ambient Earth's magnetic field, handling in the laboratory environment, or the drilling process itself. In most cases this overprint was easily removed by AF demagnetization of 10 mT so that more stable primary magnetization components of sufficient intensity were revealed. Stable declination values (Fig. 6C) are not evenly distributed but show extreme values around 60° and 300°. Declination values were not used in this study for several reasons. First, the cores were not oriented azimuthally and therefore declination values are jumping by unknown amounts at core boundaries. Second, the small horizontal magnetization components of a nearly vertical magnetization vector are widely scattered, which makes it difficult to distinguish from polarity reversals. And third, to de-

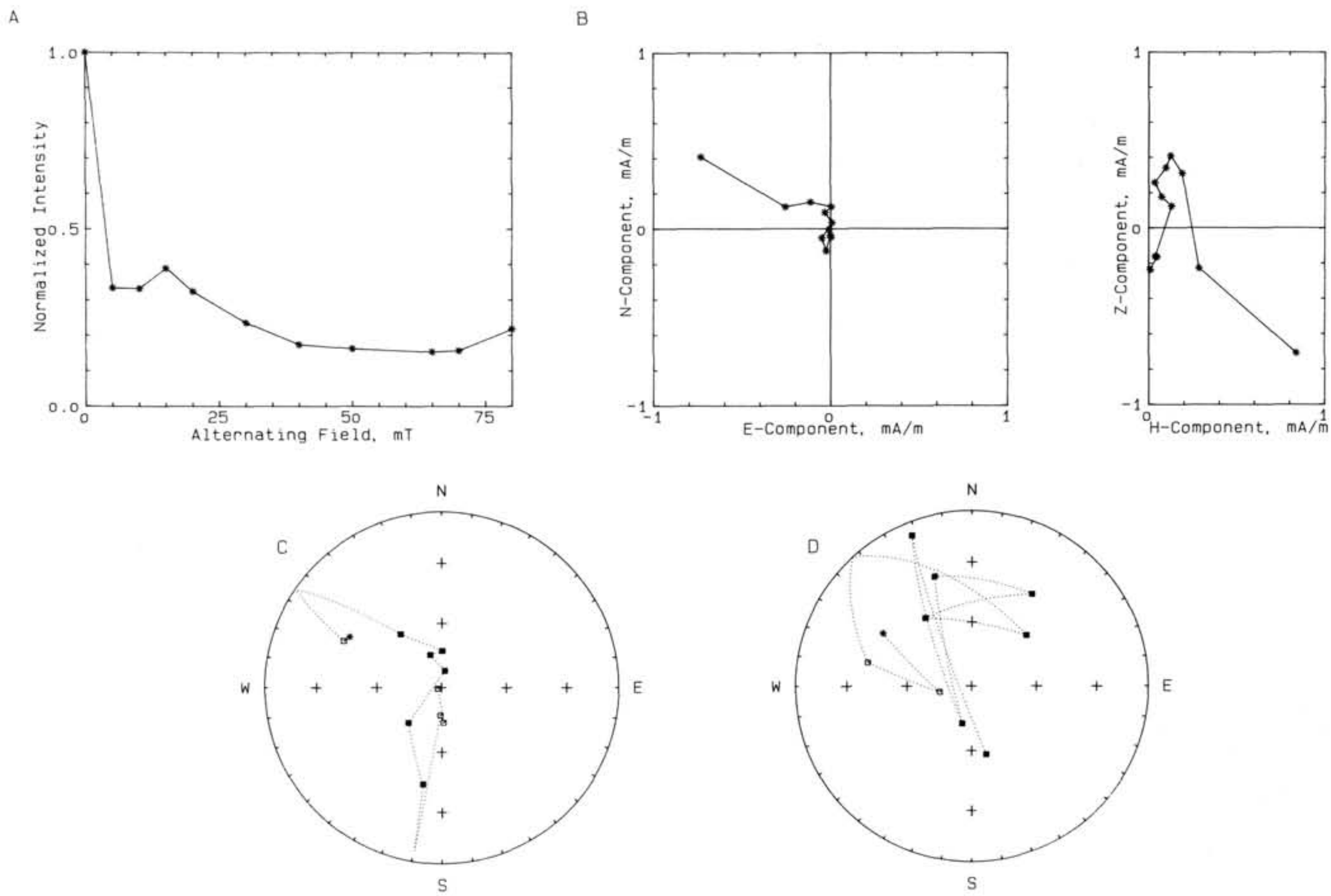

Figure 5. Demagnetization of NRM for a multicomponent remanence (Type C) of Sample 113-689B-10H-6, 20 cm. See Figure 3 for further explanation.

Table 1. Statistics of paleomagnetic properties of Hole 689B sediments. Included are geometric means and standard deviation intervals for NRM intensity and summed median destructive field values as well as the arithmetic mean and standard deviation for the stable inclination. In addition the data set was subdivided into age ranges and lithological units as defined in the text.

	689B	Neogene	Oligocene	Eocene	Lith. I	Lith. IIa	Lith. IIb	Lith. III
No. of samples	725	250	221	254	119	149	277	179
NRM intensity (mA/m)								
Geometric mean	1.53	1.66	1.82	1.21	1.71	1.59	1.59	1.29
SD interval	0.5	0.5	0.7	0.3	0.6	0.5	0.5	0.4
	4.7	5.0	4.5	4.4	4.4	5.2	5.1	4.0
Median destructive field (mT)								
Geometric mean	12.0	14.5	9.7	14.5	19.4	10.9	10.7	14.5
SD interval	6.3	7.7	5.1	8.2	11.6	6.1	5.7	7.9
Stratigraphic samples								
	681	239	220	240	113	145	275	166
Stable inclination (degrees)								
Arithmetic mean	67.8	61.8	77.2	62.4	61.6	64.0	77.4	55.5
SD	15.8	15.8	9.3	18.0	17.7	14.1	8.7	17.2

Table 2. Statistics of paleomagnetic properties of Hole 690B sediments. For further explanation see Table 1.

	690B	Neogene	Oligocene	Eocene	Lith. I	Lith. IIa	Lith. IIb	Lith. III	Lith. IV
No. of samples	822	191	168	463	94	107	158	183	280
NRM intensity (mA/m)									
Geometric mean	2.79	2.60	2.58	2.96	3.00	2.19	2.67	3.76	2.54
SD interval	1.1	1.1	1.2	1.0	1.4	0.9	1.3	2.0	0.7
	7.3	6.1	5.5	8.7	6.2	5.4	5.6	7.2	8.9
Median destructive field (mT)									
Geometric mean	11.4	12.9	10.2	11.2	19.5	8.4	10.5	8.2	13.8
SD interval	6.2	6.3	5.9	6.3	10.7	4.8	6.1	4.9	8.3
	20.9	26.3	17.7	19.8	35.7	14.6	18.3	13.8	22.9
Stratigraphic samples									
	784	183	167	434	90	103	157	177	257
Stable inclination (degrees)									
Arithmetic mean	62.3	62.9	72.4	58.1	60.6	66.1	72.3	63.4	54.4
SD	16.6	13.6	13.9	17.0	12.6	14.5	13.9	16.8	16.1

termine polarities unequivocally only inclination values are required in high latitudes, and declination values cannot improve the magnetostratigraphic results.

NRM inclination values (Fig. 6D) were biased toward normal polarities (negative inclinations), which was often observed in sediments of high biogenic content (e.g., Barton and Bloemendal, 1986). Because this is to a lesser extent still true for the 20 mT demagnetized directions of many magnetostratigraphies (see also Fig. 6E), a systematic stepwise demagnetization was applied to all samples, and stable inclinations and polarities could be clearly defined for 699 of 725 samples by magnetization component analysis. The typical bimodal distribution of stable inclinations (Fig. 6F) has a mean absolute value of 68°. From a detailed look at the inclination variation between cores, the deviation from the axial geocentric dipole field of 77° for this site can be well explained by variable core quality and preservation of primary magnetization directions.

A comparison of paleomagnetic properties for different age intervals and lithologic units (Table 1) does not show any dramatic variation. But significant differences in magnetic stability became obvious from MDF values, which were high in Unit I (~20 mT), low in Unit II (~11 mT), and medium (15 mT) below Unit II, although the distributions are very broad. Steep inclination values were apparently better preserved in Oligocene sediments (77°), whereas Eocene/Unit III inclinations are anomalously low (55°). The basic paleomagnetic data set, containing different inclination, NRM intensity, MDF values, and polarities for Hole 689B, is given in Appendix A. Together with the magnetochronologic interpretation and biostratigraphically defined hiatuses (Gersonde and Burckle, this volume; Abelmann, this volume; Wei and Wise, this volume; Pospichal and Wise, this volume, chapter 30; Thomas, et al., this volume; Lazarus, this volume), Figure 7 shows the inferred inclination, intensity, MDF, and polarity records for the Miocene/Pliocene (A), Oligocene (B), and Paleocene/Eocene (C) intervals. Details about polarity reversal boundaries, magnetochronology, sedimentation rates, and hiatuses can be extracted from Appendix A and the age-depth relationships plotted in Figure 10.

Neogene

The Neogene sedimentation history is documented in mostly biosiliceous lower Miocene to lower Pliocene sediments composed mainly of diatoms and to a lesser degree of radiolarians and silicoflagellates (Lithologic Unit I, 0.0–31.0 mbsf). Some intervals in middle Miocene and older sediments contain additional calcareous components (nannofossils >50%). The proportion of nannofossils increased with depth to a maximum carbonate content of >90% (Lithologic Unit II, 31.0–72.1 mbsf).

Frequency distributions of paleomagnetic parameters, analyzed separately for Neogene and Paleogene intervals, show similar characteristics, mean values, and statistical parameters as for the whole Cenozoic time interval (Table 1). Extraordinarily low and narrowly distributed intensities around 0.5 mA/m are found in two expanded intervals (17–21 mbsf; 33–43 mbsf). The first interval is associated partly with high amounts of silicoflagellates (12 to 21 mbsf; >30%), whereas in the second interval high nannofossil abundances (33–50 mbsf; >50%) were observed. The intensity decrease may be partly explained by a dilutional effect (high biogenic productivity; relative increase of sedimentation rates), by a decrease of magnetic input over a longer period of time, or by reductive diagenesis of magnetic material. In general, average intensities change smoothly, showing a characteristic long-term variability, which was also observed in the median destructive field. Except for the very low intensity values, an obvious correlation with lithologic changes documented in the shipboard core descriptions could not be found. Due to multicomponent magnetizations in intervals of reversed polarity, NRM intensities are often higher for normal polarity intervals. More detailed sedimentologic and rock magnetic analyses are required to explain the observed variations in the amount of magnetic material recovered at the drill site.

The NRM intensities were generally high enough for a systematic AF-treatment up to a level of at least 50 mT, and the scheme for progressive demagnetization could also be performed throughout the intervals of lower NRM intensities. From the typical bimodal grouping of inclination values, stable inclinations and polarities could easily be defined for the upper 67 m, although Cores 113-689B-1H and -2H on average show much shallower inclination values. These may be related to minor drilling disturbance observed down to Section 113-689B-2H-5, but even so an unequivocal polarity interpretation was possible. Between 12 and 42 mbsf, the inclination values scatter around the expected geocentric dipole inclination of +77° for this site. Shallower inclinations are again found between 42 and 62 mbsf, where the decrease is more pronounced in the reversed polarity intervals (~30°) than for normal polarities (10°). Steep geocen-

Table 3. Magnetochronology for Hole 689B. Boundaries of polarity intervals are given by sample name and mean depth of sample. If the interval was assigned to the geomagnetic polarity time scale (GPTS), the subchron name is added to the assigned polarity. For the polarity reversal boundary a mean depth is calculated together with the depth uncertainty. A chronostratigraphic age is given according to the noted subchron. Sedimentation rates were calculated for each subchron from the mean depth values of two adjacent reversal boundaries, if the sequence is not interrupted by a hiatus. In this case the sedimentation rate of the previous and following subchrons (given in brackets) are used to extrapolate an age for the hiatus location, which allows a rough estimate of its duration. In special cases the sedimentation rate used for extrapolation was averaged over longer intervals. For polarity intervals that could not be assigned to the GPTS the subchron wherein they appear is listed. These intervals are ignored in the calculation of sedimentation rate, but for some (Chrons C24, C25) estimated ages were given from linear interpolation.

Boundary depth (mbsf)	Range (m)	Depth (mbsf)	Sample	Polarity	Chron	Sedimentation rate (m/m.y.)	Age (Ma)
		3.06	1,3,6				
				R	C2AR-3		
		3.25	1,2,25				
3.38	0.25						3.88
		3.50	1,3,50				
				N	C3 N-1	11.3	
		4.25	1,3,125				
4.40	0.29						3.97
		4.54	1,4,4				
				R	C3 R-1		
		6.26	2,1,96				
6.41	0.29						
		6.55	2,1,125				
				N	in C3 R-1		
		6.55	2,1,125				
6.61	0.12						
		6.67	2,1,137				
				R	C3 R-1	33.8	
		8.55	2,3,25				
8.79	0.48						4.10
		9.03	2,3,73				
				N	C3 N-2	6.0	
		9.57	2,3,127				
9.63	0.11						4.24
		9.68	2,3,138				
				R	C3 R-2	11.4	
		11.34	2,5,4				
11.45	0.21						4.40
		11.55	2,5,25				
				N	C3 N-3	3.9	
		11.55	2,5,25				
11.72	0.34						4.47
		11.89	2,5,59				
				R	C3 R-3	34.5	
		15.05	3,1,25				
15.17	0.25						4.57
		15.30	3,1,50				
				N	C3 N-4	8.8	
		16.80	3,2,50				
16.92	0.25						4.77
		17.05	3,2,75				
				R	C3 R-4	(8.8)	
		17.55	3,2,125				
17.65?	0.21				hiatus		4.85–6.17
		17.76	3,2,146				
				N	?		
		17.76	3,2,146				
17.82	0.12						
		17.88	3,3,8				
				R	C3AR-2	(4.3)	
		17.88	3,3,8				
18.09	0.42						6.37
		18.30	3,3,50				
				N	C3BN	4.3	
		18.55	3,3,75				
18.67	0.25						6.50
		18.80	3,3,100				
				R	C3BR	1.3	
		18.80	3,3,100				
18.92	0.25						6.70
		19.05	3,3,125				
				N	C4 N-1/2/3	1.8	
		20.05	3,4,75				

Table 3 (continued).

Boundary depth (mbsf)	Range (m)	Depth (mbsf)	Sample	Polarity	Chron	Sedimentation rate (m/m.y.)	Age (Ma)
20.17	0.25						7.41
		20.30	3,4,100				
				R	C4 R-3	4.0	
		22.05	3,4,125				
22.15	0.21						7.90
		22.26	3,5,146				
				N	C4AN-1/2	2.5	
		23.55	3,6,125				
23.65	0.21						8.50
		23.76	3,6,146				
				R	C4AR-2	0.8	
		23.76	3,6,146				
23.81	0.10						8.71
		23.86	3,7,6				
				N	C4AN-3	4.0	
		23.86	3,7,6				
24.17	0.61						8.80
		24.47	3,C,29				
				R	C4AR-3	4.2	
		24.55	4,1,25				
24.67	0.25						8.92
		24.80	4,1,50				
				N	C5 N-1/2	6.6	
		33.55	4,7,25				
34.55	2.00						10.42
		35.55	5,2,25				
				R	C5 R-2	4.4	
		37.30	5,3,50				
37.55	0.50						11.03
		37.80	5,3,100				
				N	C5 N-3	6.3	
		37.80	5,3,100				
37.93	0.25						11.09
		38.05	5,3,125				
				R	C5 R-3	17.4	
		45.80	6,2,100				
45.93	0.25						11.55
		46.05	6,2,125				
				N	C5AN-1	2.7	
		46.27	6,2,147				
46.41	0.28						11.73
		46.55	6,3,25				
				R	C5AR-1	2.1	
		46.55	6,3,25				
46.68	0.25						11.86
		46.80	6,3,50				
				N	C5AN-2	1.9	
		47.05	6,3,75				
47.18	0.25						12.12
		47.30	6,3,100				
				R	C5AR-2/3/4	2.1	
		48.55	6,4,75				
48.68	0.25						12.83
		48.80	6,4,100				
				N	C5AN-5	2.8	
		48.80	6,4,100				
49.18	0.75						13.01
		49.55	6,5,25				
				R	C5AR-5	2.6	
		49.55	6,2,25				
49.68	0.25						13.20
		49.80	6,5,50				
				N	C5AN-6	4.7	
		50.77	6,5,147				
50.91	0.28						13.46
		51.05	6,6,25				
				R	C5AR-6	4.4	
		51.80	6,6,100				
51.93	0.25						13.69
		52.05	6,6,125				
				N	C5AN-7	1.2	
		52.27	6,6,147				
52.41	0.28						14.08
		52.55	6,7,25				
				R	C5AR-7	3.7	
		52.55	6,7,25				
52.85	0.60						14.20

Table 3 (continued).

Boundary depth (mbsf)	Range (m)	Depth (mbsf)	Sample	Polarity	Chron	Sedimentation rate (m/m.y.)	Age (Ma)
		53.15	7,1,25				
				N	C5AN-8	5.3	
		55.15	7,2,75				
55.28	0.25			hiatus			14.66-14.93
		55.40	7,2,100				
				R	C5BR-1	(6.2)	
		56.40	7,3,50				
56.53	0.25						15.13
		56.65	7,3,75				
				N	C5BN-2	6.2	
		57.15	7,3,125				
57.40	0.50						15.27
		57.65	7,4,25				
				R	C5BR-2	(6.2)	
		58.65	7,4,125				
58.75	0.20			hiatus			15.49->16.22
		58.85	7,4,145				
				N	C5CN		
		59.40	7,5,50				
59.65	0.50			hiatus			<16.98-18.02
		59.90	7,5,100				
				R	C5DR-1	(3.9)	
60.03	0.25						18.12
		60.15	7,5,125				
				N	C5DN-2?	18.5	
60.40	0.50						18.14
		60.65	7,6,25				
				R	C5DR-2	3.2	
61.76	0.22						18.56
		61.87	7,6,147				
				N	C5E—C6		
		66.75	8,3,125				
66.86	0.22			hiatus			<20.45->25.60
		66.97	8,3,147				
				R	C7 R-1	(>2.6)	
67.11	0.28						25.67
		67.25	8,4,25				
				N	C7 N-2	2.6	
		67.75	8,4,75				
67.88	0.25						25.97
		68.00	8,4,100				
				R	C7 R-2	1.8	
		68.47	8,4,147				
68.61	0.28						26.38
		68.75	8,5,25				
				N	C7AN	1.5	
		68.75	8,5,25				
68.88	0.25						26.56
		69.00	8,5,50				
				R	C7AR	1.7	
		69.25	8,5,75				
69.38	0.25						26.86
		69.50	8,5,100				
				N	C8 N-1	10.4	
		69.97	8,5,147				
70.11	0.28						26.93
		70.25	8,6,25				
				R	C8 R-1	3.4	
		70.25	8,6,25				
70.38	0.25						27.01
		70.50	8,6,50				
				N	C8 N-2	7.7	
		75.85	9,3,75				
75.98	0.25						27.74
		76.10	9,3,100				
				R	C8 R-2	8.5	
		79.35	9,5,125				
79.46	0.22						28.15
		79.57	9,5,147				
				N	C9 N-1/2	5.3	
		84.90	10,3,20				
85.05	0.30						29.21
		85.20	10,3,50				
				R	C9 R-2	9.2	
		89.70	10,6,50				

Table 3 (continued).

Boundary depth (mbsf)	Range (m)	Depth (mbsf)	Sample	Polarity	Chron	Sedimentation rate (m/m.y.)	Age (Ma)
89.82	0.25						29.73
		89.95	10,6,75				
				N	C10N-1?		
		89.95	10,6,75				
90.07	0.25						
		90.20	10,6,100				
				R	C10R-1?		
		90.20	10,6,100				
91.01	1.61						
		91.81	11,1,51				
				N	C10N-2	3.5	
		91.81	11,1,51				
91.93	0.24						30.33
		92.05	11,1,75				
				R	C10R-2	9.2	
		98.96	11,6,16				
100.23	2.54						31.23
		101.50	12,1,50				
				N	C11N-2	3.8	
		103.25	12,2,75				
103.38	0.25						32.06
		103.50	12,2,100				
				R	C11R-2	2.5	
		104.25	12,3,25				
104.38	0.25						32.46
		104.50	12,3,50				
				N	C12N	5.7	
		106.50	12,4,100				
106.88	0.75						32.90
		107.25	12,5,25				
				R	C12R	4.1	
		116.56	13,4,146				
116.71	0.29						35.29
		116.85	13,5,25				
				N	C13N-1/2	5.2	
		119.54	13,6,144				
119.70	0.31						35.87
		119.85	13,7, 25				
				R	C13R-2		
		123.97	14,3,77				
124.09	0.23						(36.57)
		124.20	14,3,100				
				N	in C13R-2		
		124.95	14,4,25				
125.07	0.25						(36.72)
		125.20	14,4,50				
				R	C13R-2	6.2	
		128.20	14,6,50				
128.33	0.25						37.24
		128.45	14,6,75				
				N	C15N-1/2		
		129.45	14,7,25				
129.70	0.49						
		129.94	14,C, 18				
				R	in C15N-1/2		
		129.94	14,C, 18				
130.05	0.21						
		130.15	15,1,25				
				N	C15N-1/2	12.9	
134.02	0.25						37.68
		134.15	15,3,125				
				R	C15R-2	4.2	
		135.40	15,4,100				
135.77	0.75						38.10
		136.15	15,5,25				
				N	C16N-1	15.3	
		139.40	15,7,50				
139.45	0.10						38.34
		139.50	15,7,60				
				R	C16R-1	0.6	
		139.50	15,7,60				
139.55	0.10						38.50
		139.60	16,1,20				
				N	C16N-2/3	7.1	
		144.65	16,4,75				
144.77	0.25						39.24
		144.90	16,4,100				
				R	C16R-3	0.9	

Table 3 (continued).

Boundary depth (mbsf)	Range (m)	Depth (mbsf)	Sample	Polarity	Chron	Sedimentation rate (m/m.y.)	Age (Ma)
		144.90	16,4,100				
145.02	0.25						39.53
		145.15	16,4,125				
				N	C17N-1/2	5.8	
		151.60	17,2,100				
151.73	0.25						40.70
		151.85	17,2,125				
				R	C17R-2	3.1	
		151.85	17,2,125				
151.95	0.20						40.77
		152.05	17,2,145				
				N	C17N-3	2.3	
		152.60	17,3,50				
152.73	0.25						41.11
		152.85	17,3,75				
				R	C17R-3	5.4	
		153.55	17,3,145				
153.70	0.30						41.29
		153.85	17,4,25				
				N	C18N-1/2	5.2	
		161.05	18,2,75				
161.17	0.25						42.73
		161.30	18,2,100				
				R	C18R-2	(5.2)	
161.54	0.47				hiatus		42.80–43.66
		161.77	18,2,147				
				N	C19N	(4.0)	
		163.05	18,3,125				
163.16	0.22						44.06
		163.27	18,3,147				
				R	C19R	4.0	
		165.30	18,5,50				
165.55	0.50						44.66
		165.80	18,5,100				
				N	C20N		
		166.55	18,6,25				
166.76	0.42						
		166.97	18,C,12				
				R	in C20N		
		169.50	19,1,100				
169.63	0.25						
		169.75	19,1,125				
				N	C20N		
		169.75	19,1,125				
170.00	0.50						
		170.25	19,2,25				
				R	in C20N?		
		170.25	19,2,75				
170.50	0.50						
		170.75	19,2,75				
				N	C20N	3.7	
171.11	0.72						46.17
		171.47	19,2,147				
				R	C20R		
		175.97	19,5,147				
176.11	0.28						
		176.25	19,6,25				
				N	in C20R		
		176.25	19,6,25				
176.50	0.50						
		176.75	19,6,75				
				R	C20R	4.7	
		183.10	20,4,50				
183.23	0.25						48.75
		183.35	20,4,75				
				N	C21N		
		183.85	20,4,125				
183.96	0.22						
		184.07	20,4,147				
				R	in C21N		
184.18	0.21						
		184.28	20,5,18				
				N	C21N		
		188.55	21,1,75				
188.67	0.25						
		188.80	21,1,100				
				R	in C21N		

Table 3 (continued).

Boundary depth (mbsf)	Range (m)	Depth (mbsf)	Sample	Polarity	Chron	Sedimentation rate (m/m.y.)	Age (Ma)
		188.80	21,1,100				
188.92	0.25						
		189.05	21,1,125				
				N	C21N	(4.7)	
		190.55	21,1,125				
190.66	0.22						
		190.77	21,2,147				
				R	in C21N	7.0	
		190.77	21,2,147				
190.91	0.28						
		191.05	21,3,25				
				N	C21N	(9.2)	
		197.75	22,1,25				
197.89	0.27						50.34
		198.02	22,1,52				
				R	C21R	(7.0)	
203.00					hiatus		51.07->56.14
		203.00					
				R	C24R		
		204.72	22,5,122				
204.85	0.25						
		204.97	22,5,147				
				N	in C24R		
		204.97	22,5,147				
205.05	0.16						
		205.13	22,6,13				
				R	C24R		
		209.20	23,2,50				
209.33	0.25						
		209.45	23,2,75				
				N	in C24R		
209.58	0.25						
		209.70	23,2,100				
				R	C24R	>6.1	
		217.87	24,1,97				
218.37	1.00						<58.64
		218.87	24,C,31				
				N		?	
		218.87	24,C,31				

tric dipole inclinations are again found in the lowermost Miocene section below 62 mbsf. Compaction of water-saturated sediments caused by the coring process or slight drilling disturbances, which on average would decrease steep inclination values, may account for these effects. Therefore a calculation of paleolatitudes appears to be adequate only after a cautious selection of samples. The general observation that inclinations are often shallower for samples of reversed polarity in comparison to axial dipole directions in normal polarity samples may be explained by an incomplete removal of a normal overprint.

The biosiliceous microfossil stratigraphy (Gersonde and Burckle, this volume; Lazarus, this volume; Abelmann, this volume) provided a number of important constraints on sedimentation rates and age assignments, although most of the biostratigraphic datums were not calibrated magnetostratigraphically for the Southern Ocean.

The close magnetic sample spacing of 25 cm, which represents a sampling interval of approximately 50,000 yr, was barely adequate to resolve short polarity intervals on the order of 50,000 yr. This is especially important for the upper and middle Miocene polarity reversal sequences, where a number of intervals could be defined only on the basis of a single sample. Although misorientation of samples cannot be excluded, and for an unequivocal identification of polarity intervals at least two samples are required, those intervals were included in the Neogene polarity reversal pattern. Confirmation and refinement of these intervals should be done at a later stage.

Dominantly reversed polarities within the upper 15 m (Fig. 7A) and diatom stratigraphic data (Gersonde and Burckle, this volume; Gersonde et al., this volume) indicate that the Brunhes to Gauss Geomagnetic Epochs were not retrieved at Hole 689B. Lower Pliocene Chrons C3N-1 to C3N-4 were identified in a sequence of normal polarity events (3–17 mbsf), which was associated with a deposition rate of 15 m/m.y. A hiatus at approximately 18 mbsf of estimated 1.3 m.y. duration covers the Miocene/Pliocene boundary (placed near Subchron boundary C3R-4/C3AN-1) and separates this interval from upper Miocene sediments (Chrons C3A/C3B/C4). There is no paleomagnetic evidence for a short hiatus between Subchrons C3N-2 and C3N-4 proposed by diatom stratigraphy (Gersonde and Burckle, this volume).

A nearly complete middle and upper Miocene reversal sequence was found between 18 and 55 mbsf from Chrons C4 to C5. Due to extremely low sedimentation rates of ~3 m/m.y., the magnetochronologic assignments depend on the resolution of biostratigraphic constraints. Such condensed intervals with average sedimentation rates of only a few meters per million years can be equally well explained by a number of short hiatuses separating intervals of higher deposition rate. Normally these hiatuses cannot be resolved by stratigraphic methods, but they degrade the characteristic paleomagnetic reversal pattern. This may account for the late Miocene interval within Chron C3B/C4/C4A, which does not show a perfect correlation with the polarity time scale. A predominantly reversed interval in the

Table 4. Magnetochronology for Hole 690B. For further explanation see Table 3.

Boundary depth (mbsf)	Range (m)	Depth (mbsf)	Sample	Polarity	Chron	Sedimentation rate (m/m.y.)	Age (Ma)
		0.49	1,1,49				
				N	C1 N-1		
		1.83	1,2,33				
2.00	0.56				hiatus		<0.73->1.88
		2.35	2,1,25				
				R	C2 R		
		3.35	2,1,125				
3.45	0.21						
		3.56	2,1,146				
				N	in C2 R (Reunion?)	(2.2)	
		3.56	2,1,146				
3.70	0.29						
		3.85	2,2,25				
				R	C2 R	>4.8	
		4.60	2,2,100				
4.83	0.46						2.47
		5.06	2,2,146				
				N	C2AN-1	4.2	
		6.56	2,3,146				
6.71	0.29						2.92
		6.85	2,4,25				
				R	C2AR-1	3.9	
		6.85	2,4,25				
6.98	0.25						2.99
		7.10	2,4,50				
				N	C2AN-2	(3.9)	
		7.10	2,4,50				
7.23	0.25				hiatus		3.05-3.18
		7.35	2,4,75				
				R	C2AR-3	(4.3)	
		10.10	2,6,50				
10.23	0.25						3.88
		10.35	2,6,75				
				N	C3 N-1	2.8	
		10.35	2,6,75				
10.48	0.25						3.97
		10.60	2,6,100				
				R	C3 R-1	5.6	
		11.06	2,6,146				
11.21	0.29						4.10
		11.35	2,7,25				
				N	C3 N-2	4.1	
		11.60	2,7,50				
11.78	0.35						4.24
		11.95	3,1,25				
				R	C3 R-3	19.8	
		18.19	3,5,49				
18.32	0.25						4.57
		18.44	3,5,74				
				N	C3 N-4	(11.8)	
		18.44	3,5,74				
18.57	0.26						
		18.70	3,5,100				
				R	?		
		18.70	3,5,100				
18.83	0.26				hiatus		4.61->7.90
		18.96	3,5,126				
				N	C4AN-1		
		19.94	3,6,74				
20.07	0.26						8.21
		20.20	3,6,100				
				R	C4AR-1		
		20.94	3,7,24				
21.07	0.25				hiatus		<8.41->8.92
		21.19	3,7,49				
				N	C5 N-1		
		22.40	4,1,100				
22.53	0.25						
		22.65	4,1,125				
				R	in C5 N-1		
		22.65	4,1,125				
22.76	0.21						
		22.86	4,1,146				
				N	C5 N-1	>4.6	
		27.90	4,5,50				
28.03	0.25						10.42

Table 4 (continued).

Boundary depth (mbsf)	Range (m)	Depth (mbsf)	Sample	Polarity	Chron	Sedimentation rate (m/m.y.)	Age (Ma)
		28.15	4,5,75				
				R	C5 R-1/2	12.5	
		29.40	4,6,50				
29.53	0.25						10.54
		29.65	4,6,75				
				N	C5 N-3	5.0	
		29.65	4,6,75				
29.78	0.25						10.59
		29.90	4,6,100				
				R	C5 R-3	(10.3)	
31.20	0.87				hiatus		10.73–11.38
				R	C5 R-3	(3.1)	
		31.60	5,1,50				
31.72	0.25						11.55
		31.85	5,1,75				
				N	C5AN-1	4.1	
		32.35	5,1,125				
32.45	0.20						11.73
		32.55	5,1,145				
				R	C5AR-1	7.9	
		33.35	5,2,75				
33.47	0.25						11.86
		33.60	5,2,100				
				N	C5AN-2	1.9	
		33.85	5,2,125				
33.95	0.20						12.12
		34.05	5,2,145				
				R	C5AR-2/3/4	3.4	
		36.10	5,4,50				
36.35	0.50						12.83
		36.60	5,4,100				
				N	C5AN-5	3.3	
		36.85	5,4,125				
36.95	0.20						13.01
		37.05	5,4,145				
				R	C5AR-5	1.3	
		37.05	5,4,145				
37.20	0.30						13.20
		37.35	5,5,25				
				N	C5AN-6	3.0	
		37.85	5,5,75				
37.97	0.25						13.46
		38.10	5,5,100				
				R	C5AR-6	4.4	
		38.85	5,6,25				
38.97	0.25						13.69
		39.10	5,6,50				
				N	C5AN-7	2.5	
		39.85	5,6,125				
39.95	0.20						14.08
		40.05	5,6,145				
				R	C5AR-7	2.1	
		40.05	5,6,145				
40.20	0.30						14.20
		40.35	5,7,25				
				N	C5AN-8	3.2	
		41.55	6,1,75				
41.68	0.25						14.66
		41.80	6,1,100				
				R	C5AR-8	2.3	
		42.05	6,1,125				
42.16	0.21						14.87
		42.26	6,1,146				
				N	C5BN-1	2.8	
		42.26	6,1,146				
42.41	0.29						14.96
		42.55	6,2,25				
				R	C5BR-1	(3.1)	
		43.55	6,2,125				
43.66	0.21				hiatus		15.36–>16.22
		43.76	6,2,146				
				N	C5C~~~C5DN-1		
		44.55	6,3,75				
44.68	0.25						17.90
		44.80	6,3,100				
				R	C5DR-1	3.3	
		45.26	6,3,146				

Table 4 (continued).

Boundary depth (mbsf)	Range (m)	Depth (mbsf)	Sample	Polarity	Chron	Sedimentation rate (m/m.y.)	Age (Ma)
45.41	0.29						18.12
		45.55	6,4,25				
				N	C5DN-2	13.5	
		45.55	6,4,25				
45.68	0.25						18.14
		45.80	6,4,50				
				R	C5DR-2	2.4	
		46.30	6,4,100				
46.68	0.75						18.56
		47.05	6,5,25				
				N	C5E~~~C6		
		51.15	7,1,75				
51.28	0.25				hiatus		<20.45->26.56
		51.40	7,1,100				
				R	C7AR		
		53.15	7,2,125				
53.25	0.20						26.86
		53.35	7,2,145				
				N	C8 N-1	21.4	
		54.65	7,3,125				
54.75	0.20						26.93
		54.85	7,3,145				
				R	C8 R-1	3.1	
		54.85	7,3,145				
55.00	0.30						27.01
		55.15	7,4,25				
				N	C8 N-2	7.0	
		59.90	7,7,50				
60.11	0.42						27.74
		60.32	7,C,15				
				R	C8 R-2	2.1	
		60.88	8,1,78				
60.99	0.22						28.15
		61.10	8,1,100				
				N	C9 N-1/2		
		67.85	8,6,25				
67.98	0.25						
		68.10	8,6,50				
				R	in C9 N-1/2		
		68.10	8,6,50				
68.23	0.25						
		68.35	8,6,75				
				N	C9 N-1/2	7.1	
		68.35	8,6,75				
68.48	0.25						29.21
		68.60	8,6,100				
				R	C9 R-2	(7.1)	
		72.05	9,2,75				
72.18	0.25				hiatus		29.73-31.96
		72.30	9,2,100				
				N	C11N-1/2	(17.1)	
		73.80	9,3,100				
73.93	0.25						32.06
		74.05	9,3,125				
				R	C11R-2		
		79.90	10,1,50				
80.02	0.25						
		80.15	10,1,75				
				N	in C11R-2		
		80.15	10,1,75				
80.27	0.25						
		80.40	10,1,100				
				R	C11R-2	17.1	
		80.65	10,1,125				
80.76	0.21						32.46
		80.86	10,1,146				
				N	C12N	7.4	
		83.88	10,3,148				
84.01	0.27						32.90
		84.15	10,4,25				
				R	C12R	(7.4)	
		91.33	11,2,73				
91.58	0.50				hiatus		33.92-38.73
		91.83	11,2,123				
				N	C16N-2	(6.3)	
		91.83	11,2,123				
91.95	0.24						38.79
		92.07	11,2,147				

Table 4 (continued).

Boundary depth (mbsf)	Range (m)	Depth (mbsf)	Sample	Polarity	Chron	Sedimentation rate (m/m.y.)	Age (Ma)
				R	C16R-2	6.5	
		92.07	11,2,147				
92.21	0.28						38.83
		92.35	11,3,25				
				N	C16N-3	8.5	
		95.57	11,5,47				
95.70	0.26						39.24
		95.83	11,5,73				
				R	C16R-3	3.1	
		96.33	11,5,123				
96.59	0.52						39.53
		96.85	11,6,25				
				N	C17N-1	2.7	
		98.78	11,7,68				
99.04	0.51						40.43
		99.29	12,1,49				
				R	C17R-1	5.3	
		99.29	12,1,49				
99.41	0.24						40.50
		99.53	12,1,73				
				N	C17N-2	(4.3)	
		101.30	12,2,100				
101.42	0.23				hiatus		40.97–?
		101.53	12,2,123				
				R	?		
		101.77	12,2,147				
101.91	0.28						?
		102.05	12,3,25				
				N	?		
		105.53	12,5,73				
105.65	0.24				hiatus		?–44.58
		105.77	12,5,97				
				R	C19R	(7.9)	
		105.99	12,5,119				
106.27	0.56						44.66
		106.55	12,6,25				
				N	C20N	7.9	
		118.00	13,7,50				
118.23	0.46						46.17
		118.46	13,C,16				
				R	C20R	(7.9)	
		118.46	13,C,16				
118.74	0.55				hiatus		46.23–49.20
		119.01	14,1,51				
				N	C21N	(4.3)	
		123.51	14,4,51				
123.63	0.24						50.34
		123.75	14,4,75				
				R	C21R	4.3	
		130.35	15,2,75				
130.48	0.25						51.95
		130.60	15,2,100				
				N	C22N		
		130.60	15,2,100				
130.64	0.08						
		130.68	15,2,108				
				R	in C22N		
		130.68	15,2,108				
130.77	0.17						
		130.85	15,2,125				
				N	C22N		
		130.85	15,2,125				
130.95	0.20						
		131.05	15,2,145				
				R	in C22N		
		131.05	15,2,145				
131.11	0.12						
		131.17	15,3,7				
				N	C22N	2.6	
		132.10	15,3,100				
132.23	0.25						52.62
		132.35	15,3,125				
				R	C22R	(2.6)	
		132.55	15,3,145				
132.70	0.30				hiatus		52.80–54.65
		132.85	15,4,25				
				N	C23N-2	(9.4)	
		133.10	15,4,50				

Table 4 (continued).

Boundary depth (mbsf)	Range (m)	Depth (mbsf)	Sample	Polarity	Chron	Sedimentation rate (m/m.y.)	Age (Ma)
133.18	0.15						54.70
		133.25	15,4,65				
				R	C23R-2	9.4	
		137.05	15,6,145				
137.33	0.55						55.14
		137.60	15,7,50				
				N	C24N-1		
		138.80	16,1,100				
138.92	0.25						
		139.05	16,1,125				
				R	in C24N-1		
		139.05	16,1,125				
139.15	0.20						
		139.25	16,1,145				
				N	C24N-1	10.2	
		139.55	16,2,25				
139.67	0.25						55.37
		139.80	16,2,50				
				R	C24R-1		
		140.30	16,2,100				
140.42	0.25						
		140.55	16,2,125				
				N	in C24R-1		
		140.55	16,2,125				
140.65	0.20						
		140.75	16,2,145				
				R	C24R-1	16.4	
		144.30	16,5,50				
144.42	0.25						55.66
		144.55	16,5,75				
				N	C24N-2		
		145.55	16,6,25				
145.67	0.25						(55.72)
		145.80	16,6,50				
				R	in C24N-2		
		146.05	16,6,75				
146.17	0.25						(55.74)
		146.30	16,6,100				
				N	C24N-2		
		147.30	16,7,50				
147.52	0.45						(55.81)
		147.75	17,1,25				
				R	in C24N-2		
		148.00	17,1,50				
148.13	0.25						
		148.25	17,1,75				
				N	C24N-2		
		148.25	17,1,75				
148.38	0.25						
		148.50	17,1,100				
				R	in C24N-2		
		148.75	17,1,125				
148.85	0.20						(55.87)
		148.95	17,1,145				
				N	C24N-2		
		149.75	17,2,75				
149.88	0.25						(55.92)
		150.00	17,2,100				
				R	in C24N-2		
		150.25	17,2,125				
150.35	0.20						(55.94)
		150.45	17,2,145				
				N	C24N-2		
		153.00	17,4,100				
153.13	0.25						
		153.25	17,4,125				
				R	in C24N-2		
		153.25	17,4,125				
153.35	0.20						
		153.45	17,4,145				
				N	C24N-2	21.3	
		154.50	17,5,100				
154.63	0.25						56.14
		154.75	17,5,125				
				R	C24R-2		
		159.20	18,2,50				
159.33	0.25						(56.52)
		159.45	18,2,75				

Table 4 (continued).

Boundary depth (mbsf)	Range (m)	Depth (mbsf)	Sample	Polarity	Chron	Sedimentation rate (m/m.y.)	Age (Ma)
				N	in C24R-2		(56.52)
		159.45	18,2,75				
159.58	0.25						
		159.70	18,2,100				
				R	C24R-2		
		159.70	18,2,100				
159.83	0.25						
		159.95	18,2,125				
				N	in C24R-2		
		160.15	18,2,145				
160.30	0.30						(56.60)
		160.45	18,3,25				
				R	C24R-2		
		166.15	18,6,145				
166.78	1.25						(57.13)
		167.40	19,1,50				
				N	in C24R-2		
		167.90	19,1,100				
168.65	1.50						(57.28)
		169.40	19,2,100				
				R	C24R-2		
		170.40	19,3,50				
170.52	0.25						(57.43)
		170.65	19,3,75				
				N	in C24R-2		
		170.65	19,3,75				
170.77	0.25						
		170.90	19,3,100				
				R	C24R-2		
		170.90	19,3,100				
171.02	0.25						
		171.15	19,3,125				
				N	in C24R-2		
		171.15	19,3,125				
171.25	0.20						(57.49)
		171.35	19,3,145				
				R	C24R-2		
		173.90	19,5,100				
174.23	0.65						
		174.55	20,1,25				
				N	in C24R-2		
		174.55	20,1,25				
174.67	0.25						
		174.80	20,1,50				
				R	C24R-2	12.3	
		185.25	21,C,5				
185.48	0.45						58.64
		185.70	22,1,50				
				N	C25N	17.4	
		195.69	23,3,149				
195.94	0.50						59.24
		196.19	23,4,49				
				R	C25R		
		200.46	24,2,76				
200.58	0.24						
		200.70	24,2,100				
				N	in C25R		
		200.70	24,2,100				
200.94	0.48						
		201.18	24,2,148				
				R	C25R		
		202.20	24,3,100				
202.33	0.25						(59.67)
		202.45	24,3,125				
				N	in C25R		
		202.45	24,3,125				
202.56	0.22						
		202.67	24,3,147				
				R	C25R		
		202.67	24,3,147				
202.82	0.29						
		202.96	24,4,26				
				N	in C25R		
		203.46	24,4,76				
203.58	0.24						(59.76)
		203.70	24,4,100				
				R	C25R		
		205.45	25,1,125				

Table 4 (continued).

Boundary depth (mbsf)	Range (m)	Depth (mbsf)	Sample	Polarity	Chron	Sedimentation rate (m/m.y.)	Age (Ma)
205.56	0.22						
		205.67	25,1,147				
				N	in C25R		
		205.67	25,1,147				
205.81	0.28						
		205.95	25,2,25				
				R	C25R		
		207.69	25,3,49				
207.95	0.51						(60.04)
		208.20	25,3,100				
				N	in C25R		
		208.45	25,3,125				
208.56	0.22						(60.10)
		208.67	25,3,147				
				R	C25R	14.7	
		209.70	25,4,100				
210.20	0.99						60.21
		210.69	25,5,49				
				N	C26N	>5.3	
		212.95	25,6,125				
213.06	0.22						60.75
		213.17	25,6,147				
				R	?		
		213.17	25,6,147				

lower part of Chron C4A could not be identified in Hole 689B, which may suggest a hiatus at around 24.5 mbsf. Chron C5, which contains a long normal interval of 1.5 m.y. duration, is characterized by a higher sedimentation rate due to a higher proportion of calcareous nannofossils. A further increase downcore from 7 to 17 m/m.y. is observed in Core 113-689B-4H at the middle/late Miocene boundary (near Subchron boundary C5R-1/C5N-1). The interpretation of the middle Miocene Chron C5A as a continuous sequence in Hole 689B conflicts with the diatom stratigraphy of Gersonde and Burckle (this volume). The detection of the short Subchrons C5AN-3 and -4 (30,000 and 40,000 yr) within more than one sample is very unlikely due to the sample spacing of nearly 80,000 yr at 3 m/m.y. accumulation rate. Strong fluctuations in sedimentation rates by a factor of 5 (3–16 m/m.y.) would be implied by the alternative interpretation of Gersonde and Burckle (this volume). Further constraints from more detailed paleomagnetic and biostratigraphic analyses of this time interval and of the duplicate APC Hole 689D are needed to solve this problem. Thus the hiatus in the upper middle Miocene at 44 mbsf based on diatom stratigraphic data is not included at this stage of analysis. From magnetostratigraphy an apparently well defined and complete middle and upper Miocene section was drilled at Site 689. Due to a number of hiatuses at 55, 59, 60, 65, and 67 mbsf, consecutive polarity intervals could be interpreted only by use of diatom stratigraphic age assignments (Gersonde and Burckle, this volume). But seven reversal boundaries within this interval were used to refine these assignments. Parts of Chrons C5B to C5E and C6 may be represented in this interval and are tentatively identified according to Table 3. Crude estimates for sedimentation rates lie again within the range of 3 to 6 m/m.y.

A major hiatus at 67 mbsf, including the Oligocene/Miocene boundary, is located near a transition between biosiliceous and calcareous lithological units. The hiatus of estimated duration more than 5 m.y. was identified by diatom and radiolarian stratigraphies (Gersonde and Burckle, this volume; Abelmann, this volume).

Paleogene

Slow changes in the overall paleomagnetic characteristics are also seen in Paleogene sediments. Long-term variations in NRM intensity and MDF show similar periods to the Neogene (Fig. 7B, C). Again, extraordinarily low NRM intensities are observed between 144 and 152 mbsf and between 159 and 162 mbsf, which fall in an interval of high quartz and clay content (135–180 mbsf; >15%), but magnetization intensities allow AF demagnetization up to 50 mT peak field. Between 67 and 155 mbsf stable inclinations show the expected distribution for high-quality magnetostratigraphic records, with a small scatter around steep dipole inclination values (Table 1). The definition of stable magnetization directions becomes more difficult below 155 mbsf due to multicomponent magnetization, which results in a shallower average inclination of 55°.

Oligocene sediments lie between the unconformity at 67 mbsf between Subchrons C6N and C7R-1 and 131 mbsf. Nannofossil stratigraphy (Wei and Wise, this volume) places zones CP17 to CP19, which cover most of the Oligocene, into the depth interval 67–107 mbsf. The nannofossil datums at 107 mbsf (boundary CP16/CP17; Subchron C12R) and at 132 mbsf (boundary CP15a/CP15b; Subchron C15R/C13R) were used as constraints for the magnetochronologic assignment of the inferred polarity sequence. Although the zonal boundary CP15b/CP16 is apparently missing in the nannofossil zonation scheme, the magnetostratigraphic sequence was assumed to be continuous due to the pattern and number of polarity intervals encountered in this interval. On the basic assumption of smoothly varying or continuous sedimentation, the interpretation for the whole interval between 88 and 161 mbsf is straightforward, covering a complete part of the geomagnetic polarity time scale from Chrons C10 through the normal part of Chron C18. From the assignment of Subchron C12R at 107 mbsf the underlying normal interval between 117 and 120 mbsf must be interpreted as Subchron C13N. If younger than upper Eocene Chron C15, as indicated by biostratigraphic data (Thomas et al., this volume), the normal interval between 124 and 125 mbsf, represented by four samples, cannot be assigned to the geomagnetic polarity timescale. By interpolation of Chron C13 sedimentation-rate ages of 36.72 and 36.57 for this "Chron C14" polarity interval were estimated.

Poor biostratigraphic constraints were available for the depth range 67 to 88 mbsf overlying the sequence discussed above. An extrapolation of the interpretation of Chrons C18 to C10 up to the hiatus at 67 mbsf identifies Chrons C9 (79–88 mbsf) and C8

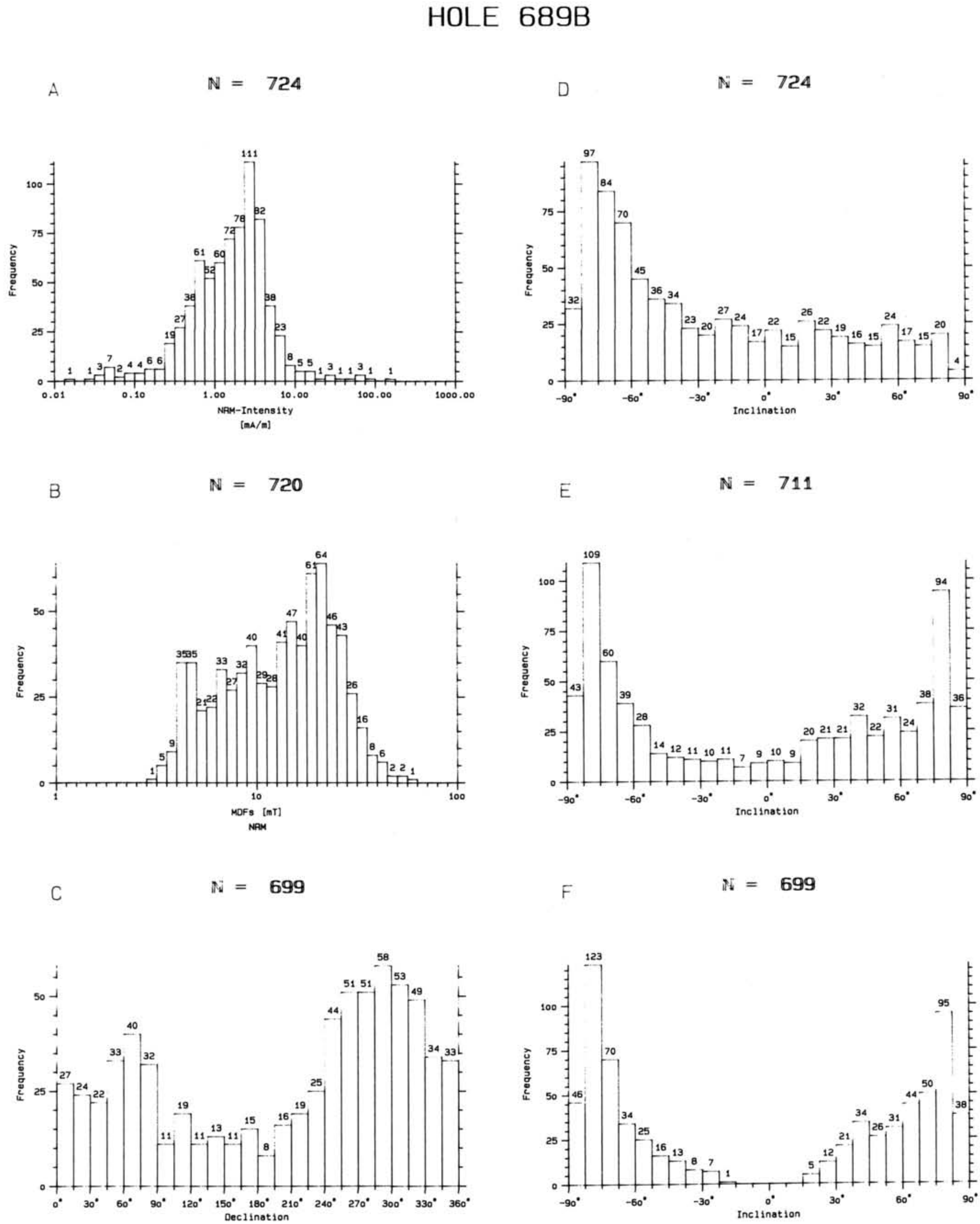

Figure 6. Frequency distribution of paleomagnetic parameters for Hole 689B. See Table 1 for statistical properties. The number N denotes the total number of samples included in the histogram. Numbers above the columns give the frequencies for the corresponding classes. **A.** Geometric distribution of NRM intensities. **B.** Geometric distribution of median destructive field values calculated from summed difference vector decay curves. **C.** Distribution of stable declination values. **D.** NRM inclination values. **E.** Inclination values for 20 mT demagnetization steps. **F.** Stable inclination.

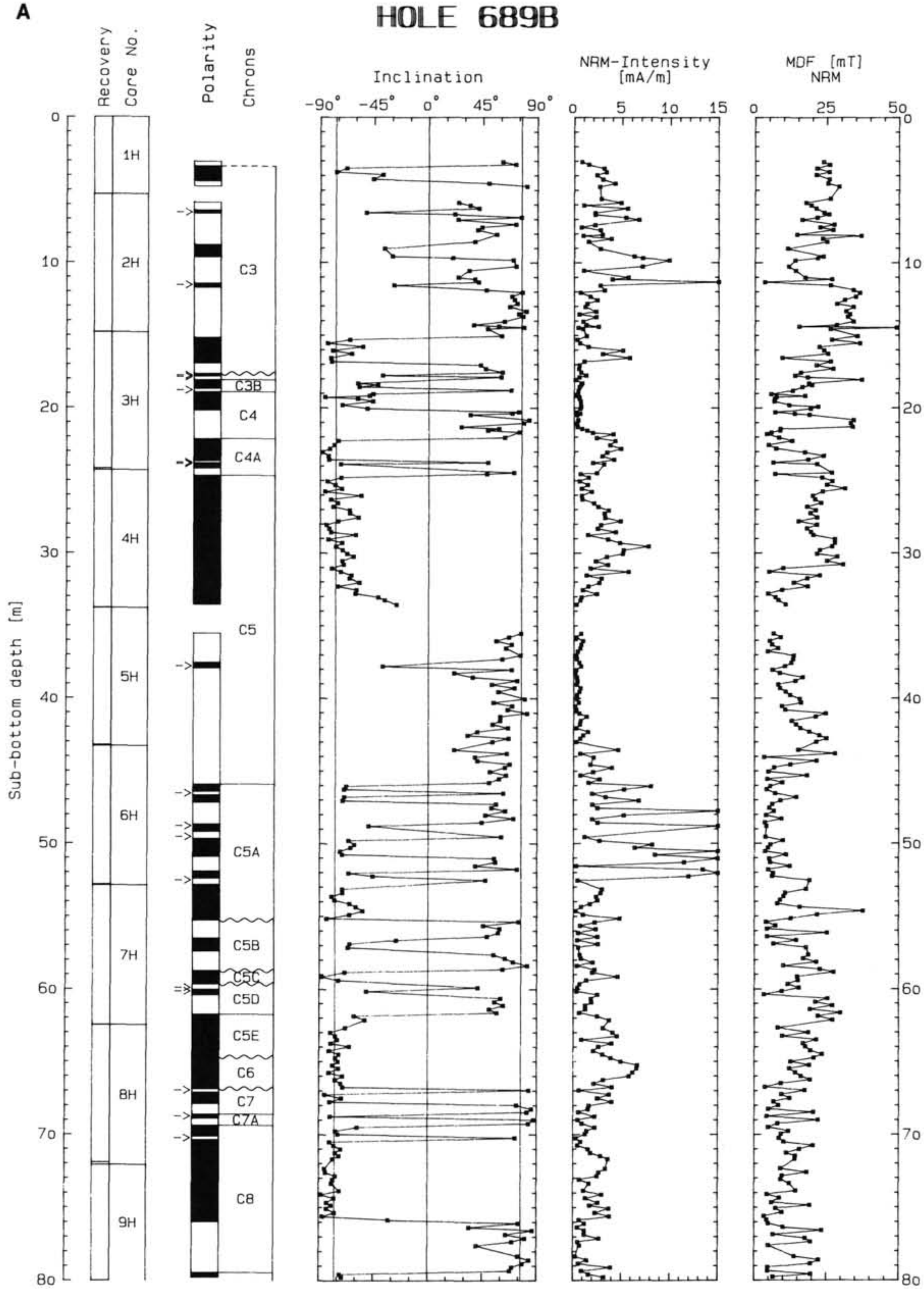

Figure 7. Magnetostratigraphic results for Hole 689B. The downhole variation of NRM intensity, median destructive field calculated from difference vectors (see text for explanation) and stable inclination together with lines for the geocentric axial dipole inclination is plotted as a function of depth together with the polarity reversal pattern and its magnetochronologic interpretation, which includes biostratigraphically defined hiatuses (see Table 3 for details). Core number, coring technique (H = HPC, X = XCB) and core boundaries are shown with recovered interval. Gaps of material loss are dotted in the recovery arrow. For clarity the magnetostratigraphic record is subdivided into three parts with an overlap of 10 m. **A.** 0–80 mbsf. **B.** 70–150 mbsf. **C.** 140–220 mbsf.

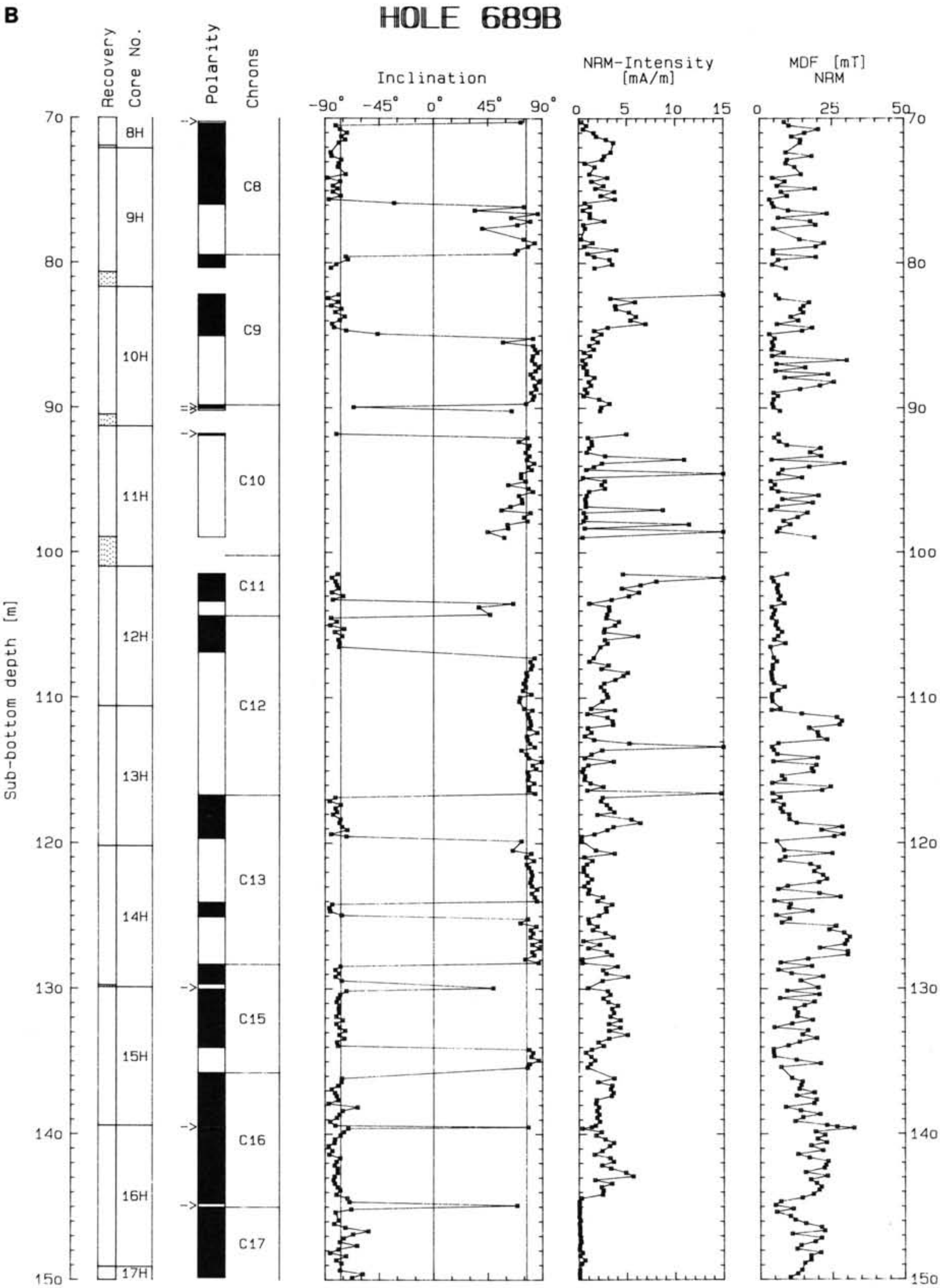

Figure 7 (continued).

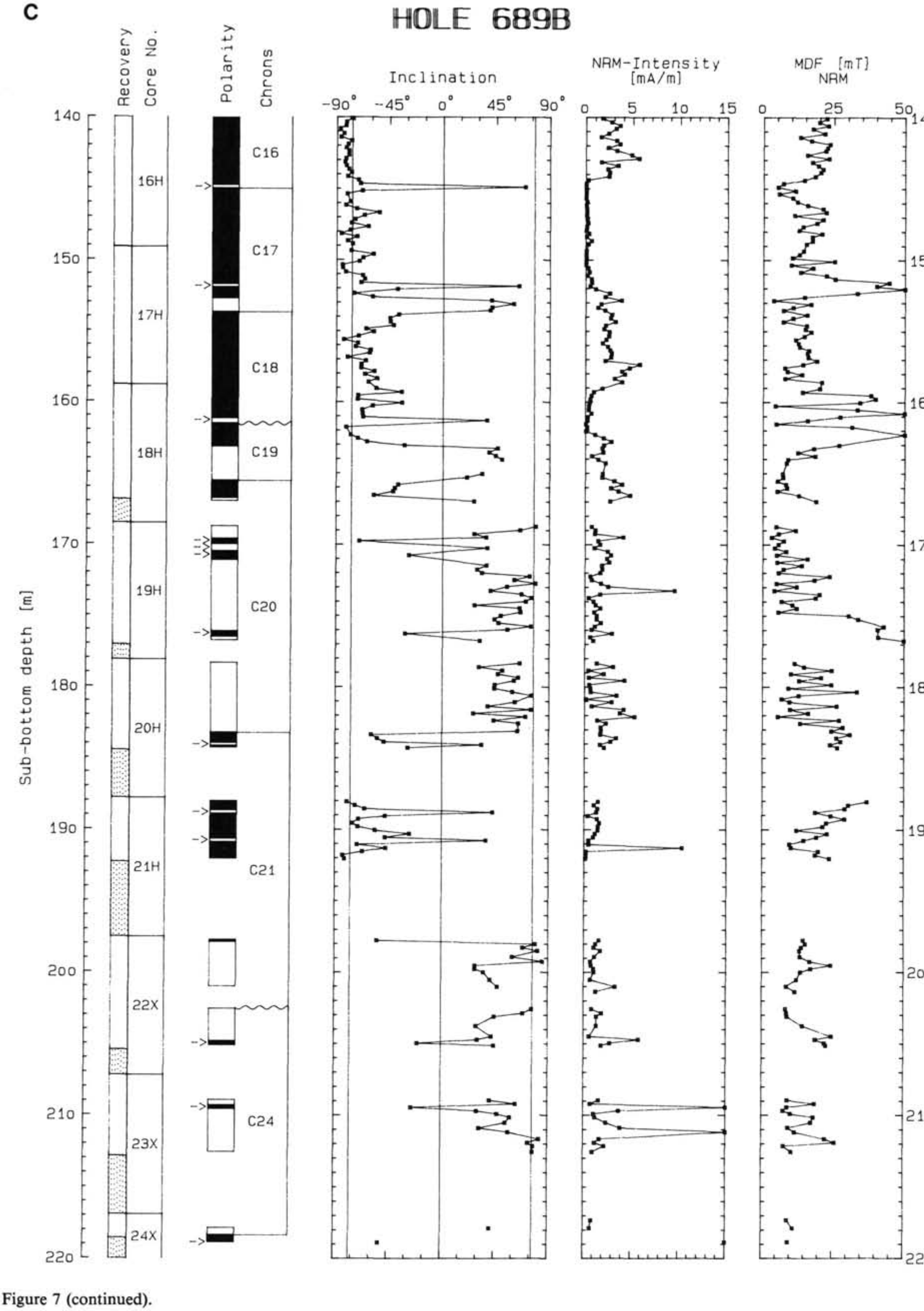

Figure 7 (continued).

(69–79 mbsf) in two long normal and reversed polarity intervals. Uniform sedimentation rates derived from the age-depth curve (Fig. 10B) do not provide any evidence of hiatuses within this interval.

Predominantly normal polarities between 128 and 161 mbsf were identified as Chrons C15 through C18 of late middle to late Eocene age. Short intervals of reversed polarity indicate that the sediments are capable of carrying primary magnetization of reversed polarity, and therefore a total normal overprint of this sequence is rather unlikely. However, intervals of reversed polarity are generally too short, which may be caused by an incomplete removal of a normal overprint and/or overlapping coercivity spectra of antiparallel directional magnetization components. Except for Subchron C17R-3, reversed intervals are based on single samples and have to be used with caution. The age assignment is in agreement with nannofossil (zones CP15 and CP14; Wei and Wise, this volume) and foraminiferal data (zones AP10 through AP12; Stott and Kennett, this volume, chapter 34).

A normal interval at the bottom of Core 113-689B-8H and another group of normal samples at the top of Core 113-689B-9H with two reversed intervals in between were subsumed under Chron C20N. The large gap between them may be produced by the standard ODP procedure of assuming nonrecovered intervals at the bottom of each core. The gap of 1.5 m may well be absent or shorter. Constraining age data at the bottom of Core 113-689B-19H provided by calcareous microfossil stratigraphy define the nannofossil zone boundary CP13/CP14 (Pospichal and Wise, this volume, chapter 30) and foraminiferal zone AP9/AP10 (Stott and Kennett, this volume, chapter 34), which is associated with the lowermost part of Subchron C20N (Berggren et al., 1985; Aubry et al., 1988).

Although larger gaps in recovery in Cores 113-689B-20H and -21H make the interpretation more difficult, normal polarities indicate the presence of Subchron C21N between 184 and 198 mbsf. If the single normal sample at the top of Core 113-689B-22X is disturbed, which may be caused by the beginning of XCB coring, the mean depth of the C21N/C21R boundary may in fact occur at 194 or 190 mbsf instead of 198 mbsf. Sedimentation rates based on these assumptions vary from 5 to 9 m/m.y. and change the extrapolated age at the hiatus at 203 mbsf accordingly. A biostratigraphically defined hiatus at 203 mbsf separates upper lower Eocene (Subchron C21R) from middle lower Eocene sediments (Subchron C24R) within a reversed polarity interval. Apparently, benthic foraminiferal assemblage 6 (207.99–223.59 mbsf, Thomas, this volume) is completely deposited within a reversed polarity interval. If the gap in Core 113-689B-23X (210–218 mbsf) does not contain any normal polarity intervals, the assignment to Chron C24R-2 constrains the minimum sedimentation rate to 6.1 m/m.y. above the hiatus between Core 113-689B-24X and -25X (223 mbsf).

Further constraints may be taken from the placement of the Paleocene/Eocene boundary within Subchron C24R-2. Two single samples of normal polarity appear within Subchron C24R-2, which may be compared to the Eocene sequence encountered at Hole 690B, where ages could be derived for a number of short polarity intervals. Resampling of this interval may provide additional tiepoints for a cross-correlation with Hole 690B and yield more precise estimates of the sedimentation rates.

Site 690

Site 690 (65°9.63′S, 1°12.30′E) is situated on the southern flank of Maud Rise in a water depth of 2914 m. In comparison with Site 689, a duplication of the pelagic sedimentary sequences was expected with a higher biosiliceous component in the Neogene, due to the greater water depth. The first of three drill holes at Site 690 did not contain the mud line in the only core taken, whereas Hole 690B penetrated the upper 213.6 m into Paleocene sediments with the advanced piston corer. Hole 690C duplicates the upper 83.6 mbsf of Neogene and Oligocene sediments and was continued from 204.2 mbsf using the XCB coring technique into the Mesozoic. For a detailed magnetostratigraphic study of Cenozoic sediments, 822 samples in Cores 113-689B-1H to -25H from Hole 690B were selected representing Pleistocene to late Paleocene ages. The lithologic description of Hole 690B is similar to Hole 689B with a general trend from biosiliceous Neogene sediments to calcareous Paleogene sediment components. Nonbiogenic components became important below the Paleocene/Eocene boundary with higher amounts of quartz, clay, and mica. Lithologic Unit I is subdivided into a Pleistocene foraminiferal ooze (0–2.4 mbsf) and diatom and radiolarian-bearing biosiliceous oozes in Subunit Ib (2.4–24.4 mbsf) of Pliocene and Miocene age. A variable mixture of biosiliceous and calcareous components with a larger proportion of biosilica is found in Subunit IIa (24.4–53.4 mbsf) and dominantly nannofossil oozes in Subunit IIb (53.4–92.9 mbsf). Unit III (92.9–137.8 mbsf) represents purely calcareous sediments, whereas additional terrigenous components are observed in Subunits IVa (nannofossil ooze, >15% quartz, clay, mica; 137.8–177.3 mbsf) and IVb (diagenetically altered nannofossil ooze, minor terrigenous constituents; 177.3–252.5 mbsf).

Table 2 summarizes the paleomagnetic properties of Hole 690B sediments, subdivided into several classes of age and lithology. A complete progressive AF-demagnetization was carried out for all 822 paleomagnetic samples from Hole 690B. The geometrically distributed NRM intensities (Fig. 8A) average to 2.8 mA/m, a value nearly twice as high as for Hole 689B. The downcore variation between Lithological Units I and IV is less than a factor of 2. The median destructive field (MDF) is higher (~20 mT) in the upper ~25 m than for the rest of the sedimentary sequence (11.4 mT) and follows a broad geometric distribution (Fig. 8B). The distribution of stable declination values (Fig. 8C) is even more biased toward values around 270° than in Hole 689B, which can hardly be explained by paleomagnetic processes. More likely this was caused by the subsampling effect, first described and investigated by Lovlie et al. (1986), which produces additional magnetization components in each sample perpendicular to the core split surface (90° or 270°) in sample box push direction.

The bias of NRM and 20 mT inclination values was comparable to Hole 6B9B (Fig. 8D, E) and provides strong arguments for a systematic laboratory treatment of each sample. Thus the analysis of magnetization components was used to define stable inclinations and derive polarities from their typical bimodal distribution (Fig. 8F) for 784 of 822 samples. As in Hole 689B the effect of normal overprint is least pronounced in Lithologic Unit IIb, representing the only interval where the use of 20 mT demagnetization steps would have been of any value. The mean inclination value of 62° is significantly lower than for Hole 689B, but a gradual decrease with increasing age could be derived from average values (Table 2) only for sediments of Lithologic Units IIb to IV. Best preservation of axial dipole direction is observed between 45 and 120 mbsf (Unit IIb, 72°), with lower values around 63° above and below.

Results of magnetostratigraphic analyses on each sample of Hole 690B are given in Appendix B and plotted against depth in Figure 9 together with the magnetochronologic age assignments and inferred hiatuses. A summary of this chronology is given in Table 4, and an age-depth plot is in Figure 10.

Neogene

The Neogene biosiliceous sedimentary sequence encountered at Hole 690B is about 16 m shorter than in Hole 689B but covers basically the same age range. Diatoms and radiolarians as

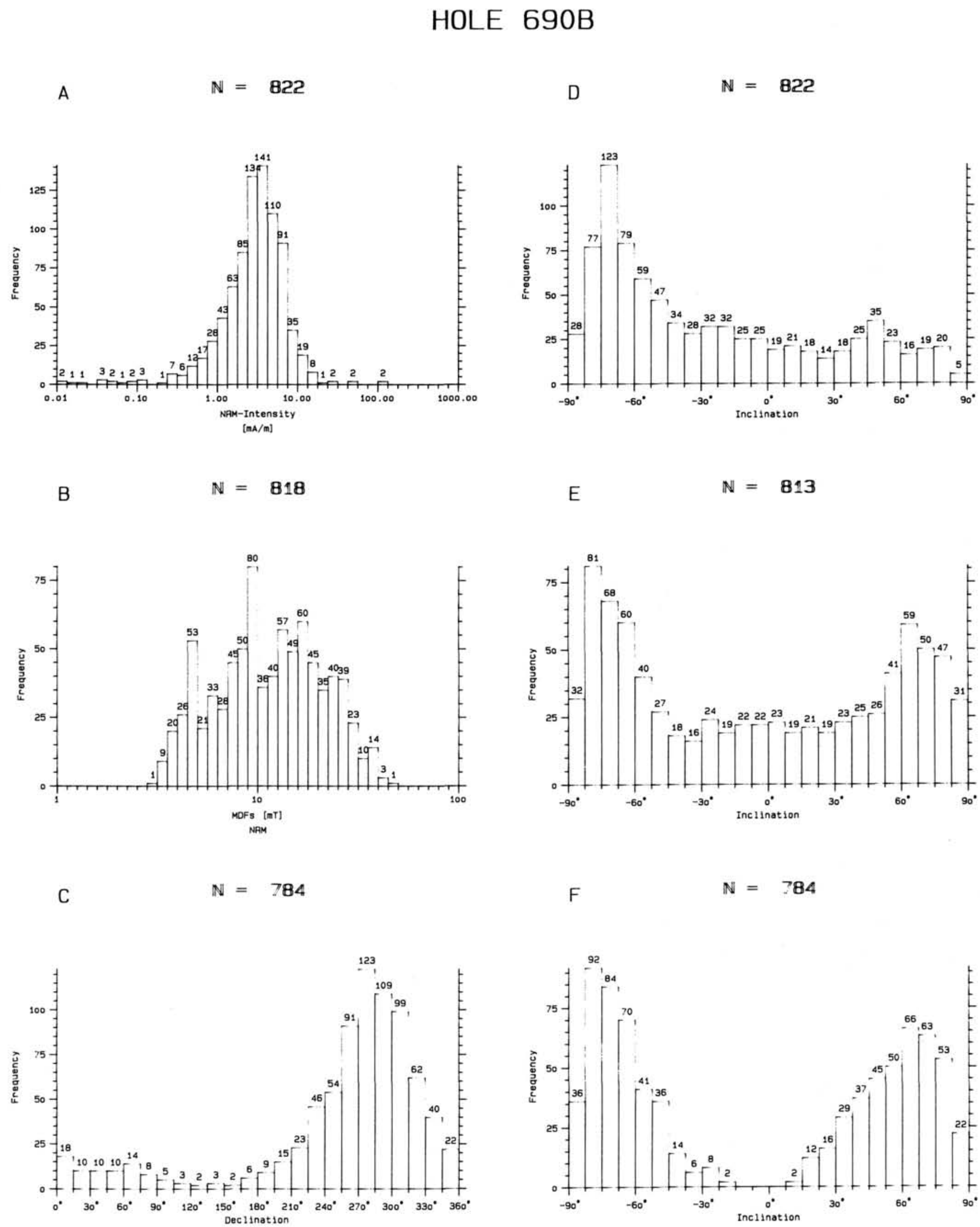

Figure 8. Frequency distribution of paleomagnetic parameters for Hole 690B. See Table 2 for statistical properties. For further explanation see Figure 6.

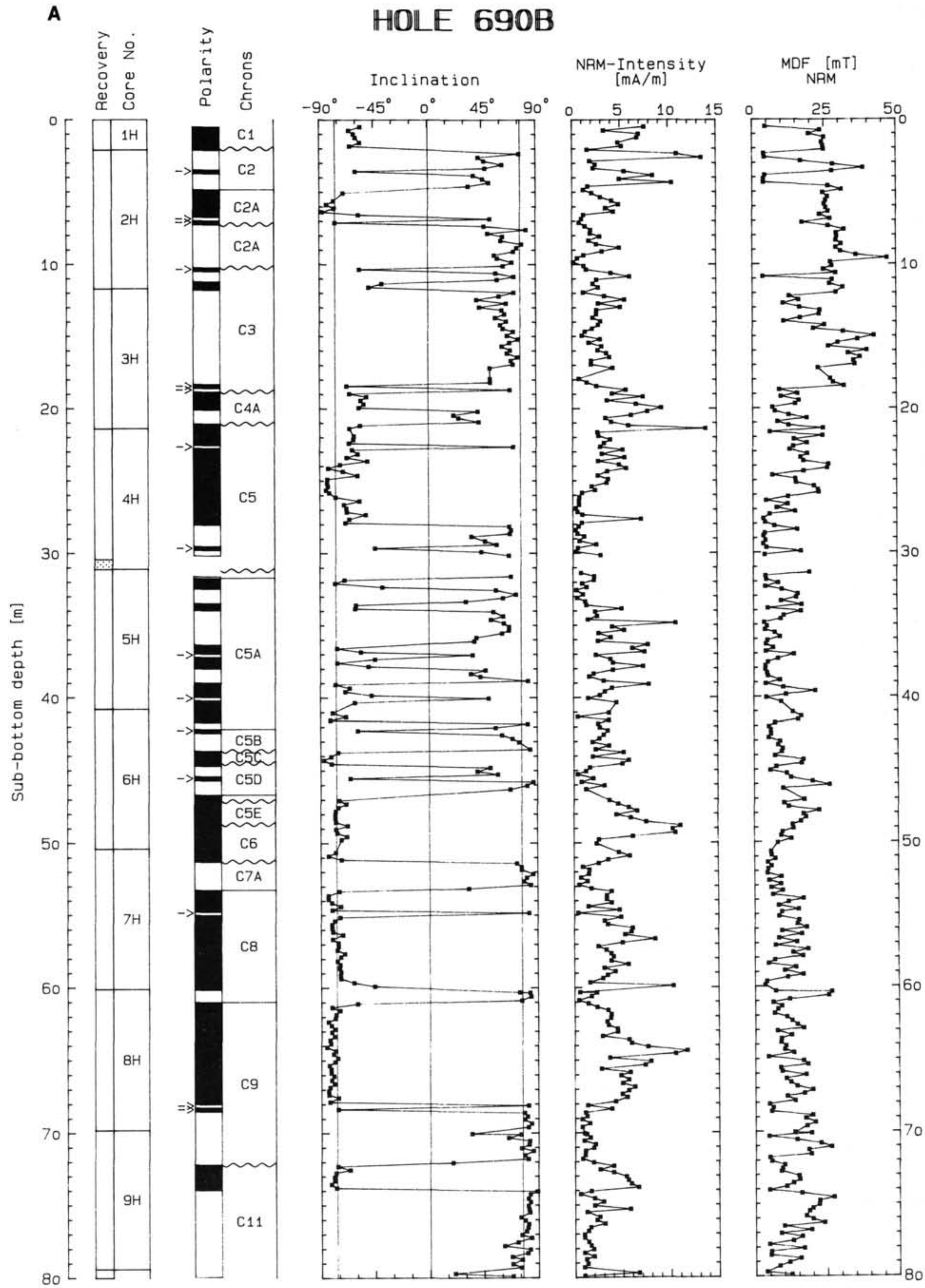

Figure 9. Magnetostratigraphic results for Hole 690B. **A.** 0–80 mbsf. **B.** 70–150 mbsf. **C.** 140–220 mbsf. For further explanation see Figure 7. See also Table 4 for details of the magnetochronostratigraphy.

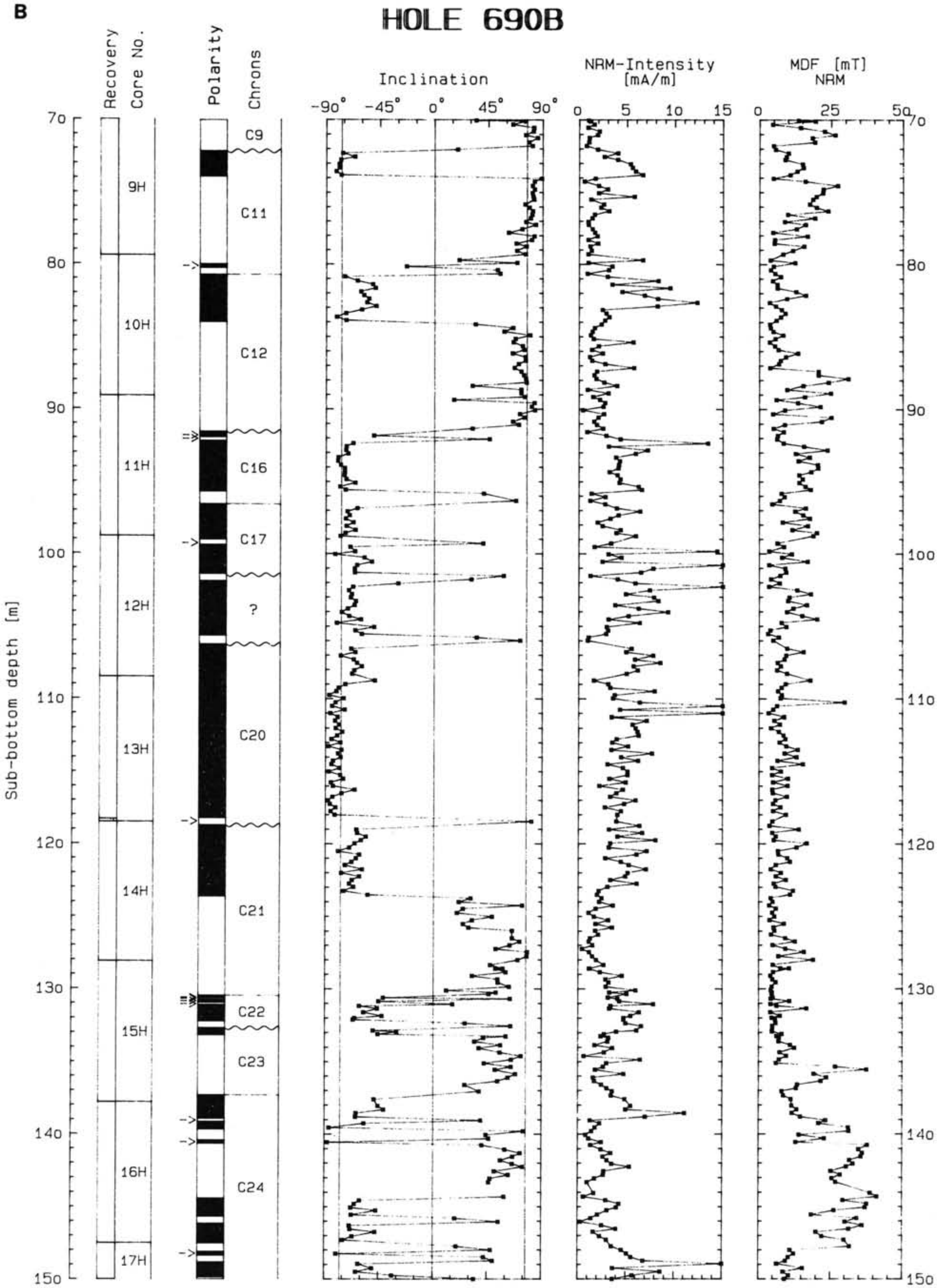

Figure 9 (continued).

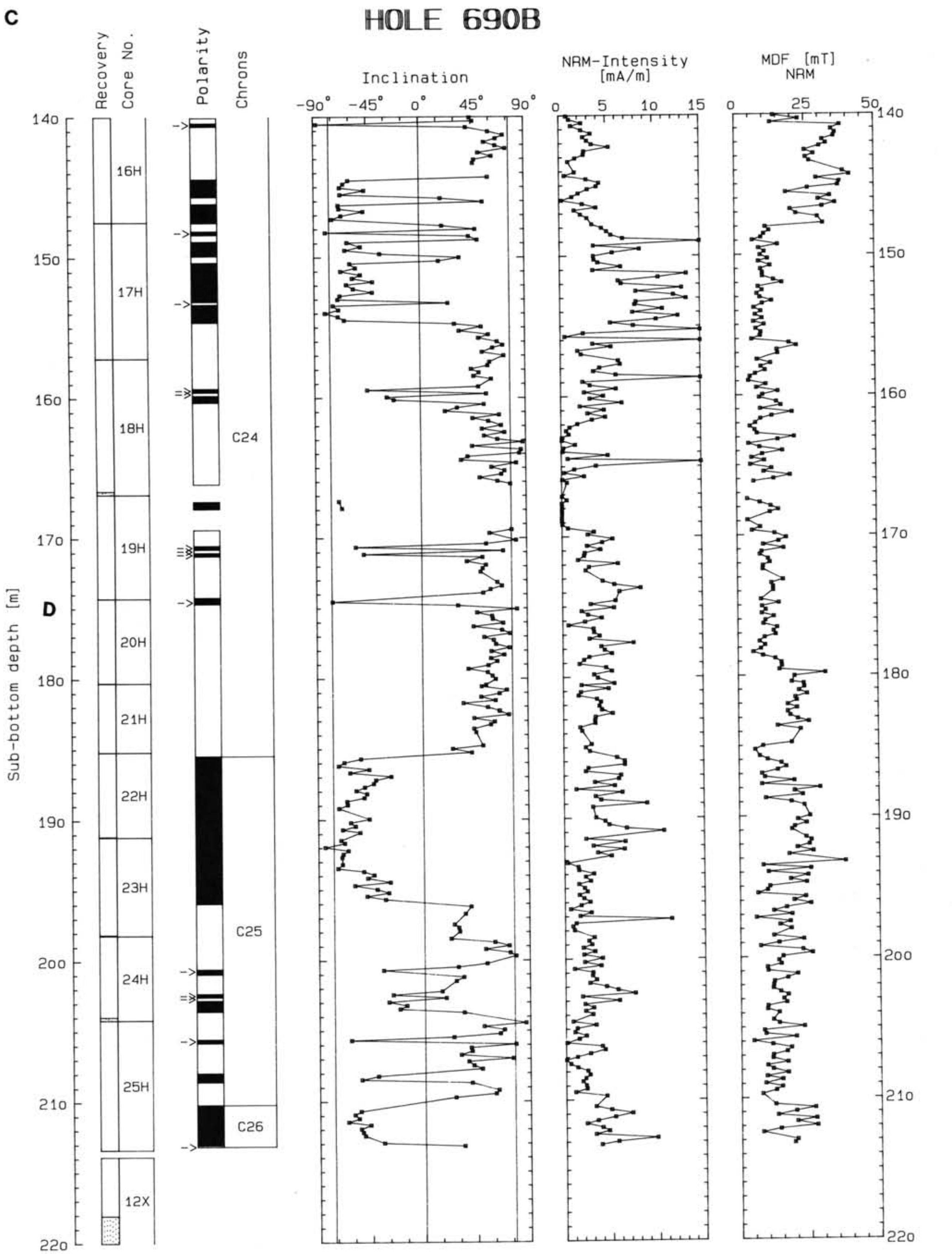

Figure 9 (continued).

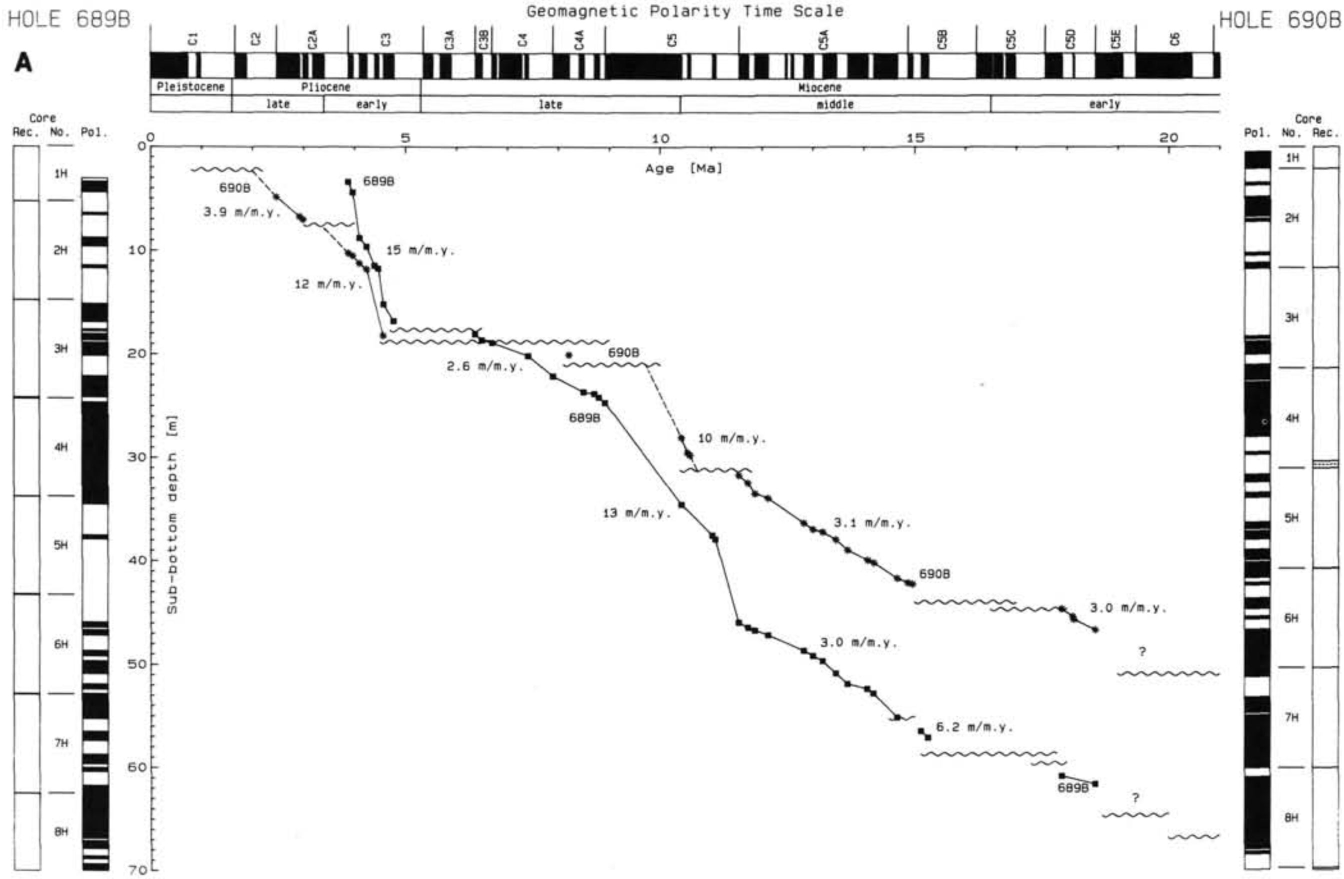

Figure 10. Magnetostratigraphic age-depth relationship and sedimentation rates for Holes 689B and 690B. Hiatuses shown as undulating lines are defined from biostratigraphic data. Broken lines represent extrapolations, alternative interpretations, or constraining assignments. Sedimentation rates were estimated from linear intervals of the age-depth curve. Magnetochronologic assignments for Hole 689B are plotted as solid squares, for Hole 690B as asterisks. **A.** Neogene (0–21 Ma). **B.** Oligocene (20–40 Ma). **C.** Paleocene/Eocene (38–63 Ma). Note that different age and depth scales were chosen to optimize graphic resolution.

major constituents provide the basic biostratigraphic age information for this interval (Gersonde and Burckle, this volume; Abelmann, this volume; Lazarus, this volume), correlating in detail with zonation schemes for Hole 689B. Entirely biosiliceous sediments in the upper 24 m are followed by a mixture with calcareous components.

Stable inclination values were generally lower than the axial dipole inclination down to a depth of 45 mbsf, but due to sufficiently high NRM intensities polarities could unambiguously be derived from the inclination record after standard paleomagnetic laboratory treatment. Long-term variations in intensity run parallel to Hole 689B overlain by a high-frequency scatter of 2–3 mA/m amplitude. A significant drop in magnetic stability downcore from 25 to 15 mT is revealed in the MDF curve at a depth of 19 mbsf, which coincides with a hiatus at the Miocene/Pliocene boundary. A further decrease with depth to a level of 5 mT is detected at 26 mbsf, which persists through the underlying 18 m. A broad cycle of 10 m wavelength and 15–20 mT amplitude continues downcore.

According to diatom stratigraphic data, the shallowest polarity reversal around 2 mbsf represents the Brunhes/Matuyama boundary or a hiatus of similar age. Parts of the lower Matuyama (C2R) and Gauss Chron (C2AN-1, -2) are encountered between 2 and 7 mbsf above a short hiatus leading directly into the upper Gilbert Chron (C2AR-3). The short normal interval within the lower Matuyama polarity record is constrained by diatom biostratigraphy (Gersonde and Burckle, this volume) to late Pliocene age and might be identified as the Reunion Event, which has been reported from several places (McDougall, 1977; Bleil, 1985, 1989) with an estimated age around 2.1 Ma. Late Pliocene sedimentation rates can be estimated as 4 m/m.y., whereas no value is available for the upper Pleistocene. The latest two events within the Gilbert Chron were recognized from 10 to 12 mbsf, but the earlier long reversed interval extends to Subchron C3N-4 with a comparatively high sedimentation rate (20 m/m.y.). The absence of Subchron C3N-3 can be explained according to diatom stratigraphy by a hiatus of short duration (Gersonde and Burckle, this volume).

A major hiatus at 19 mbsf includes the Miocene/Pliocene boundary and extends from Subchron C3R-4 through the younger portion of Chron C4A. Another hiatus (21 mbsf) of short duration leads into the long normal polarity interval unambiguously identified as Subchron C5N-1. Two single reversed samples within the upper part cannot be assigned to the geomagnetic polarity time scale. These short intervals within Subchron C5N-1 may be compared to those reported repeatedly in the literature (e.g., McDougall et al., 1976; LaBrecque et al., 1977; Bleil, 1989), but the resolution of the inferred magnetostratigraphic record is not adequate to provide precise estimates of age and duration. A biostratigraphically defined hiatus at 31.2 mbsf within the lower reversed part of Chron C5 cannot be sustained by magnetostratigraphy.

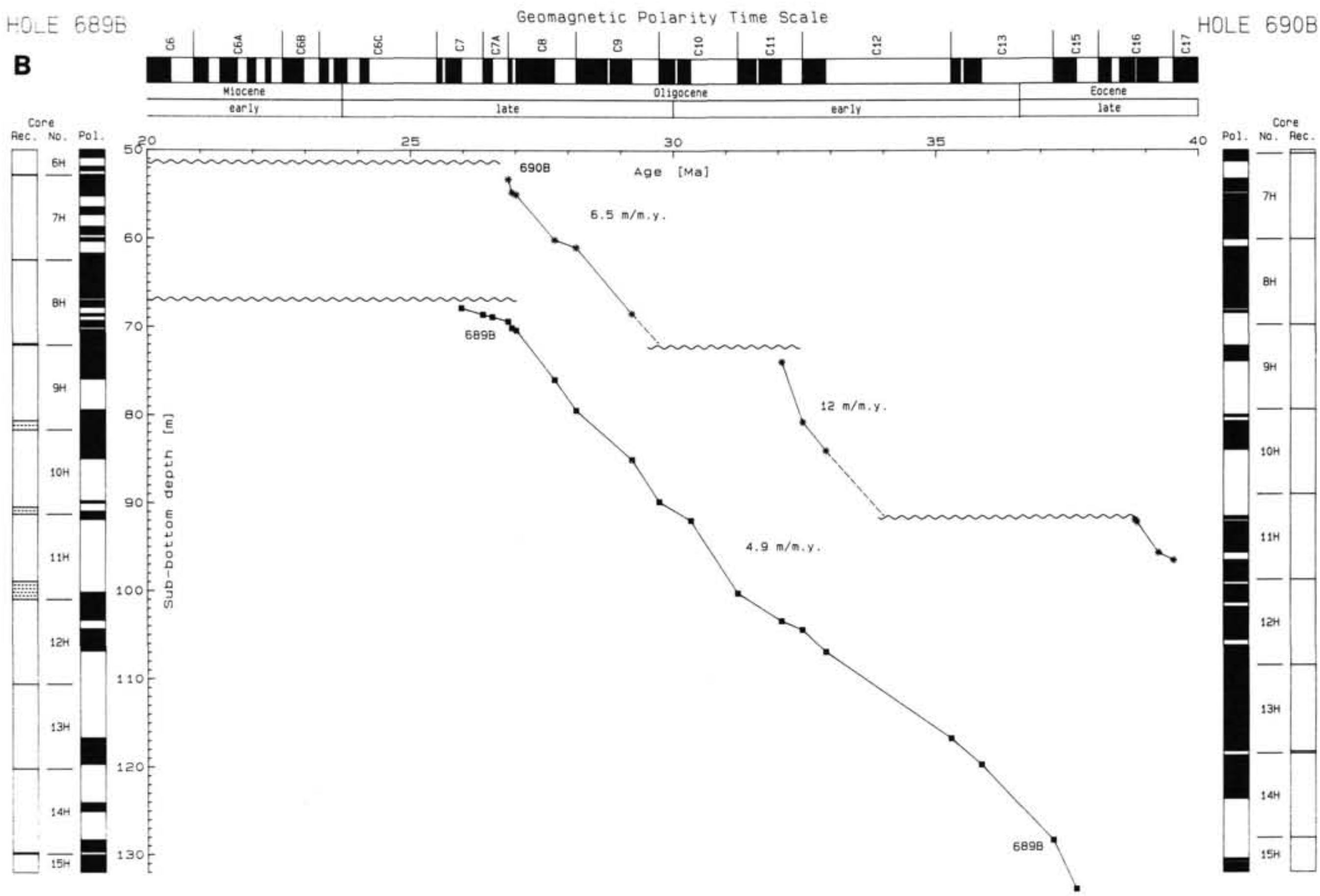

Figure 10 (continued).

Analysis of the polarity pattern together with sedimentation rates indicates an apparently complete polarity reversal pattern between 31 and 43 mbsf. An average deposition rate of 4 m/m.y. was obtained in middle Miocene sediments. An alternative interpretation derived from diatom biostratigraphy (Gersonde and Burckle, this volume) would imply strong variations of the sedimentation rate as was already discussed for Hole 689B. Based on the correlation between Holes 689B and 690B, Gersonde and Burckle expect Chrons C5AN-5 and -6 to be missing, but on the other hand we are unlikely to resolve the two very short geomagnetic Chrons C5AN-3 and -4 with a sampling scheme of 25 cm. These magnetostratigraphic results are comparable to an interval of the same age with constant sedimentation rate encountered at Hole 689B. Discrepancies with diatom stratigraphic results at both sites will have to be resolved on the basis of a more detailed paleomagnetic sampling of this interval to identify shorter polarity intervals. The lower portion of Chron C5, in which high sedimentation rates were derived in Hole 689B, may be absent due to a hiatus proposed by Gersonde and Burckle (this volume).

Diatom data had to be used exclusively to provide age ranges for the sedimentary sequences between 44 and 51 mbsf with hiatuses at 45, 47, 49, and 51 mbsf. Only a small portion (45–47 mbsf) was tentatively assigned to Chrons C5D and C5E, from which the accumulation rate above the major Oligocene/Miocene hiatus was roughly estimated at 3 m/m.y.

Paleogene

More than 6 m.y. are missing at the Oligocene/Miocene unconformity, which was identified also at Hole 689B and separates early Miocene from late Oligocene sediments. Paleomagnetic properties do not change dramatically across this boundary. Inclination values are generally steep down to a depth of 120 mbsf. An acceptable level above 45° inclination is maintained down to a depth of 195 mbsf, but below that primary magnetization directions were less perfectly preserved, and short normal polarity intervals, especially within Subchron C25R, have to be evaluated with caution. NRM intensities (Fig. 9) tend to increase with depth from 1–2 mA/m in the upper Oligocene to 5 mA/m in dominantly normal intervals in the upper Eocene. The general feature of lower intensities within and near reversed chronozones is closely related to a normal overprint together with an overlap of coercivity spectra of both magnetization components. Stabilities cluster around 10 mT with some increased values between 135 and 150 mbsf (~30 mT) and from 180 through 195 mbsf (~25 mT).

Subchron C7AR and the predominantly normal geomagnetic chrons C8 and C9 of late Oligocene age are found just below the Paleogene/Neogene hiatus at 51 mbsf. The top of this sequence is located in Core 113-690B-7H and continues downward with a sedimentation rate of ~7 m/m.y. to ~70 mbsf. Due to constraints provided by nannofossil data (Wei and Wise, this vol-

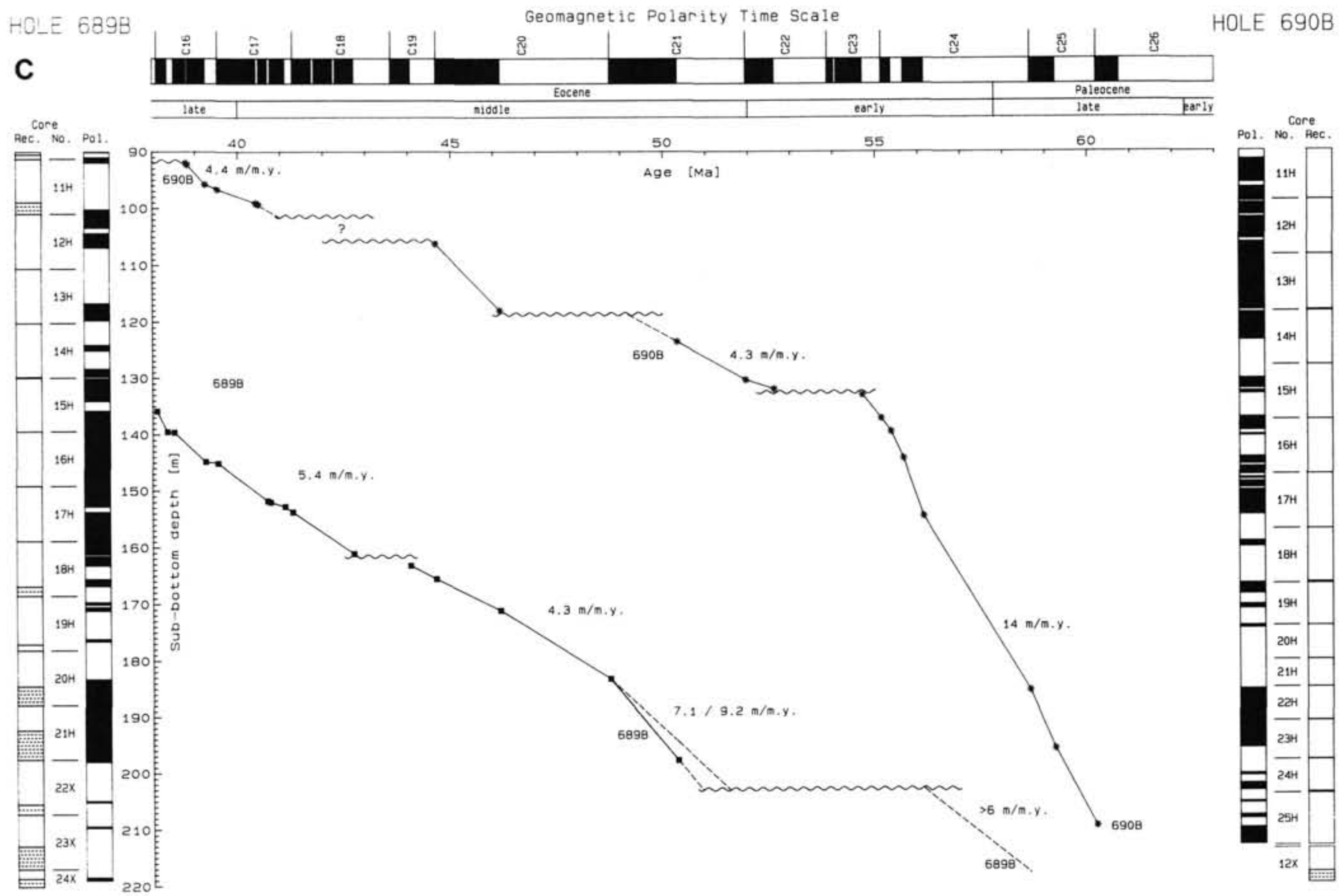

Figure 10 (continued).

ume) an early Oligocene age is assigned to the polarity sequence below. This is interpreted as Chrons C11 and C12, and thus a hiatus is inferred, eliminating Chrons C9 to C11, which were not resolved with biostratigraphic methods at this stage of the investigations. Subchron C11 N between 72 and 74 mbsf is extraordinarily short in comparison to C11R, and for this reason a hiatus of 2.2 m.y. estimated duration might be placed at the top of this normal interval (72 mbsf) within C11 N-2 adjacent to the reversed part of Subchron C9R-2. The average deposition rate can be roughly estimated at 12 m/m.y.

The lower boundary of the Oligocene sedimentary sequence is formed by another major hiatus at around 92 mbsf, including the Eocene/Oligocene boundary. Extrapolating the early Oligocene sedimentation rates, the more than 2-m.y.-long reversed Subchron C12R is apparently not completely represented in Hole 690B. From magnetostratigraphic results this unconformity is placed at a depth of 92 mbsf, just above the short normal polarity interval. This part of Subchron C16N-2, which is in contact with sediments deposited at mid-Chron C12R times, represents the top of a dominantly normal polarity sequence. Within this normal interval calcareous microfossil stratigraphy must be exclusively used to define hiatuses and/or condensed intervals between 102 and 107 mbsf leading from Subchron C20N (106–118 mbsf) to Chrons C17 and C16 above.

Missing calcareous microfossil zones indicate another hiatus in the middle Eocene, within the very long normal polarity interval between 107 and 124 mbsf. If sedimentation rates are assumed as for the late and middle Eocene and the hiatus is placed at ~118 mbsf, the polarity pattern suggests the deletion of Subchron C20R. Below the complete Chron C21 and the normal portion of Chron C22 is identified with a sedimentation rate of 4 m/m.y.

Another hiatus leads from the uppermost Subchron C22R into Chron C23 (Thomas et al., this volume). Chron C24 is characterized by two normal intervals of 0.23 and 0.48 m.y. duration and a long reversed portion below. A high number of polarity reversals was found in this chronozone, which ranges from 133 to 210 mbsf according to calcareous microfossil stratigraphy. An accumulation rate of 14 m/m.y. gives the highest resolution in time of the magnetostratigraphic record on Maud Rise. Thus, polarity intervals can be interpreted requiring more than a single sample. On this basis the predominantly normal intervals (138–140 mbsf and 144–155 mbsf) can be assigned to Subchron C24N-1 and -2. A number of biostratigraphic reference datums (Thomas et al., this volume) as well as a large $\delta^{13}C$ shift support this interpretation (Kennett and Stott, this volume; Stott et al., this volume).

Analysis of magnetization components in early Eocene/Paleocene sediments is more difficult than in other parts of the Hole 690B paleomagnetic record because of multicomponent systems and intervals of weak intensities. But accepting all intervals based on two or more samples as real allows an estimation of age and duration of these additional polarity events (see Table 4) not yet included in the geomagnetic polarity time scale. Normal intervals are found around 56.56, 57.20, 57.46, 59.72, and 60.03 Ma, reversed zones around 55.73, 55.84, and 55.93 Ma, their duration is estimated to be 0.08, <0.15, 0.06, 0.09, and 0.06 m.y. and 0.02, 0.06, and 0.02 m.y., respectively. Similarly, within Chron C25 the same phenomenon was observed in Subchron C25R between 200 and 210 mbsf, where two normal intervals can be detected, but in this case shallower inclinations raise questions about the reliability of the paleomagnetic record. The lowermost portion of Hole 690B, with a normal interval of 3 m, must be assigned to the uppermost section of Subchron C26N.

SUMMARY AND CONCLUSIONS

The Cenozoic sedimentary series from two sites on the Maud Rise plateau were successfully retrieved with the Advanced Piston Corer and the Extended Core Barrel with more than 90% recovery. The biogenic sediments were dominated by biosiliceous components in the upper 67 and 51 m sediments of Neogene age and calcareous microfossils in the Paleogene.

The upper ~220 m of both holes were investigated in some detail with a high-resolution sampling program and a systematic paleomagnetic laboratory treatment of more than 1500 specimens. Magnetization component analysis based on alternating field demagnetization provided reliable information about characteristic remanence of each sample. Correlation of the derived polarity pattern with a geomagnetic polarity timescale was closely tied to the biostratigraphic framework to provide a magnetochronostratigraphy for the low-sedimentation-rate environment of a remote oceanic plateau. In addition, this study should serve as a tool to establish a detailed chronostratigraphy for the Southern Ocean, which should later be combined with the results from the subsequent legs in this region. The interpretation given here represents a first step toward integration of the different data sets, and thus not all inconsistencies between the different stratigraphic methods were resolved; they need further refinement.

Paleomagnetic properties of the sediments did not vary significantly with depth and age but remain more or less constant across lithologic boundaries. Preservation of the primary magnetization was better than expected from other studies on sediments of high biogenic content (e.g., Barton and Bloemendal, 1986). Sufficiently high intensities and stabilities provided the basis for stepwise AF demagnetization and a reliable determination of stable inclination values and polarities for the vast majority of the samples.

Generally the sediments drilled at both sites cover the same age intervals, although distribution and range of the high number of hiatuses detected with biostratigraphic methods vary in some parts (Fig. 10). Pleistocene and late Pliocene sediments are found only in Hole 690B at 4 m/m.y. sedimentation rate, but the early Pliocene is characterized in both holes by higher deposition rates above 10 m/m.y. A hiatus across the Miocene/Pliocene boundary extends into late Miocene sediments, beneath a condensed section in Hole 689B (2.6 m/m.y. deposition rate) and a hiatus in Hole 690B. Increased accumulation, above 10 m/m.y., is encountered around the middle/late Miocene boundary, but the preceding, apparently complete middle Miocene Chron C5A shows lower rates of 3 m/m.y. For a more precise dating of this interval, discrepancies with biostratigraphy need to be resolved. A large number of hiatuses is typical for the early Miocene, one of which covers the Oligocene/Miocene boundary with a duration of about 6 m.y.

The middle late Oligocene features, partly due to the lack of precise biostratigraphic zonation, apparently continuous sedimentation at 5 m/m.y. as far as the middle Eocene in Hole 689B. In contrast, two hiatuses covering Chrons C10/C11 and C12 to C16, together with higher accumulation rates between 7 and 12 m/m.y., were obtained in Hole 690B. Parts of the middle Eocene were missing in both holes, but the sedimentary sequences differ significantly. In Hole 689B the stratigraphic record is interrupted at Chron C20 and between C21 and C24, and thus no precise age constraints could be derived from magnetostratigraphy for this interval. Sediments drilled in Hole 690B contain a complete late Paleocene to early Eocene series with a high average sedimentation rate of 14 m/m.y. Hiatuses were identified between Chrons C17 and C21 as well as in Subchron C21R and near the C22/C23 boundary. The sedimentation rate of the portion in between is estimated at 4 m/m.y.

The cyclic changes in sedimentation rate run more or less parallel in both holes. This indicates a similarity of the depositional environments, which is also expressed in the comparable paleomagnetic properties and a similar cyclicity in NRM intensity for both holes. The paleomagnetic results from Maud Rise provide the first high-quality magnetostratigraphy in the Southern Ocean for a large portion of the Cenozoic. A basic data set is now available, which can be used on the one hand as a chronological framework for regional and global paleoceanographic studies, and on the other hand for a more detailed elaboration of southern high-latitude biochronologies together with ODP Legs 114, 119, and 120 from this region.

ACKNOWLEDGMENTS

I am very grateful to the many people responsible for the success of ODP Leg 113, in particular the scientific party for their friendly cooperation and voluntary assistance in an extensive shipboard sampling program. I especially appreciate the helpful discussions with Norman Hamilton, Rainer Gersonde, and the shipboard biostratigraphic group, as well as the discussions, valuable comments, and support of this scientific work by Ulrich Bleil. Anja Heuermann, Tamara Krüger, Christoph Stadler, and Maria Tegeler did most of the laboratory work.

The financial support of the Deutsche Forschungsgemeinschaft both toward the Ocean Drilling Program and the paleomagnetic laboratory in Bremen is gratefully acknowledged.

REFERENCES

Aubry, M.-P., Berggren, W. A., Kent, D. V., Flynn, J. J., Klitgord, K. D., Obradovich, J. D., and Prothero, D. R., 1988. Paleogene geochronology: an integrated approach. *Paleoceanography,* 3:707–742.

Barker, P. F., Kennett, J. P., et al., 1988. *Proc. ODP, Init. Repts.,* 113: College Station, TX (Ocean Drilling Program).

Barton, C. E., and Bloemendal, J., 1986. Paleomagnetism of sediments collected during Leg 90, Southwest Pacific. *In* Kennett, J. P., von der Borch, C. C., et al., *Init. Repts. DSDP,* 90: Washington (U.S. Govt. Printing Office), 1273–1316.

Berggren, W. A., Kent, D. V., Flynn, J. J., and Van Couvering, J. A., 1985. Cenozoic geochronology. *Geol. Soc. Am. Bull.,* 96:1407–1418.

Bleil, U., 1985. The magnetostratigraphy of Northwest Pacific Sediments, Deep Sea Drilling Project Leg 86. *In* Heath, G. R., Burckle, L. H., et al., *Init. Repts. DSDP,* 86: Washington (U.S. Govt. Printing Office), 441–458.

———, 1989. Magnetostratigraphy of Neogene and Quaternary sediment series from the Norwegian Sea: Ocean Drilling Program, Leg 104. *In* Thiede, J., Eldholm, O., et al. *Proc. ODP, Sci. Results,* 104: College Station, TX (Ocean Drilling Program), 829–901.

Hoffman, K. A., and Day, R., 1978. Separation of multi-component NRM, a general method. *Earth Planet. Sci. Lett.,* 40:433–438.

LaBrecque, J. L., Kent, D. V., and Cande, S. C., 1977. Revised magnetic polarity time scale for Late Cretaceous and Cenozoic time. *Geology,* 5:330–335.

LaBrecque, J. L., Hsü, K. J., Carman, M. F., Jr., Karpoff, A., McKenzie, J. A., Percifal, S. F., Jr., Petersen, N. P., Pisciotto, K. A., Schreiber, E., Tauxe, L., Tucker, P., Weissert, H. J., and Wright, R., 1983. DSDP Leg 73: contributions to Paleogene stratigraphy in nomenclature, chronology and sedimentations rates. *Palaeogeogr., Palaeoclimatol., Palaeoecol.,* 42:91–125.

Lovlie, R., Markussen, B., Sejrup, H. P., and Thiede, J., 1986. Magnetostratigraphy in three Arctic Ocean sediment cores; arguments for geomagnetic excursions within oxygen-isotope stage 2-3. *Phys. Earth Planet. Int.,* 43:173–184.

McDougall, L., 1977. *The present status of the geomagnetic polarity time scale.* Research School of Earth Sciences, Austr. Nat. Univ. Publ. 1288.

McDougall, L., Watkins, N. D., Walker, G., and Kristjansson, L., 1976. K-Ar and paleomagnetic analysis of Icelandic lava flows: limits on the age of Anomaly 5. *J. Geophys. Res.*, 81:1505–1512.

Weinreich, N., and Theyer, F., 1985. Paleomagnetism of Deep Sea Drilling Project Leg 85 sediments: Neogene magnetostratigraphy and tectonic history of the central equatorial Pacific. *In* Mayer, L., Theyer, F., et al. *Init. Repts. DSDP,* 85: Washington (U.S. Govt. Printing Office), 849–901.

Date of initial receipt: 5 May 1989
Date of acceptance: 26 October 1989
Ms 113B-182

APPENDIX A

Paleomagnetic results for 725 samples of Hole 689B. Basic data for the magnetostratigraphic interpretation are given from left to right: Sample location and depth, NRM intensity, intensity calculated from the vector sum of difference vectors, NRM inclination, inclination of the 20 mT demagnetization step, stable inclination and declination, assigned polarity, median destructive field of NRM intensity decay curve, and median destructive field, calculated from difference vector sum decay curve.

Core, section, interval (cm)	Depth (mbsf)	J NRM (mA/m)	Js NRM (mA/m)	Incl. NRM (deg)	Incl. 20 mT (deg)	Incl. stable (deg)	Decl. stable (deg)	Pol.	MDF (mT)	MDFs (mT)
Hole 689B										
1-3, 5-7	3.06	0.84	1.35	+10.7	+50.2	+60.9	36.2	R	43.4	23.9
1-3, 24-26	3.25	1.54	1.71	+56.7	+70.7	+71.7	322.0	R	28.4	26.0
1-3, 49-51	3.50	3.13	3.73	−73.5	−66.5	−68.1	147.2	N	18.3	21.5
1-3, 74-76	3.75	3.35	3.59	−75.9	−65.3	−76.8	34.0	N	27.4	25.8
1-3, 94-96	3.95	2.38	2.50	−33.5	−35.6	−38.0	215.0	N	20.5	21.2
1-3, 124-126	4.25	3.00	3.10	−48.8	−45.8	−46.1	295.0	N	26.4	25.8
1-4, 3-5	4.54	4.27	4.50	+46.5	+50.0	+49.6	321.2	R	26.4	25.3
1-4, 24-26	4.75	2.66	3.01	+72.7	+79.3	+81.0	245.9	R	32.2	29.2
2-1, 28-30	5.59	2.86	3.14	+4.8	+11.9	no	no		28.4	26.3
2-1, 56-58	5.87	4.92	5.09	+16.6	+21.3	+24.7	334.5	R	17.7	17.7
2-1, 74-76	6.05	1.02	1.58	−7.6	+31.9	+34.3	52.1	R	28.5	19.6
2-1, 95-97	6.26	5.59	6.03	+22.5	+31.8	+41.7	42.6	R	22.0	21.3
2-1, 124-126	6.55	2.19	2.34	−47.2	−49.6	−51.9	352.0	N	25.4	24.1
2-1, 136-138	6.67	2.21	2.31	+18.2	+21.0	+21.5	30.0	R	26.9	25.8
2-2, 8-10	6.89	5.40	6.21	+57.3	+64.5	+76.6	110.7	R	23.6	21.6
2-2, 22-24	7.03	6.76	7.31	+22.2	+20.7	+23.9	120.7	R	17.4	16.4
2-2, 56-58	7.37	2.18	2.42	+62.8	+63.0	+72.1	175.7	R	29.9	27.6
2-2, 74-76	7.55	0.76	1.83	−11.4	+25.9	+43.9	159.9	R	35.5	22.6
2-2, 92-94	7.73	2.75	2.91	+26.9	+35.7	+40.3	348.5	R	28.5	27.2
2-2, 124-126	8.05	2.94	3.95	+20.9	+58.2	+56.3	330.7	R	15.8	14.5
2-2, 132-134	8.13	0.94	2.42	+21.0	+36.8	no	no		14.6	36.9
2-3, 3-5	8.34	3.87	5.79	−38.4	−10.9	no	no		28.4	23.5
2-3, 24-26	8.55	1.49	2.37	+23.2	+26.3	+38.0	126.7	R	36.3	25.0
2-3, 72-74	9.03	2.73	3.46	+15.3	−27.5	−36.9	128.8	N	14.8	11.3
2-3, 126-128	9.57	6.23	7.13	−30.1	−29.1	−30.4	71.4	N	27.0	23.8
2-3, 137-139	9.68	7.14	8.03	−9.2	+2.7	+19.7	279.0	R	23.9	21.8
2-4, 3-5	9.84	9.90	12.39	+51.2	+81.4	+70.2	170.8	R	14.4	14.0
2-4, 46-48	10.27	7.11	8.27	−7.7	+11.7	+72.5	267.8	R	12.0	11.8
2-4, 74-76	10.55	1.00	3.55	−27.3	+17.8	+33.3	108.2	R		14.2
2-4, 121-123	11.02	5.64	6.09	+12.2	+21.0	+24.1	87.7	R	19.0	17.5
2-4, 133-135	11.14	3.98	5.50	+29.9	+35.5	+38.2	276.6	R	25.6	26.8
2-5, 3-5	11.34	28.58	38.49	−48.1	+43.1	+41.3	291.6	R	3.3	3.4
2-5, 24-26	11.55	2.72	2.87	−21.8	−19.0	−29.0	99.6	N	27.3	26.4
2-5, 58-60	11.89	3.17	4.01	+34.1	+34.7	+47.7	354.4	R	26.0	34.3
2-5, 75-77	12.06	0.65	1.35	+44.1	+74.9	+77.5	16.4	R		36.5
2-5, 103-105	12.34	1.69	2.00	+59.1	+69.9	+68.7	355.3	R	34.9	35.1
2-5, 125-127	12.56	2.42	2.45	+68.4	+71.0	+70.9	49.5	R	31.6	31.3
2-6, 2-4	12.83	1.36	1.64	+63.5	+72.4	+73.2	11.4	R	32.7	28.5
2-6, 24-26	13.05	1.16	1.39	+58.7	+63.3	+66.9	224.3	R	37.1	34.2
2-6, 54-56	13.35	2.29	2.47	+77.7	+82.2	+80.7	109.3	R	31.5	31.7
2-6, 74-76	13.55	0.51	.80	+53.0	+73.4	+74.2	339.6	R	42.3	33.0
2-6, 91-93	13.72	2.29	2.44	+71.5	+78.4	+77.9	346.6	R	32.8	32.2
2-6, 124-126	14.05	0.93	1.03	+47.3	+56.5	+62.4	213.4	R	36.5	34.2
2-6, 147-149	14.28	1.26	1.86	+16.2	+34.7	+37.0	318.7	R	31.5	28.4
2-7, 7-9	14.38	2.57	4.10	−21.3	+31.2	+58.0	39.1	R	9.3	15.4
2-7, 16-18	14.47	0.45	1.44	+76.5	+79.6	+78.8	67.8	R		49.3
2-7, 24-26	14.55	0.94	1.05	+37.7	+41.2	+48.7	134.0	R	23.9	26.3
3-1, 24-26	15.05	1.33	2.13	−15.7		+60.4	48.8	R	21.0	35.7
3-1, 49-51	15.30	0.32	0.48	−33.0	−23.0	−65.3	329.7	N	28.8	26.7
3-1, 73-75	15.54	0.62	0.85	−66.7	−85.2	−83.9	313.8	N	40.7	36.5
3-1, 98-100	15.79	1.50	1.67	−60.1	−54.1	−54.5	357.2	N	25.2	22.3
3-1, 123-125	16.04	5.09	5.59	−87.2	−77.4	−79.6	139.4	N	26.3	24.0
3-1, 145-147	16.26	2.97	3.17	−56.4	−61.4	−63.6	58.9	N	27.0	25.4
3-2, 24-26	16.55	5.80	6.66	−52.7	−83.0	−81.3	351.5	N	13.5	9.4
3-2, 49-51	16.80	1.07	1.19	−80.7	−79.2	−80.7	114.4	N	28.0	26.4
3-2, 74-76	17.05	0.55	0.73	+15.4	+24.1	+43.0	308.0	R	25.8	21.3
3-2, 99-101	17.30	0.49	0.70	+25.5	+40.8	+47.1	115.0	R	30.2	27.2
3-2, 124-126	17.55	0.72	1.10	+36.4	−19.9	+60.9	206.7	R	12.5	15.9
3-2, 145-147	17.76	1.25	1.36	−4.2	−16.5	−38.4	76.5	N	13.7	13.9
3-3, 7-9	17.88	0.53	0.75	+46.9	+28.7	+60.0	53.7	R	16.6	18.3
3-3, 24-26	18.05	0.12	1.14	−21.1	−0.9	no	no			37.1
3-3, 49-51	18.30	0.84	1.46	−62.6	−54.0	−58.9	41.5	N	23.1	18.6
3-3, 61-63	18.42	0.70	0.91	−5.7	−22.8	−42.2	135.3	N	21.3	19.8
3-3, 74-76	18.55	0.54	1.03	−64.2	−53.3	−57.7	303.1	N	28.4	16.4
3-3, 99-101	18.80	0.44	0.87	+26.2	+51.6	+68.3	348.4	R	4.9	13.1
3-3, 124-126	19.05	0.41	0.49	−57.1	+7.2	−46.1	60.8	N	5.3	5.6
3-3, 135-137	19.16	0.32	0.54	−39.4	−45.1	−48.9	137.6	N	12.2	17.5
3-3, 145-147	19.26	0.55	0.69	−78.2	−19.5	−86.0	39.5	N	5.7	7.5

Appendix A (continued).

Core, section, interval (cm)	Depth (mbsf)	J NRM (mA/m)	Js NRM (mA/m)	Incl. NRM (deg)	Incl. 20 mT (deg)	Incl. stable (deg)	Decl. stable (deg)	Pol.	MDF (mT)	MDFs (mT)
Hole 689B (Cont.)										
3-4, 6-8	19.37	0.59	0.69	−19.6	−16.2	−58.5	49.0	N	6.8	6.9
3-4, 24-26	19.55	0.70	1.03	−57.2	+5.5	−46.0	170.1	N	4.5	6.8
3-4, 49-51	19.80	0.72	1.03	−59.4	+7.5	−71.7	289.9	N	7.8	11.9
3-4, 61-63	19.92	0.74	1.36	+13.7	+3.0	no	no		13.8	22.0
3-4, 74-76	20.05	0.65	1.25	−62.4	−46.6	−50.7	200.5	N	16.8	19.4
3-4, 99-101	20.30	0.20	0.44	−57.0	+73.8	+74.6	207.6	R	3.6	7.0
3-4, 108-110	20.39	0.65	0.68	+65.4	+67.9	+69.1	40.1	R	13.1	13.8
3-4, 116-118	20.47	0.30	0.65	−17.5	+42.9	+34.3	326.5	R	24.8	19.0
3-5, 3-5	20.84	0.42	0.51	+76.7	+78.6	+83.2	54.7	R	37.1	34.3
3-5, 24-26	21.05	0.30	0.54	+73.0	+66.6	+78.5	313.7	R	44.4	33.3
3-5, 49-51	21.30	0.35	0.95	−61.3	−33.0	+26.7	350.6	R	23.1	34.0
3-5, 62-64	21.43	0.83	1.21	+1.3	+57.2	+58.1	10.7	R	4.9	8.8
3-5, 74-76	21.55	1.38	2.57	−50.9	+21.3	+48.7	272.7	R	3.8	8.8
3-5, 88-90	21.69	1.96	2.64	−50.0	+42.0	+74.9	67.5	R	4.2	5.7
3-5, 99-101	21.80	4.10	5.14	−66.0	−8.5	no	no		3.3	4.1
3-5, 124-126	22.05	2.35	3.73	−76.4	+2.0	+62.8	255.4	R	6.0	8.3
3-5, 145-147	22.26	4.28	4.76	−82.9	−72.2	−75.1	278.4	N	16.0	13.0
3-6, 24-26	22.55	3.73	4.10	−64.9	−76.4	−78.5	349.0	N	4.9	4.7
3-6, 49-51	22.80	4.89	5.04	−67.5	−79.8	−82.2	122.0	N	7.7	7.3
3-6, 74-76	23.05	3.41	3.60	−81.7	−88.2	−88.6	78.4	N	18.9	17.3
3-6, 99-101	23.30	2.94	3.10	−82.1	−81.7	−83.2	147.3	N	25.1	24.0
3-6, 124-126	23.55	4.19	4.51	−70.4	−82.3	−82.6	122.2	N	20.4	18.6
3-6, 145-147	23.76	2.00	4.67	−51.6	+44.6	+49.3	268.3	R	21.1	6.4
3-7, 5-7	23.86	3.15	3.56	−68.3	−74.2	−72.8	96.7	N	24.5	21.7
3-C, 28-30	24.47	2.40	2.43	+72.2	+70.3	+70.8	122.8	R	26.8	26.9
4-1, 24-26	24.55	0.67	0.81	+63.0	+40.1	+48.3	155.6	R	5.6	7.0
4-1, 49-51	24.80	1.56	1.61	−65.0	−69.7	−72.5	184.2	N	23.7	23.4
4-1, 74-76	25.05	0.59	0.78	−75.3	−84.8	−84.2	63.4	N	34.6	27.0
4-1, 99-101	25.30	1.45	1.58	−78.8	−77.0	−77.4	306.5	N	27.3	25.1
4-1, 125-127	25.56	0.80	1.26	−57.6	−69.9	−71.9	122.6	N	40.8	31.4
4-1, 145-147	25.76	1.87	1.93	−80.3	−87.1	−85.9	42.4	N	23.6	23.6
4-2, 24-26	26.05	0.80	0.99	−55.6	−48.3	−55.7	264.1	N	27.2	20.1
4-2, 49-51	26.30	0.86	1.04	−78.9	−81.0	−81.2	279.9	N	22.8	20.9
4-2, 74-76	26.55	2.09	2.19	−69.7	−74.8	−75.3	277.1	N	24.1	23.1
4-2, 99-101	26.80	2.53	2.84	−75.2	−77.5	−79.2	213.6	N	20.0	18.1
4-2, 124-126	27.05	3.62	4.45	−38.6	−59.5	−65.4	286.5	N	25.6	21.1
4-2, 144-146	27.25	3.16	3.94	−54.7	−66.6	−65.1	316.7	N	24.6	19.3
4-3, 24-26	27.55	3.23	3.93	−29.7	−47.8	−57.9	276.5	N	25.9	21.6
4-3, 49-51	27.80	4.86	5.00	−71.2	−75.4	−75.1	257.5	N	15.9	15.2
4-3, 74-76	28.05	2.83	3.25	−82.8	−84.0	−84.6	172.1	N	24.9	21.7
4-3, 99-101	28.30	2.49	2.51	−77.8	−80.1	−82.3	165.3	N	18.2	18.2
4-3, 124-126	28.55	4.37	4.64	−69.9	−81.5	−80.7	245.5	N	21.2	19.6
4-3, 144-146	28.75	1.49	1.76	−38.3	−57.2	−60.0	288.4	N	25.3	20.4
4-4, 24-26	29.05	3.56	3.76	−81.5	−82.5	−83.1	214.3	N	29.2	28.0
4-4, 49-51	29.30	4.80	5.31	−71.7	−71.2	−71.5	253.4	N	30.7	27.9
4-4, 74-76	29.55	7.77	7.98	−71.6	−76.2	−76.8	255.8	N	27.5	26.9
4-4, 99-101	29.80	5.17	5.81	−74.2	−70.5	−71.2	277.5	N	25.6	22.6
4-4, 124-126	30.05	5.10	5.21	−62.3	−66.4	−67.3	225.2	N	22.1	21.6
4-4, 144-146	30.25	3.42	3.69	−54.1	−61.4	−61.9	324.6	N	30.5	28.7
4-5, 24-26	30.55	2.28	2.80	−64.8	−61.4	−71.6	223.2	N	29.5	25.1
4-5, 49-51	30.80	3.55	3.79	−70.8	−69.9	−70.2	297.1	N	32.4	30.8
4-5, 74-76	31.05	1.73	2.08	−44.4	−72.3	−80.3	203.3	N	12.3	9.9
4-5, 99-101	31.30	5.69	8.28	−22.0	−71.8	−72.7	269.8	N	4.3	5.0
4-5, 124-126	31.55	1.33	1.46	−43.6	−57.4	−63.8	266.4	N	25.3	22.6
4-5, 144-146	31.75	2.89	2.97	−64.5	−65.6	−65.5	291.3	N	19.0	18.2
4-6, 24-26	32.05	2.65	2.68	−56.9	−53.8	−57.1	279.1	N	13.3	13.5
4-6, 49-51	32.30	1.51	1.58	−71.8	−74.3	−75.4	306.2	N	18.4	18.4
4-6, 74-76	32.55	0.96	1.38	−35.8	−60.0	−59.4	294.3	N	15.2	9.6
4-6, 99-101	32.80	2.43	2.50	−70.0	−56.8	−60.3	322.5	N	4.6	4.6
4-6, 124-126	33.05	0.81	0.98	−35.2	−42.7	−41.4	326.6	N	5.0	7.3
4-6, 144-146	33.25	0.71	0.94	−36.7	−31.8	−36.1	235.7	N	10.1	8.3
4-7, 24-26	33.55	0.29	0.38	−14.5	−26.3	−26.3	258.7	N	9.2	10.8
5-2, 24-26	35.55	0.76	1.65	−52.1	+60.2	+76.6	268.0	R	4.9	6.5
5-2, 49-51	35.80	0.25	0.55	−14.6	+70.1	+66.5	234.1	R	4.7	9.0
5-2, 74-76	36.05	0.98	1.21	−20.1	+44.1	+56.0	292.7	R	4.7	5.2
5-2, 99-101	36.30	0.77	1.04	−3.1	+49.0	+68.8	336.9	R	8.1	6.0
5-2, 124-126	36.55	0.67	1.27	−27.5	+47.9	+64.0	265.7	R	4.6	8.1
5-2, 146-148	36.77	0.40	0.66	−2.9	+4.7	no	no		3.4	4.5
5-3, 24-26	37.05	0.29	0.97	+20.6	+76.0	+76.4	284.4	R	35.3	13.6
5-3, 49-51	37.30	0.34	0.46	−10.8	+22.0	+61.3	288.8	R	14.3	13.4
5-3, 74-76	37.55	0.61	0.68	−23.2	−11.4	no	no		14.1	12.8
5-3, 99-101	37.80	0.79	0.86	−38.4	−38.8	−37.9	321.7	N	13.8	10.5
5-3, 124-126	38.05	0.28	0.65	+4.0	+64.2	+69.1	112.0	R	28.8	6.2
5-3, 146-148	38.27	0.16	0.58	−42.5	+13.2	+21.0	215.8	R	46.5	8.8
5-4, 24-26	38.55	0.33	0.64	−15.7	+38.8	+36.7	214.3	R	27.1	16.8
5-4, 49-51	38.80	0.40	0.77	+40.2	+79.4	+73.6	253.5	R	33.4	14.2

Appendix A (continued).

Core, section, interval (cm)	Depth (mbsf)	J NRM (mA/m)	Js NRM (mA/m)	Incl. NRM (deg)	Incl. 20 mT (deg)	Incl. stable (deg)	Decl. stable (deg)	Pol.	MDF (mT)	MDFs (mT)
Hole 689B (Cont.)										
5-4, 74-76	39.05	0.34	0.59	−36.5	+51.0	+52.4	242.8	R	4.9	8.1
5-4, 99-101	39.30	0.73	1.17	−.1	+56.4	+71.4	252.6	R	19.4	8.8
5-4, 124-126	39.55	0.60	1.44	−37.1	+37.3	+57.7	328.1	R	30.4	10.8
5-4, 146-148	39.77	0.33	0.67	−49.7	−14.4	no	no		25.4	12.3
5-5, 24-26	40.05	0.34	1.04	+40.5	+80.3	+79.7	220.8	R	43.2	15.7
5-5, 49-51	40.30	0.54	0.74	+15.0	+52.4	+53.8	151.1	R	25.0	16.1
5-5, 74-76	40.55	0.14	0.71	−4.3	+68.4	+69.3	236.6	R	38.5	9.4
5-5, 99-101	40.80	0.27	0.66	+8.1	+64.9	+65.4	139.2	R	30.3	10.6
5-5, 124-126	41.05	0.59	1.16	+62.7	+83.4	+81.6	165.3	R	38.9	24.7
5-5, 146-148	41.27	1.36	1.85	+28.1	+51.5	+59.2	227.2	R	28.6	21.2
5-6, 24-26	41.55	0.75	1.23	+10.5	+55.3	+59.5	154.5	R	28.9	12.9
5-6, 49-51	41.80	0.69	0.99	+3.0	+38.2	+53.2	231.3	R	24.8	14.5
5-6, 74-76	42.05	0.29	0.69	+6.9	+58.6	+66.1	180.6	R	37.6	16.0
5-6, 99-101	42.30	1.54	1.86	−53.5	−32.8	+40.5	284.8	R	20.6	19.1
5-6, 124-126	42.55	1.02	1.37	+7.4	+27.2	+32.4	241.8	R	28.8	22.5
5-6, 146-148	42.77	0.71	1.15	+37.4	+55.5	+66.5	245.3	R	34.0	25.1
5-7, 19-21	43.00	0.25	0.92	+7.2	+48.5	+53.0	236.4	R	46.0	21.5
6-1, 24-26	43.55	4.66	5.21	+4.4	+20.6	+21.1	323.9	R	15.1	15.2
6-1, 50-52	43.81	0.69	0.96	+32.8	+50.3	+65.0	340.8	R	33.8	28.0
6-1, 74-76	44.05	2.11	2.59	−70.1	+15.0	+38.5	23.8	R	2.8	3.3
6-1, 99-101	44.30				+15.6	+40.5	309.3	R	38.5	21.6
6-1, 124-126	44.55	1.77	3.68	−40.8	+28.4	+67.4	7.2	R	29.6	12.4
6-1, 146-148	44.77	3.99	4.28	+64.0	+59.2	+63.3	323.6	R	11.2	6.8
6-2, 24-26	45.05	2.05	3.03	−49.5	+33.4	+50.8	59.0	R	3.8	4.8
6-2, 49-51	45.30	0.71	3.29	+47.7	+62.6	+64.4	328.0	R	62.5	18.3
6-2, 74-76	45.55	2.72	5.72	+10.9	+57.5	+58.4	342.8	R	25.2	4.4
6-2, 99-101	45.80	1.55	3.51	−31.8	+42.9	+50.2	346.7	R	33.9	9.7
6-2, 124-126	46.05	8.05	8.77	−52.1	−63.3	−67.9	164.7	N	5.3	5.4
6-2, 146-148	46.27	5.28	6.30	−60.4	−15.3	−69.5	345.4	N	4.2	4.3
6-3, 24-26	46.55	1.96	5.05	−49.0	+59.7	+62.4	21.6	R	29.7	7.3
6-3, 49-51	46.80	3.36	3.81	−72.3	−64.2	−69.5	283.9	N	13.4	14.6
6-3, 74-76	47.05	6.82	7.28	−75.8	−64.2	−70.9	294.2	N	9.5	9.1
6-3, 99-101	47.30	1.98	3.76	−44.9	+48.9	+56.3	339.6	R	4.5	6.2
6-3, 124-126	47.55	2.52	4.19	−65.0	+38.8	+52.3	324.0	R	4.5	5.2
6-3, 146-148	47.77	150.41	152.40	−37.4	+33.6	+63.9	330.9	R	6.7	6.8
6-4, 24-26	48.05	5.22	9.58	−19.9	+43.6	+47.3	327.2	R	3.5	4.0
6-4, 49-51	48.30	1.94	3.00	−2.5	+42.0	+70.7	346.6	R	22.5	9.4
6-4, 74-76	48.55	2.52	2.87	−43.3	+27.6	+44.3	248.4	R	3.2	3.6
6-4, 99-101	48.80	26.03	26.34	−48.9	−47.4	−49.3	277.8	N	4.2	4.2
6-5, 24-26	49.55	1.17	1.92	−12.7	+40.2	+60.5	159.8	R	2.9	3.8
6-5, 49-51	49.80	2.70	3.08	−70.7	−65.3	−66.1	241.6	N	9.2	9.9
6-5, 78-80	50.09	8.17	8.47	−29.6	−58.2	−61.1	275.7	N	5.4	5.5
6-5, 99-101	50.30	6.36	7.49	−54.4	−63.5	−64.3	269.4	N	5.4	4.7
6-5, 124-126	50.55	18.22	24.33	+17.1	−73.3	−73.0	248.9	N	3.1	3.7
6-5, 146-148	50.77	8.46	8.76	−63.9	−68.3	−71.1	256.7	N	11.4	11.1
6-6, 24-26	51.05	65.87	67.06	−15.9	+52.5	+54.8	320.2	R	5.1	5.2
6-6, 49-51	51.30	11.47	12.79	+26.7	+58.6	+55.9	326.5	R	5.0	5.5
6-6, 74-76	51.55	0.30	1.41	+55.9	+37.7	+39.1	271.0	R		12.4
6-6, 99-101	51.80	13.45	13.96	+59.5	+63.8	+73.7	308.9	R	4.7	4.8
6-6, 124-126	52.05	29.14	29.58	−44.1	−63.1	−65.8	223.9	N	6.5	6.5
6-6, 146-148	52.27	11.94	12.39	−19.8	−43.6	−45.7	254.3	N	5.9	6.1
6-7, 24-26	52.55	0.44	0.61	+21.5	+20.0	+47.6	165.1	R	18.5	19.2
7-1, 24-26	53.15	2.98	3.05	−68.2	−71.2	−71.1	292.8	N	18.3	18.0
7-1, 49-51	53.40	2.84	3.22	−51.4	−71.8	−70.9	354.2	N	13.3	10.7
7-1, 74-76	53.65	2.37	2.46	−76.3	−81.5	−80.0	20.3	N	10.3	10.1
7-1, 99-101	53.90	2.51	3.55	−43.7	−77.4	−77.6	337.9	N	7.0	8.9
7-1, 124-126	54.15	1.73	1.84	−69.8	−61.5	−65.0	290.7	N	7.5	7.9
7-1, 146-148	54.37	0.81	1.21	−78.1	−52.8	−59.7	286.3	N	14.4	15.7
7-2, 24-26	54.65	0.21	1.32	−77.6	−53.0	−54.1	209.7	N	9.0	37.6
7-2, 49-51	54.90	1.00	1.11	−67.5	−66.7	−65.2	108.0	N	22.6	21.7
7-2, 74-76	55.15	4.82	4.96	−75.1	−83.6	−84.0	354.5	N	13.2	12.6
7-2, 99-101	55.40	2.26	3.15	−31.5	+70.1	+75.1	195.0	R	3.1	4.1
7-2, 124-126	55.65	0.72	0.98	−66.9	+41.3	+45.7	310.1	R	5.0	7.4
7-2, 146-148	55.87	2.36	4.80	−76.3	+64.4	+59.4	234.9	R	3.5	4.4
7-3, 24-26	56.15	0.51	0.64	+48.7	+57.8	+58.0	324.4	R	31.6	25.3
7-3, 49-51	56.40	2.55	4.40	−48.9	+53.1	+48.8	241.3	R	3.3	4.4
7-3, 74-76	56.65	0.43	1.42	−79.0	−15.8	−26.5	249.8	N	9.4	14.6
7-3, 99-101	56.90	2.57	3.05	−78.2	−54.8	−64.8	289.9	N	5.6	6.6
7-3, 124-126	57.15	0.51	1.17	+25.4	−6.3	−66.2	240.2	N	26.0	18.0
7-4, 24-26	57.65	0.67	1.49	+4.4	+55.9	+54.4	259.0	R	17.7	18.7
7-4, 49-51	57.90	0.79	2.01	+2.7	+56.8	+63.7	247.8	R	40.3	16.9
7-4, 74-76	58.15	2.04	3.51	+38.9	+72.0	+70.3	287.6	R	32.0	21.6
7-4, 99-101	58.40	0.35	0.93	−14.2	+73.4	+82.2	296.2	R	37.1	9.9
7-4, 124-126	58.65	2.23	2.35	+63.7	+61.5	+61.7	288.3	R	24.4	22.7
7-4, 144-146	58.85	1.97	2.01	−65.2	−66.7	−68.9	256.8	N	27.4	27.5
7-5, 24-26	59.15	4.61	4.70	−80.8	−88.0	−87.9	263.7	N	15.3	14.8

Appendix A (continued).

Core, section, interval (cm)	Depth (mbsf)	J NRM (mA/m)	Js NRM (mA/m)	Incl. NRM (deg)	Incl. 20 mT (deg)	Incl. stable (deg)	Decl. stable (deg)	Pol.	MDF (mT)	MDFs (mT)
Hole 689B (Cont.)										
7-5, 49-51	59.40	1.36	1.54	−86.8	−70.0	−74.3	244.8	N	17.3	15.1
7-5, 74-76	59.65	0.67	1.01	−12.1	+9.3	no	no		15.4	11.5
7-5, 99-101	59.90	0.45	0.97	−29.8	+29.6	+41.5	253.7	R	32.7	15.6
7-5, 124-126	60.15	0.37	1.06	−54.8	−39.6	−50.8	276.7	N	30.7	9.5
7-5, 145-147	60.36	2.54	3.41	−5.1	+13.3	no	no		3.4	3.3
7-6, 24-26	60.65	1.87	3.10	+31.2	+55.2	+60.2	262.6	R	36.9	25.5
7-6, 49-51	60.90	1.92	3.03	+13.9	+52.8	+55.2	281.2	R	35.1	21.2
7-6, 74-76	61.15	1.27	2.54	+43.3	+61.3	+62.5	252.1	R	42.1	27.1
7-6, 99-101	61.40	1.28	3.07	−6.4	+48.0	+50.7	253.7	R	40.1	19.4
7-6, 124-126	61.65	0.62	0.77	+32.2	+37.9	+57.0	262.4	R	31.9	29.9
7-6, 146-148	61.87	2.50	2.70	−61.7	−51.4	−61.1	288.7	N	20.9	22.0
7-7, 24-26	62.15	3.73	3.77	−50.7	−52.1	−52.0	322.9	N	27.3	27.2
8-1, 18-20	62.69	3.09	3.57	−78.2	−66.1	−68.3	27.6	N	10.0	8.1
8-1, 49-51	63.00	4.10	4.34	−73.7	−82.3	−80.7	6.7	N	20.1	18.7
8-1, 74-76	63.25	4.55	4.75	−69.3	−73.5	−76.6	354.7	N	10.4	9.6
8-1, 99-101	63.50	0.85	1.00	−74.5	−75.6	−75.0	20.7	N	25.9	21.5
8-1, 124-126	63.75	3.98	4.06	−84.0	−78.8	−80.4	19.1	N	17.1	16.9
8-1, 146-148	63.97	2.61	2.73	−66.6	−65.2	−64.9	332.2	N	18.4	17.7
8-2, 24-26	64.25	2.12	2.94	−65.2	−77.6	−81.7	13.2	N	27.8	19.5
8-2, 49-51	64.50	3.07	3.19	−75.7	−74.4	−73.4	3.3	N	24.1	23.6
8-2, 74-76	64.75	3.92	4.03	−72.0	−76.2	−76.2	355.5	N	21.3	20.7
8-2, 99-101	65.00	4.96	5.73	−60.3	−71.8	−74.1	9.2	N	13.3	12.6
8-2, 124-126	65.25	6.69	6.99	−74.2	−80.3	−78.8	14.0	N	18.6	19.1
8-2, 146-148	65.47	6.62	6.89	−84.2	−74.2	−73.8	6.0	N	12.7	12.2
8-3, 24-26	65.75	6.19	6.76	−79.1	−80.6	−81.9	40.3	N	16.4	14.3
8-3, 49-51	66.00	5.81	6.08	−76.0	−69.8	−70.3	346.1	N	17.0	16.2
8-3, 74-76	66.25	3.13	3.30	−83.6	−75.7	−76.6	18.9	N	20.0	19.4
8-3, 99-101	66.50	2.15	2.52	−77.2	−71.0	−71.9	12.8	N	9.6	9.2
8-3, 124-126	66.75	4.05	4.98	−29.2	−68.4	−70.2	328.1	N	3.5	3.7
8-3, 146-148	66.97	0.62	2.38	−28.8	+84.0	+83.6	51.0	R	37.1	17.5
8-4, 24-26	67.25	3.74	3.90	−87.7	−84.0	−85.4	37.1	N	9.5	9.4
8-4, 49-51	67.50	2.52	2.83	−74.0	−66.4	−71.3	18.9	N	9.8	12.3
8-4, 74-76	67.75	4.02	4.18	−78.0	−80.4	−81.3	50.5	N	6.8	6.7
8-4, 99-101	68.00	1.65	2.87	−81.5	+84.1	+73.4	24.3	R	4.3	8.4
8-4, 124-126	68.25	1.56	2.85	−42.3	+83.6	+85.7	167.1	R	2.8	4.8
8-4, 146-148	68.47	0.54	1.77	+50.8	+86.2	+82.0	67.0	R	44.9	20.5
8-5, 24-26	68.75	2.28	2.47	−77.8	−70.4	−80.7	26.0	N	4.2	4.3
8-5, 49-51	69.00	0.52	1.85	+67.6	+80.6	+87.6	338.9	R	44.3	22.2
8-5, 74-76	69.25	0.94	2.80	−23.5	+81.4	+83.4	202.9	R	38.7	8.2
8-5, 99-101	69.50	2.29	2.57	−58.7	−56.9	−58.3	7.5	N	4.4	4.8
8-5, 124-126	69.75	1.45	1.64	−75.0	−77.9	−76.2	3.0	N	14.5	11.9
8-5, 146-148	69.97	1.28	1.46	−86.2	−68.9	−74.2	357.0	N	8.7	9.3
8-6, 24-26	70.25	0.31	0.50	−65.9	+34.3	+72.4	9.0	R	5.8	8.6
8-6, 49-51	70.50	0.81	0.96	−87.8	−76.3	−81.2	32.7	N	9.1	10.2
8-6, 74-76	70.75	0.48	0.51	−77.1	−77.4	−77.6	14.1	N	21.4	20.4
8-6, 99-101	71.00	1.59	1.64	−70.6	−73.1	−71.8	356.6	N	16.1	15.7
8-6, 124-126	71.25	1.84	1.91	−62.9	−78.1	−76.3	2.5	N	11.8	11.1
8-6, 146-148	71.47	2.86	3.10	−61.7	−73.7	−73.2	2.4	N	15.9	14.3
8-7, 17-19	71.68	3.63	3.91	−75.8	−79.7	−78.5	53.4	N	16.1	14.1
9-1, 24-26	72.35	3.35	3.46	−74.5	−86.0	−85.2	213.8	N	9.3	9.1
9-1, 49-51	72.60	2.66	2.76	−79.5	−84.2	−84.6	145.1	N	19.0	18.2
9-1, 74-76	72.85	2.48	2.83	−57.3	−81.7	−76.4	158.9	N	11.8	9.6
9-1, 99-101	73.10	0.64	0.86	−55.2	−79.4	−78.7	82.7	N	9.4	9.1
9-1, 124-126	73.35	1.70	2.79	−56.7	−80.3	−79.4	114.3	N	26.1	12.2
9-2, 24-26	73.85	1.12	1.27	−73.9	−80.2	−72.7	143.1	N	16.2	14.5
9-2, 49-51	74.10	3.01	3.36	−73.5	−85.1	−88.2	138.5	N	4.1	4.4
9-2, 74-76	74.35	1.33	1.49	−63.6	−78.1	−77.2	36.9	N	9.3	8.8
9-2, 105-107	74.66	2.62	2.83	−67.4	−85.6	−83.4	48.9	N	6.1	6.0
9-2, 124-126	74.85	1.74	1.95	−72.7	−80.1	−79.6	77.8	N	21.9	19.3
9-2, 146-148	75.07	3.75	4.35	−82.9	−82.2	−83.6	72.6	N	5.5	7.4
9-3, 24-26	75.35	2.30	2.34	−75.2	−77.9	−76.9	68.0	N	9.5	9.6
9-3, 49-51	75.60	3.79	4.95	+48.1	−87.3	−87.0	58.6	N	3.0	3.4
9-3, 74-76	75.85	0.64	1.00	+24.3	−20.1	−32.5	314.9	N	3.3	4.3
9-3, 99-101	76.10	1.21	1.73	−71.4	+36.3	+75.1	206.2	R	3.4	4.9
9-3, 124-126	76.35	0.45	0.94	−22.8	+41.2	+34.1	325.1	R	31.8	10.0
9-3, 146-148	76.57	1.19	1.85	+56.4	+86.0	+86.5	240.7	R	35.1	23.4
9-4, 24-26	76.85	1.17	2.64	−61.3	+67.7	+64.3	306.5	R	3.4	6.5
9-4, 49-51	77.10	2.70	2.78	+81.2	+80.5	+80.3	264.4	R	17.1	17.6
9-4, 74-76	77.35	0.48	1.64	+34.7	+72.2	+69.5	309.2	R	43.6	19.5
9-4, 99-101	77.60	0.68	1.36	+27.0	+39.4	+40.0	242.7	R	3.7	4.8
9-5, 24-26	78.35	0.24	1.69	+16.9	+78.6	+74.7	321.9	R		13.9
9-5, 49-51	78.60	1.47	2.79	+60.8	+82.0	+84.0	260.1	R	36.6	22.4
9-5, 74-76	78.85	0.58	1.59	+33.9	+78.4	+78.3	318.9	R	38.8	19.6
9-5, 99-101	79.10	3.92	5.45	−74.1	+68.9	+69.7	259.6	R	3.4	4.7
9-5, 124-126	79.35	0.91	1.43	−64.3	+54.9	+68.0	281.1	R	3.1	4.7
9-5, 146-148	79.57	1.64	2.39	−53.5	−73.5	−72.8	126.9	N	17.1	19.6

Appendix A (continued).

Core, section, interval (cm)	Depth (mbsf)	J NRM (mA/m)	Js NRM (mA/m)	Incl. NRM (deg)	Incl. 20 mT (deg)	Incl. stable (deg)	Decl. stable (deg)	Pol.	MDF (mT)	MDFs (mT)
Hole 689B (Cont.)										
9-6, 16–18	79.77	3.23	3.36	−83.4	−81.7	−70.9	10.6	N	6.1	6.5
9-6, 49–51	80.10	3.50	3.75	−66.3	−76.0	−80.7	69.1	N	4.2	4.4
9-6, 74–76	80.35	1.66	1.74	−81.2	−85.3	−85.1	19.6	N	8.7	9.2
10-1, 49–51	82.20	15.87	16.29	−69.9	−79.9	−78.6	274.3	N	5.9	5.7
10-1, 74–76	82.45	3.28	3.68	−66.6	−84.4	−87.5	284.6	N	8.0	6.7
10-1, 99–101	82.70	5.87	6.24	−74.7	−79.7	−79.0	286.2	N	18.6	17.2
10-1, 124–126	82.95	3.78	3.85	−78.5	−83.0	−84.9	290.9	N	15.6	15.2
10-1, 146–148	83.17	3.84	3.96	−68.4	−75.7	−76.2	290.4	N	14.5	14.2
10-2, 19–21	83.40	5.23	5.29	−82.8	−79.4	−81.6	296.7	N	15.2	15.2
10-2, 49–51	83.70	5.96	6.16	−73.3	−74.4	−73.5	289.3	N	11.5	10.7
10-2, 74–76	83.95	5.38	5.40	−75.4	−76.6	−77.7	275.9	N	13.6	13.5
10-2, 99–101	84.20	6.95	7.18	−80.6	−81.0	−84.2	267.3	N	6.1	6.0
10-2, 124–126	84.45	3.02	3.15	−71.9	−82.0	−82.5	259.0	N	19.2	18.3
10-2, 146–148	84.67	1.59	1.68	−70.9	−71.2	−72.3	313.6	N	14.7	14.8
10-3, 19–21	84.90	2.36	2.49	−37.3	+1.4	−46.3	219.7	N	3.3	3.3
10-3, 49–51	85.20	1.46	2.49	−31.4	+83.5	+82.6	242.5	R	3.1	5.2
10-3, 74–76	85.45	2.00	2.32	−79.5	+27.6	+57.5	265.6	R	3.8	4.4
10-3, 99–101	85.70	1.10	2.45	−49.3	+82.5	+82.7	96.4	R	3.8	4.8
10-3, 124–126	85.95	1.57	2.35	+9.7	+85.9	+84.2	172.8	R	2.8	4.2
10-3, 146–148	86.17	0.53	2.39	−9.5	+85.3	+86.0	112.2	R	49.2	8.4
10-4, 19–21	86.40	1.20	2.50	−61.3	+86.4	+82.4	168.6	R	3.5	4.3
10-4, 49–51	86.70	0.39	1.72	−44.3	+80.5	+81.7	261.2	R	3.0	30.2
10-4, 74–76	86.95	0.72	2.27	−76.1	+81.7	+84.1	36.8	R	33.1	5.9
10-4, 99–101	87.20	0.51	2.92	+42.1	+83.7	+87.1	58.7	R		15.9
10-4, 124–126	87.45	0.85	2.21	−21.9	+86.3	+84.5	331.7	R	31.3	5.5
10-4, 146–148	87.67	0.83	1.79	+64.9	+81.8	+80.3	94.6	R	34.9	23.8
10-5, 19–21	87.90	1.64	4.37	+6.5	+80.8	+82.4	119.9	R	35.5	8.7
10-5, 49–51	88.20	1.05	3.13	+44.4	+87.1	+87.4	110.9	R	39.1	25.8
10-5, 74–76	88.45	1.28	3.60	+61.0	+81.8	+83.9	89.4	R	43.9	20.9
10-5, 99–101	88.70	0.66	1.31	+33.3	+86.9	+85.0	152.1	R	34.4	14.1
10-5, 124–126	88.95	0.89	2.49	−39.9	+82.9	+80.9	64.0	R	35.4	4.8
10-5, 146–148	89.17	0.49	1.68	−22.8	+79.3	+83.3	315.3	R	39.2	6.4
10-6, 19–21	89.40	2.14	3.64	−76.1	+74.1	+82.3	321.3	R	3.0	4.9
10-6, 49–51	89.70	3.21	3.90	+54.8	+78.4	+76.7	175.0	R	3.9	4.4
10-6, 74–76	89.95	2.33	2.59	−75.8	−60.4	−66.3	279.8	N	4.5	4.8
10-6, 99–101	90.20	2.22	4.04	−40.9	+63.7	+64.9	257.1	R	3.3	7.1
11-1, 50–52	91.81	4.98	5.07	−69.9	−78.8	−80.6	13.7	N	6.7	6.6
11-1, 74–76	92.05	0.94	3.45	−80.5	+83.9	+77.9	198.5	R	39.7	5.0
11-1, 100–102	92.31	1.34	2.70	−10.4	+74.6	+70.6	190.4	R	24.3	6.8
11-1, 125–127	92.56	1.38	3.17	+29.8	+81.0	+79.6	185.3	R	34.3	9.4
11-1, 145–147	92.76	1.09	3.09	+26.2	+78.6	+78.3	231.2	R	33.2	21.1
11-2, 25–27	93.06	0.81	4.51	+52.8	+78.9	+76.4	231.0	R	47.7	17.5
11-2, 50–52	93.31	2.74	7.47	+74.2	+79.3	+79.6	210.6	R	40.6	21.4
11-2, 76–78	93.57	10.95	13.05	+0.6	+81.4	+77.5	203.7	R	3.7	4.1
11-2, 101–103	93.82	2.40	2.87	+84.3	+84.1	+83.5	220.9	R	33.0	29.4
11-2, 126–128	94.07	1.58	4.37	+38.4	+81.2	+78.6	200.2	R	38.7	17.2
11-2, 146–148	94.27	0.77	3.53	−5.3	+83.7	+81.4	233.2	R	43.2	7.9
11-3, 24–26	94.55	71.30	71.42	+71.7	+75.9	+72.5	210.7	R	6.5	6.5
11-3, 51–53	94.82	0.43	1.50	−21.8	+70.9	+72.5	168.5	R	3.4	14.7
11-3, 75–77	95.06	2.72	3.73	+73.7	+81.3	+76.5	227.3	R	3.1	3.8
11-3, 100–102	95.31	2.39	4.10	−56.9	+61.4	+61.8	227.2	R	3.4	5.3
11-3, 126–128	95.57	2.74	3.83	+19.7	+78.1	+78.7	185.0	R	3.8	4.1
11-3, 147–149	98.78	1.07	3.76	−24.7	+84.6	+82.5	249.1	R	38.6	6.4
11-4, 25–27	96.06	0.82	2.06	+37.4	+74.1	+70.8	224.3	R	42.1	20.5
11-4, 51–53	96.32	0.67	2.48	−29.1	+73.6	+73.2	208.4	R	39.4	7.8
11-4, 75–77	96.56	0.75	3.48	+51.8	+74.7	+73.6	205.4	R		18.5
11-4, 101–103	96.82	0.73	1.64	−58.3	+69.8	+63.8	214.5	R	3.5	6.1
11-4, 126–128	97.07	8.75	10.06	+32.3	+55.7	+56.1	255.2	R	3.2	3.7
11-4, 144–146	97.25	0.51	1.88	+30.7	+83.6	+80.4	217.8	R	44.9	16.6
11-5, 25–27	97.56	0.74	2.82	+25.3	+78.6	+75.0	239.5	R	45.4	13.2
11-5, 51–53	97.82	0.49	2.09	−17.3	+79.4	+77.9	239.1	R	45.5	8.2
11-5, 75–77	98.06	11.43	33.47	−71.7	+55.0	+61.2	274.8	R	13.9	10.6
11-5, 101–103	98.32	0.61	2.19	−34.4	+61.1	+61.8	227.9	R	39.6	6.8
11-5, 126–128	98.57	35.30	35.67	+48.5	+28.8	+44.6	294.9	R	6.0	6.0
11-6, 15–17	98.96	0.39	1.77	+2.5	+54.5	+58.6	336.0	R		18.9
12-1, 49–51	101.50	4.58	6.01	−69.4	−76.3	−79.6	79.6	N	10.6	9.4
12-1, 74–76	101.75	17.06	20.30	+16.0	−83.9	−84.3	73.8	N	3.7	4.2
12-1, 99–101	102.00	8.02	8.68	−71.4	−81.0	−81.3	228.1	N	4.5	4.8
12-1, 124–126	102.25	6.41	6.68	−71.7	−79.7	−80.1	40.0	N	6.5	6.3
12-1, 146–148	102.47	4.45	7.24	−43.0	−77.8	−78.7	334.6	N	15.9	6.0
12-2, 24–26	102.75	6.26	6.40	−77.4	−85.3	−84.4	77.2	N	6.5	6.3
12-2, 49–51	103.00	5.20	5.48	−72.0	−74.4	−74.9	101.9	N	7.8	7.1
12-2, 74–76	103.25	3.39	3.68	−87.7	−86.1	−83.6	357.8	N	5.5	6.5
12-2, 99–101	103.50	1.06	2.83	−23.5	+68.6	+66.0	330.4	R	34.7	8.5
12-2, 124–126	103.75	3.13	4.93	−12.2	+23.6	+37.1	315.2	R	3.6	4.1
12-2, 146–148	103.97	3.16	4.38	−58.3	−7.9	no	no		4.3	5.3

Appendix A (continued).

Core, section, interval (cm)	Depth (mbsf)	J NRM (mA/m)	Js NRM (mA/m)	Incl. NRM (deg)	Incl. 20 mT (deg)	Incl. stable (deg)	Decl. stable (deg)	Pol.	MDF (mT)	MDFs (mT)
Hole 689B (Cont.)										
12-3, 24–26	104.25	2.95	4.61	−83.2	+46.2	+46.7	282.7	R	3.2	4.7
12-3, 49–51	104.50	2.84	3.10	−84.5	−84.5	−85.1	19.9	N	3.8	4.1
12-3, 74–76	104.75	4.17	4.46	−61.8	−80.2	−80.2	82.5	N	6.0	5.8
12-3, 99–101	105.00	3.75	4.01	−70.0	−83.4	−85.8	351.1	N	5.9	5.5
12-3, 124–126	105.25	2.66	2.97	−61.7	−75.4	−74.0	58.2	N	6.9	6.3
12-3, 146–148	105.47	2.58	3.08	−67.3	−78.9	−81.9	14.4	N	9.2	7.7
12-4, 24–26	105.75	6.17	6.28	−69.9	−77.2	−75.8	108.1	N	6.4	6.3
12-4, 49–51	106.00	2.67	2.84	−68.2	−82.2	−79.0	98.5	N	5.0	4.9
12-4, 74–76	106.25	2.97	3.08	−68.2	−77.5	−77.8	111.3	N	9.4	8.9
12-4, 99–101	106.50	2.21	2.32	−68.4	−55.4	−78.4	191.2	N	3.5	3.6
12-5, 24–26	107.25	1.53	3.86	−39.9	+81.8	+83.6	308.2	R	4.7	4.8
12-5, 49–51	107.50	1.06	3.13	−41.1	+74.6	+80.1	288.1	R	34.9	5.9
12-5, 74–76	107.75	3.08	5.98	−62.6	+81.1	+81.8	307.4	R	2.9	4.4
12-5, 99–101	108.00	2.33	4.60	−51.4	+78.3	+80.7	319.0	R	3.1	4.4
12-5, 125–127	108.26	5.10	8.18	−63.2	+76.8	+76.7	314.6	R	2.8	3.9
12-5, 146–148	108.47	4.64	7.99	−54.4	+79.2	+77.4	312.0	R	3.0	4.1
12-6, 24–26	108.75	3.79	6.35	−61.9	+77.3	+76.2	337.0	R	2.6	4.2
12-6, 49–51	109.00	2.61	7.05	−53.7	+74.2	+74.4	347.0	R	4.4	4.9
12-6, 74–76	109.25	2.27	5.97	+19.1	+72.7	+76.4	307.1	R	36.9	8.6
12-6, 99–101	109.50	2.62	6.66	+2.6	+74.8	+73.8	329.0	R	32.2	6.4
12-6, 125–127	109.76	2.90	6.06	−72.2	+78.6	+81.0	294.1	R	3.4	4.2
12-6, 145–147	109.96	3.01	4.62	−45.5	+67.1	+71.5	277.3	R	2.9	4.1
12-7, 24–26	110.25	2.43	4.22	−78.8	+72.7	+70.9	274.2	R	2.8	4.3
12-C, 11–13	110.74	1.23	2.91	−2.6	+72.1	+74.9	271.8	R	33.0	7.1
13-1, 24–26	110.85	3.75	6.50	−8.5	+76.9	+81.9	312.6		3.8	4.0
13-1, 49–51	111.10	0.86	4.10	+26.3	+79.5	+77.8	270.5	R	46.1	14.5
13-1, 74–76	111.35	2.95	3.42	+68.3	+78.4	+78.9	268.4	R	29.9	26.6
13-1, 99–101	111.60	3.49	4.47	+76.6	+79.4	+80.2	265.6	R	33.7	28.4
13-1, 124–126	111.85	3.57	5.17	+84.4	+80.6	+80.5	270.2	R	35.4	27.6
13-1, 145–147	112.06	0.92	5.07	+56.5	+79.8	+79.4	285.4	R	49.8	17.0
13-2, 24–26	112.35	1.29	3.40	+52.1	+85.9	+85.8	252.3	R	39.1	20.0
13-2, 49–51	112.60	0.59	2.89	+74.7	+80.2	+77.2	252.8	R	49.4	20.2
13-2, 74–76	112.85	1.56	4.04	+75.7	+81.9	+77.9	257.9	R	41.4	23.3
13-2, 99–101	113.10	5.26	7.67	+28.5	+79.8	+79.8	258.6	R	20.3	6.4
13-2, 124–126	113.35	16.43	17.55	+37.9	+84.5	+83.8	252.7	R	3.9	4.1
13-2, 145–147	113.56	2.39	4.63	−40.2	+73.5	+72.5	265.4	R	2.9	4.8
13-3, 24–26	113.85	1.29	3.44	−39.3	+77.6	+77.1	275.1	R	4.3	6.0
13-3, 49–51	114.10	0.58	3.04	+66.8	+79.7	+78.9	273.7	R		20.0
13-3, 74–76	114.35	3.62	3.72	+78.0	+87.3	+89.5	236.1	R	4.6	4.6
13-3, 99–101	114.60	0.96	2.71	+55.4	+82.2	+82.0	277.3	R	41.4	19.6
13-3, 124–126	114.85	0.47	3.68	+71.1	+85.4	+84.9	279.5	R		17.9
13-3, 145–147	115.06	0.36	3.19	+60.6	+77.1	+77.7	272.7	R		18.5
13-4, 24–26	115.35	0.64	3.04	−41.2	+80.5	+78.7	274.2	R	48.3	7.6
13-4, 49–51	115.60	0.57	2.25	−34.4	+77.2	+77.9	295.0	R	43.5	8.6
13-4, 74–76	115.85	1.19	1.43	+59.6	+77.8	+83.3	252.7	R	3.6	4.2
13-4, 99–101	116.10	2.55	3.98	+64.4	+77.4	+78.8	270.2	R	34.3	24.5
13-4, 124–126	116.35	0.86	2.67	+67.2	+79.4	+78.8	245.3	R	43.9	21.5
13-4, 145–147	116.56	14.78	15.05	+63.0	+82.3	+84.0	321.6	R	4.2	4.3
13-5, 24–26	116.85	2.44	2.51	−73.6	−84.4	−81.6	160.9	N	7.1	7.1
13-5, 49–51	117.10	2.27	2.49	−76.3	−36.8	−86.3	207.3	N	4.3	4.5
13-5, 74–76	117.35	2.88	2.97	−69.5	−78.4	−76.9	83.9	N	8.5	8.2
13-5, 99–101	117.60	3.22	3.25	−75.7	−85.2	−81.4	88.4	N	7.1	7.1
13-5, 124–126	117.85	3.68	3.70	−80.1	−78.8	−80.0	85.9	N	7.8	7.8
13-5, 141–143	118.02	1.90	2.31	−63.7	−82.8	−83.5	304.2	N	13.4	10.1
13-6, 24–26	118.35	5.47	5.68	−79.7	−76.7	−77.2	77.7	N	11.7	10.2
13-6, 49–51	118.60	6.39	6.49	−76.3	−79.5	−78.0	63.5	N	13.0	12.7
13-6, 76–78	118.87	3.57	3.75	−76.4	−76.3	−75.8	63.5	N	29.5	28.4
13-6, 98–100	119.09	2.94	3.05	−72.9	−71.1	−71.5	92.6	N	22.0	21.2
13-6, 127–129	119.38	1.59	1.65	−82.1	−84.1	−85.1	94.2	N	29.2	28.9
13-6, 143–145	119.54	0.26	0.28	−72.8	−71.1	−72.3	67.0	N	27.6	25.6
13-7, 24–26	119.85	0.27	0.42	+41.1	+76.0	+72.8	319.7	R	17.8	5.8
13-C, 24–26	120.48	1.74	2.95	−38.2	+74.8	+65.4	205.4	R	6.0	8.3
14-1, 49–51	120.70	3.71	4.31	+80.4	+81.1	+80.8	60.0	R	28.6	25.0
14-1, 74–76	120.95	0.52	3.04	−17.5	+77.9	+76.8	38.0	R		8.7
14-1, 99–101	121.20	1.41	5.10	−56.2	+83.1	+83.1	3.0	R	41.6	6.8
14-1, 124–126	121.45	0.82	4.50	+17.7	+81.2	+76.9	74.8	R		17.5
14-1, 146–148	121.67	0.47	3.35	+85.4	+79.8	+79.0	65.3	R		20.4
14-2, 24–26	121.95	0.49	3.45	+55.1	+81.6	+80.8	57.0	R		18.7
14-2, 49–51	122.20	0.81	2.59	+58.4	+81.6	+81.6	70.2	R	45.6	21.8
14-2, 76–78	122.47	1.34	3.91	+67.9	+80.8	+80.7	70.5	R	44.9	23.1
14-2, 99–101	122.70	0.93	4.32	+76.2	+81.8	+79.9	77.0	R		20.4
14-2, 124–126	122.95	0.53	3.34	−2.7	+82.8	+81.3	69.8	R		9.5
14-2, 146–148	123.17	1.06	4.19	−53.5	+86.6	+85.6	33.5	R	43.4	6.2
14-3, 24–26	123.45	0.95	4.42	+59.1	+82.1	+81.1	88.7	R		20.5
14-3, 49–51	123.70	2.46	4.26	+75.8	+85.2	+83.7	87.7	R	38.3	27.9
14-3, 76–78	123.97	1.90	3.56	−67.1	+84.5	+85.4	27.7	R	2.8	4.8

Appendix A (continued).

Core, section, interval (cm)	Depth (mbsf)	J NRM (mA/m)	Js NRM (mA/m)	Incl. NRM (deg)	Incl. 20 mT (deg)	Incl. stable (deg)	Decl. stable (deg)	Pol.	MDF (mT)	MDFs (mT)
Hole 689B (Cont.)										
14-3, 99-101	124.20	3.45	3.49	−83.9	−83.0	−84.2	265.7	N	10.5	10.6
14-3, 124-126	124.45	2.77	3.76	−69.6	−84.4	−86.6	252.6	N	17.5	10.0
14-3, 146-148	124.67	2.85	8.91	−83.9	−87.6	−85.8	93.9	N	9.1	18.1
14-4, 24-26	124.95	2.07	2.39	−76.6	−80.1	−76.3	230.9	N	4.7	5.5
14-4, 49-51	125.20	0.94	3.61	+10.2	+81.2	+78.0	117.1	R	45.5	10.3
14-4, 76-78	125.47	1.03	3.44	−34.1	+76.3	+71.7	127.9	R	41.2	7.4
14-4, 99-101	125.70	1.92	3.61	+77.7	+83.8	+84.9	69.2	R	39.1	26.3
14-4, 124-126	125.95	1.42	3.33	+71.9	+79.2	+80.3	94.6	R	38.9	23.9
14-4, 146-148	126.17	2.72	4.20	+85.5	+81.8	+82.3	87.6	R	37.6	29.0
14-5, 24-26	126.45	3.58	4.72	+81.6	+79.7	+80.0	108.7	R	36.6	31.0
14-5, 49-51	126.70	0.42	2.25	+28.0		+88.8	177.6	R	63.5	30.0
14-5, 74-76	126.95	2.17	3.70	+77.4	+81.0	+81.4	89.1	R	40.3	29.3
14-5, 99-101	127.20	0.93	3.49	+58.8	+87.9	+87.4	25.7	R	48.9	20.6
14-5, 124-126	127.45	2.89	4.69	+78.6	+80.6	+81.4	76.0	R	40.1	30.3
14-5, 146-148	127.67	3.38	4.38	+82.4	+84.2	+83.2	118.7	R	35.9	30.3
14-6, 24-26	127.95	0.31	2.54	+38.4	+76.1	+75.6	70.9	R		16.5
14-6, 49-51	128.20	0.34	1.33	−60.9	+88.5	+86.8	141.4	R	43.1	7.0
14-6, 74-76	128.45	4.02	4.11	−73.9	−74.4	−77.3	284.7	N	18.4	17.9
14-6, 99-101	128.70	2.46	2.54	−76.4	−76.4	−81.5	342.9	N	6.3	6.2
14-6, 124-126	128.95	2.82	2.97	−79.4	−81.4	−78.5	16.6	N	11.6	10.8
14-6, 146-148	129.17	5.09	5.15	−82.7	−82.1	−81.4	337.7	N	21.9	21.7
14-7, 24-26	129.45	2.42	2.50	−73.0	−76.2	−76.2	296.5	N	14.4	13.9
14-C, 17-19	129.94	0.90	1.68	+51.8	+51.1	+49.3	66.0	R	35.0	20.1
15-1, 24-26	130.15	2.98	3.12	−77.8	−70.4	−72.4	57.8	N	9.0	9.3
15-1, 49-51	130.40	3.24	3.36	−70.8	−79.1	−77.5	66.7	N	21.3	20.5
15-1, 74-76	130.65	2.51	2.54	−78.7	−80.9	−79.4	66.7	N	6.7	6.7
15-1, 99-101	130.90	3.03	3.11	−76.3	−81.8	−80.5	51.4	N	18.5	18.8
15-1, 124-126	131.15	4.05	4.07	−80.5	−77.4	−78.1	69.4	N	15.3	15.3
15-1, 145-147	131.36	3.42	3.45	−75.7	−79.2	−78.7	71.3	N	11.9	11.9
15-2, 24-26	131.65	3.61	3.70	−85.9	−79.5	−78.3	51.2	N	13.6	13.0
15-2, 49-51	131.90	3.24	3.28	−75.2	−81.3	−80.8	58.7	N	13.0	12.7
15-2, 74-76	132.15	4.32	4.37	−78.4	−75.1	−75.4	69.4	N	18.2	18.1
15-2, 99-101	132.40	3.06	3.18	−85.4	−82.2	−80.7	72.2	N	11.9	11.0
15-2, 124-126	132.65	4.31	4.98	−32.8	−78.1	−78.1	72.7	N	4.9	4.8
15-2, 145-147	132.86	3.09	3.18	−81.6	−72.1	−73.4	76.1	N	17.1	16.5
15-3, 24-26	133.15	5.07	5.26	−81.3	−79.0	−78.3	76.8	N	15.8	14.5
15-3, 49-51	133.40	3.10	3.71	−63.6	−69.4	−74.0	83.5	N	19.1	19.6
15-3, 74-76	133.65	1.99	2.27	−65.8	−80.9	−80.2	60.9	N	12.2	13.6
15-3, 99-101	133.90	2.56	2.79	−66.7	−74.8	−79.5	76.8	N	9.7	9.7
15-3, 124-126	134.15	1.30	1.92	−51.0	+76.0	+79.0	351.5	R	3.1	4.5
15-3, 145-147	134.36	0.69	1.41	−61.1	+81.3	+82.3	279.7	R	2.8	4.6
15-4, 24-26	134.65	1.26	2.64	−12.6	+80.6	+80.8	267.1	R	4.7	4.8
15-4, 49-51	134.90	1.66	3.43	+33.8	+85.9	+86.9	290.0	R	33.2	12.5
15-4, 74-76	135.15	1.19	2.90	+56.9	+79.0	+79.3	287.4	R	40.9	20.9
15-4, 99-101	135.40	0.87	2.33	−20.3	+77.8	+77.6	271.3	R	35.1	7.2
15-5, 24-26	136.15	3.67	4.28	−51.7	−74.8	−76.2	75.7	N	13.5	10.9
15-5, 49-51	136.40	1.94	2.10	−62.5	−77.6	−76.4	65.8	N	16.1	14.6
15-5, 74-76	136.65	3.44	3.53	−78.1	−82.0	−79.2	50.6	N	14.6	14.1
15-5, 99-101	136.90	3.29	3.37	−86.6	−84.0	−84.6	111.6	N	14.2	13.5
15-5, 124-126	137.15	3.58	3.64	−83.9	−81.3	−81.8	85.9	N	19.2	18.8
15-5, 145-147	137.36	3.38	3.43	−78.0	−79.9	−80.4	76.0	N	12.5	12.5
15-6, 24-26	137.65	1.81	1.83	−76.5	−81.4	−79.0	76.8	N	19.6	19.4
15-6, 49-51	137.90	1.75	1.82	−82.1	−86.3	−87.1	96.9	N	19.3	18.6
15-6, 74-76	138.15	2.05	2.12	−66.3	−61.7	−62.9	120.5	N	8.3	8.7
15-6, 99-101	138.40	1.86	2.17	−56.5	−75.9	−75.5	63.5	N	15.3	13.9
15-6, 124-126	138.65	2.09	2.26	−85.4	−79.8	−78.0	79.0	N	22.0	20.7
15-6, 145-147	138.86	1.88	2.46	−84.9	−78.9	−80.2	105.7	N	21.2	14.7
15-7, 22-24	139.13	2.15	2.21	−88.0	−83.8	−85.9	141.9	N	13.7	12.0
15-7, 49-51	139.40	1.71	1.78	−80.0	−82.9	−81.5	60.1	N	24.0	23.0
15-7, 59-61	139.50	1.30	1.41	+75.7	+77.5	+78.3	176.1	R	28.5	26.5
16-1, 19-21	139.60	0.32	0.46	−65.1	−61.5	−70.9	27.3	N	38.4	32.4
16-1, 44-46	139.85	2.34	2.37	−79.2	−74.6	−74.5	72.5	N	19.1	19.1
16-1, 67-69	140.08	1.76	1.87	−79.3	−78.2	−77.2	58.4	N	21.1	22.4
16-1, 94-96	140.35	2.72	2.77	−81.9	−81.1	−81.8	71.2	N	19.7	19.7
16-1, 119-121	140.60	3.62	3.65	−78.3	−82.0	−82.2	58.8	N	23.1	23.0
16-1, 140-142	140.81	3.18	3.24	−85.4	−86.4	−87.1	3.2	N	17.7	17.5
16-2, 24-26	141.15	2.40	2.66	−77.8	−83.3	−83.9	37.3	N	24.1	21.7
16-2, 49-51	141.40	1.58	1.64	−76.1	−87.4	−86.6	50.3	N	13.2	13.0
16-2, 74-76	141.65	3.24	3.38	−76.7	−77.5	−77.4	44.8	N	17.6	16.9
16-2, 99-101	141.90	3.60	3.62	−80.7	−81.4	−80.5	47.7	N	23.6	23.5
16-2, 124-126	142.15	2.37	2.42	−79.7	−81.8	−82.0	28.3	N	22.6	22.7
16-2, 145-147	142.36	3.30	3.33	−81.1	−80.0	−79.5	56.7	N	22.3	22.1
16-3, 24-26	142.65	4.87	5.20	−80.0	−81.7	−79.4	60.3	N	17.4	15.6
16-3, 49-51	142.90	5.65	5.72	−84.9	−83.8	−82.0	69.6	N	23.5	23.2
16-3, 74-76	143.15	1.65	1.66	−82.9	−81.8	−83.0	43.6	N	17.3	17.3
16-3, 99-101	143.40	3.42	3.45	−81.2	−82.1	−81.7	32.9	N	19.6	19.5

Appendix A (continued).

Core, section, interval (cm)	Depth (mbsf)	J NRM (mA/m)	Js NRM (mA/m)	Incl. NRM (deg)	Incl. 20 mT (deg)	Incl. stable (deg)	Decl. stable (deg)	Pol.	MDF (mT)	MDFs (mT)
Hole 689B (Cont.)										
16-3, 124–126	143.65	2.32	2.35	−80.0	−78.9	−79.5	57.4	N	21.3	21.1
16-3, 145–147	143.86	2.52	2.55	−79.5	−78.2	−77.3	48.5	N	20.5	20.3
16-4, 24–26	144.15	2.47	2.51	−80.7	−82.7	−80.7	68.0	N	18.5	18.4
16-4, 49–51	144.40	0.25	0.33	−59.7	−80.4	−71.5	45.0	N	12.0	14.5
16-4, 74–76	144.65	0.04	0.10	−39.0		−69.9	84.2	N		7.0
16-4, 99–101	144.90	0.03	0.11	+3.3		+69.1	293.7	R		5.1
16-4, 124–126	145.15	0.05	0.11	−56.8	−31.3	−68.4	23.6	N	17.5	11.3
16-4, 145–147	145.36	0.05	0.08	−73.2		−81.3	16.0	N	6.3	5.5
16-5, 24–26	145.65	0.01	0.07	+52.7		no	no			10.4
16-5, 49–51	145.90	0.12	0.20	−63.5	−72.0	−78.6	22.3	N	18.8	12.0
16-5, 74–76	146.15	0.05	0.21	−73.8	−58.7	−82.6	79.5	N	8.9	15.7
16-5, 99–101	146.40	0.08	0.17	−76.1	−56.0	−73.2	83.7	N	33.2	21.1
16-5, 124–126	146.65	0.10	0.20	−57.0	−49.9	−54.1	66.1	N	40.0	22.2
16-5, 145–147	146.86	0.07	0.08	−67.9	−66.8		7.8	N	11.6	11.0
16-6, 24–26	147.15	0.14	0.21	−73.4	−80.6	−74.6	56.2	N	18.1	21.1
16-6, 49–51	147.40	0.22	0.25	−74.9	−69.2	−77.8	51.4	N	18.8	18.9
16-6, 74–76	147.65	0.08	0.16	−76.8	−69.0	−63.4	105.7	N	22.5	14.0
16-6, 99–101	147.90	0.05	0.08	−71.8		−78.8	137.7	N		12.6
16-6, 124–126	148.15	0.35	0.49	−85.3	−71.2	−85.9	6.0	N	22.2	20.9
16-6, 145–147	148.36	0.10	0.14	−77.5	−69.9	−72.5	19.8	N	22.1	17.4
16-7, 24–26	148.65	0.63	0.81	−75.0	−86.2	−80.8	51.9	N	19.5	17.5
16-7, 45–47	148.86	0.30	0.76	−82.7	−79.3	−76.3	35.8	N	12.0	15.3
17-1, 24–26	149.35	0.07	0.14	−72.4	−84.4	−77.7	339.7	N		14.3
17-1, 49–51	149.60	0.05	0.08	−62.8		−58.7	11.7	N	9.5	12.8
17-1, 74–76	149.85	0.08	0.12	−54.4		−67.6	269.2	N	4.88	10.3
17-1, 99–101	150.10	0.04	0.15	−73.7	−57.3	−70.7	345.0	N		25.3
17-1, 124–126	150.35	0.03	0.07	−62.1		−85.1	251.0	N		9.9
17-1, 144–146	150.55	0.26	0.53	−62.2	−68.8	−84.9	353.6	N	33.0	17.7
17-2, 24–26	150.85	0.40	0.50	−72.4	−83.4	−82.4	342.6	N	14.3	13.3
17-2, 49–51	151.10	0.18	0.21	−66.8	−71.2	−67.9	341.6	N	25.6	22.4
17-2, 74–76	151.35	0.63	0.69	−63.1	−67.3	−66.2	338.0	N	28.4	25.4
17-2, 99–101	151.60	0.64	0.73	−67.9	−69.9	−69.5	310.8	N		44.5
17-2, 124–126	151.85	0.47	1.10	+24.8	+47.9	+64.0	270.3	R	78.2	40.1
17-2, 144–146	152.05	1.07	1.43	−46.7	−38.3	−38.7	288.5	N		60.4
17-3, 24–26	152.35	2.56	3.01	−78.3	−77.9	−75.5	324.3	N	38.6	33.2
17-3, 49–51	152.60	2.06	2.31	−69.4	−54.3	−59.6	322.8	N	16.7	14.6
17-3, 74–76	152.85	3.80	6.38	+62.3	+22.2	+40.8	265.6	R	3.2	3.6
17-3, 99–101	153.10	1.64	3.18	−21.0	+48.1	+59.4	296.2	R	10.0	16.9
17-3, 124–126	153.35	1.29	2.62	−29.6	+35.6	+41.0	306.6	R	25.5	10.5
17-3, 144–146	153.55	2.05	2.49	−19.3	+23.0	+39.6	307.6	R	6.6	7.1
17-4, 24–26	153.85	2.80	2.94	−31.1	−35.9	−37.6	307.7	N	15.5	15.7
17-4, 49–51	154.10	2.68	2.85	−51.8	−46.5	−44.7	314.0	N	9.6	10.6
17-4, 74–76	154.35	3.20	3.30	−48.1	−43.9	−44.5	306.5	N	6.9	7.1
17-4, 99–101	154.60	2.15	2.45	−26.2	−39.3	−41.7	313.1	N	17.3	15.5
17-4, 124–126	154.85	1.97	2.82	−45.1	−61.9	−65.1	337.6	N	23.4	15.0
17-4, 144–146	155.05	2.54	3.08	−58.1	−58.4	−58.4	329.9	N	21.0	17.1
17-5, 24–26	155.35	2.48	3.12	−80.5	−70.2	−71.3	292.0	N	20.0	14.6
17-5, 49–51	155.60	2.20	2.81	−64.4	−84.4	−84.0	322.1	N	17.1	11.5
17-5, 74–76	155.85	1.80	2.36	−64.3	−67.3	−71.8	330.1	N	17.8	12.5
17-5, 99–101	156.10	2.37	2.64	−68.4	−74.6	−73.9	321.0	N	10.4	12.9
17-5, 124–126	156.35	2.60	2.86	−53.1	−61.5	−61.1	324.0	N	18.4	16.2
17-5, 144–146	156.55	2.76	2.85	−54.4	−61.9	−62.0	306.0	N	16.3	15.7
17-6, 24–26	156.85	2.71	3.20	−79.1	−80.6	−80.7	306.2	N	21.5	16.0
17-6, 49–51	157.10	2.09	2.25	−64.3	−66.0	−65.3	303.9	N	19.3	19.1
17-6, 74–76	157.35	5.75	6.14	−62.2	−68.2	−69.0	311.2	N	15.5	14.1
17-6, 99–101	157.60	4.66	4.82	−56.5	−69.3	−69.2	297.8	N	8.0	7.6
17-6, 124–126	157.85	3.85	4.06	−62.0	−59.3	−57.9	303.4	N	8.3	8.6
17-6, 144–146	158.05	4.16	4.36	−61.5	−65.9	−66.2	298.8	N	14.7	13.8
17-7, 24–26	158.35	3.07	3.13	−48.4	−55.6	−55.6	291.1	N	7.9	7.7
17-7, 49–51	158.60	3.87	4.64	−51.8	−63.8	−63.1	325.0	N	25.1	20.8
18-1, 24–26	159.05	1.77	1.95	−51.8	−60.2	−56.4	274.1	N	14.4	20.1
18-1, 49–51	159.30	0.85	1.42	−48.5	−24.5	−34.9	311.8	N	12.8	13.9
18-1, 74–76	159.55	0.61	0.76	−74.8	−71.1	−71.8	318.3	N		38.1
18-1, 99–101	159.80	0.52	0.75	−74.8	−68.7	−72.0	1.9	N		39.8
18-1, 124–126	160.05	0.45	0.94	−42.1	−40.7	−34.4	308.7	N	57.5	34.3
18-1, 146–148	160.27	0.37	1.35	+78.4	−62.7	−59.1	338.8	N		4.4
18-2, 24–26	160.55	0.35	0.87	−68.0	−69.6	−68.2	329.9	N		33.4
18-2, 49–51	160.80	0.63	0.93	−70.4	−72.1	−67.7	346.4	N	64.5	51.9
18-2, 74–76	161.05	0.24	0.34	−61.8	−62.8	−67.2	59.9	N	28.0	27.2
18-2, 99–101	161.30	0.22	0.30	+45.0	+6.4	+37.4	89.0	R	15.4	15.8
18-2, 124–126	161.55	0.04	0.06	−65.7		no	no			4.7
18-2, 146–148	161.77	0.17	0.24	−82.7	−85.4	−81.6	355.9	N	39.4	31.5
18-3, 24–26	162.05	0.05	0.06	−65.8		no	no			
18-3, 49–51	162.30	1.03	1.46	−78.2	−76.1	−77.9	308.5	N		53.7
18-3, 74–76	162.55	1.93	2.07	−71.4	−71.5	−71.8	269.6	N		
18-3, 99–101	162.80	2.76	3.11	−64.9	−63.1	−64.0	320.5	N		

Appendix A (continued).

Core, section, interval (cm)	Depth (mbsf)	J NRM (mA/m)	Js NRM (mA/m)	Incl. NRM (deg)	Incl. 20 mT (deg)	Incl. stable (deg)	Decl. stable (deg)	Pol.	MDF (mT)	MDFs (mT)
Hole 689B (Cont.)										
18-3, 124–126	163.05	1.96	2.45	−51.9	−40.1	−32.3	299.3	N	33.0	26.8
18-3, 146–148	163.27	1.80	2.74	−10.9	+22.0	+46.4	288.5	R	32.0	18.0
18-4, 24–26	163.55	1.89	2.93	−19.7	+22.1	+39.0	301.1	R	24.0	12.3
18-4, 49–51	163.80	0.67	2.76	+27.3	+25.4	+44.6	296.6	R	40.6	18.5
18-4, 74–76	164.05	1.37	2.90	−25.6	+55.3	+49.8	23.7	R	4.0	8.8
18-4, 99–101	164.30	2.14	3.83	−61.8	+1.3	no	no		6.9	8.3
18-5, 24–26	165.05	1.82	3.41	−58.4	+41.4	+33.2	301.7	R	7.2	6.9
18-5, 49–51	165.30	1.78	2.63	−19.3	+18.2	+20.3	274.8	R	11.4	7.1
18-5, 74–76	165.55	3.07	4.17	−76.5	−8.8	no	no		7.0	5.2
18-5, 99–101	165.80	3.93	4.63	−68.7	−33.5	−37.7	289.5	N	10.7	8.2
18-5, 124–126	166.05	2.73	2.98	−61.6	−38.3	−40.5	291.6	N	9.3	8.6
18-5, 146–148	166.27	3.53	4.06	−59.5	−40.5	−41.9	260.9	N	5.8	5.1
18-6, 24–26	166.55	4.78	5.19	−59.6	−58.2	−58.1	268.8	N	14.8	12.8
18-C, 11–13	166.97	2.66	3.68	+43.7	+25.8	+26.7	302.7	R	26.5	18.9
19-1, 24–26	168.75	0.70	1.42	+21.1	+70.8	+78.6	312.9	R	3.2	4.8
19-1, 49–51	169.00	1.10	3.45	−51.1	+49.3	+65.3	269.7	R	3.8	11.7
19-1, 74–76	169.25	1.03	1.59	−78.8	+19.1	+26.5	261.0	R	3.9	5.6
19-1, 99–101	169.50	4.04	4.79	−67.2	+16.0	+36.7	298.6	R	2.9	3.1
19-1, 124–126	169.75	1.36	1.68	−80.7	−58.0	−70.4	272.2	N	6.1	7.5
19-1, 149–151	170.00	1.58	2.04	−43.2	−5.3	no	no		5.0	5.6
19-2, 24–26	170.25	0.98	1.39	−69.0	+22.6	+37.8	296.1	R	3.3	4.2
19-2, 49–51	170.50	2.40	3.37	−49.2	−5.7	no	no		10.3	8.3
19-2, 74–76	170.75	2.75	3.41	−79.8	−23.1	−28.6	286.0	N	4.4	4.9
19-2, 99–101	171.00	2.31	2.89	−39.7	−10.6	no	no		17.6	15.9
19-2, 124–126	171.25	2.55	3.14	−75.9	−26.8	no	no		4.7	5.1
19-2, 146–148	171.47	1.80	2.81	−5.7	+37.1	+37.2	300.2	R	21.6	13.9
19-3, 24–26	171.75	1.84	3.00	−56.8	+8.7	+29.3	275.0	R	6.8	7.4
19-3, 49–51	172.00	1.64	2.38	−61.5	+19.2	+33.4	346.5	R	5.2	5.6
19-3, 74–76	172.25	0.59	2.03	+53.2	+75.5	+73.7	260.1	R	43.7	23.8
19-3, 99–101	172.50	0.73	2.46	+18.8	+57.7	+60.7	305.7	R	43.6	18.4
19-3, 124–126	172.75	1.70	2.84	−38.5	+75.1	+78.6	352.7	R	3.5	4.9
19-3, 146–148	172.97	2.47	3.13	+10.5	+52.0	+54.5	298.0	R	20.3	12.1
19-4, 24–26	173.25	9.49	10.72	−11.0	+37.3	+40.5	307.1	R	3.7	4.1
19-4, 49–51	173.50	1.61	2.44	+35.3	+65.7	+66.8	267.1	R	30.6	20.2
19-4, 74–76	173.75	0.39	0.91	−34.7	+40.5	+75.3	318.9	R	54.4	18.8
19-4, 99–101	174.00	0.91	2.41	−16.9	+66.6	+70.4	300.7	R	43.4	6.6
19-4, 124–126	174.25	1.14	1.63	−73.9	−36.0	+26.9	235.2	R	8.8	10.5
19-4, 146–148	174.47	1.64	5.36	+48.1	+61.2	+65.1	291.6	R	45.0	12.1
19-5, 24–26	174.75	0.96	1.88	−34.2	+61.3	+65.8	309.2	R	40.0	5.5
19-5, 49–51	175.00	1.25	1.80	+32.8	+48.3	+49.1	277.4	R	43.0	30.4
19-5, 74–76	175.25	1.24	2.16	+6.3	+24.1	+43.8	290.7	R		33.8
19-5, 99–101	175.50	1.69	1.98	+32.4	+42.3	+47.2	301.5	R		
19-5, 124–126	175.75	1.04	1.62	+79.2	+77.2	+74.6	338.4	R		42.9
19-5, 146–148	175.97	0.68	0.91	+54.1	+56.1	+54.7	5.8	R		40.6
19-6, 24–26	176.25	2.86	3.22	−36.0	−31.5	−31.7	243.0	N		
19-6, 49–51	176.50	0.54	1.04	−7.2	+12.5	no	no			40.8
19-6, 74–76	176.75	0.87	1.30	+29.6	+31.0	+31.6	292.8	R		49.9
20-1, 24–26	178.35	1.28	3.55	−10.2	+57.1	+65.6	338.3	R	4.2	11.3
20-1, 49–51	178.60	3.02	3.87	+35.7	+26.8	+30.9	263.2	R	18.9	14.8
20-1, 74–76	178.85	0.40	0.90	+11.7	+43.9	+50.9	341.2	R	48.4	24.5
20-1, 99–101	179.10	2.04	3.86	−18.4	+56.3	+47.0	285.1	R	20.9	10.0
20-1, 124–126	179.35	0.44	1.41	+4.8	+31.0	+64.2	298.5	R	49.3	20.8
20-1, 145–147	179.56	4.22	7.70	+10.6	+67.3	+60.6	285.1	R	24.9	12.9
20-2, 24–26	179.85	0.48	1.33	−25.3	+30.7	+44.3	330.9	R	47.7	24.4
20-2, 49–51	180.10	0.61	5.24	−9.0	+56.4	+43.9	271.3	R	49.8	9.1
20-2, 74–76	180.35	0.63	0.91	+47.4	+56.7	+59.1	329.0	R	39.6	33.4
20-2, 99–101	180.60	3.38	12.96	+19.2	+77.9	+75.3	262.7	R	39.6	12.8
20-2, 124–126	180.85	0.11	0.13	−32.7		no	no		6.9	6.7
20-2, 145–147	181.06	2.87	11.02	−39.2	+67.9	+61.3	245.1	R	37.7	9.5
20-3, 24–26	181.35	0.74	0.89	+34.3	+36.7	+38.2	330.0	R	31.1	26.3
20-3, 49–51	181.60	4.14	10.39	+6.1	+77.0	+74.8	255.1	R	34.7	9.7
20-3, 74–76	181.85	3.72	15.64	+22.0	+23.0	+26.0	313.9	R	9.2	16.2
20-3, 99–101	182.10	5.28	88.18	+39.4	+73.9	+70.3	249.1	R	18.9	5.5
20-3, 124–126	182.35	1.33	1.55	+40.1	+44.1	+43.2	299.2	R	31.0	27.1
20-3, 145–147	182.56	2.26	6.66	+1.1	+66.2	+64.2	250.5	R	39.4	13.3
20-4, 24–26	182.85	1.70	1.84	−8.8	−5.5	no	no		30.5	28.4
20-4, 49–51	183.10	1.73	2.16	+60.7	+66.9	+63.7	301.1	R	27.8	24.4
20-4, 74–76	183.35	1.69	1.96	−54.3	−54.7	−59.7	325.4	N	35.1	31.1
20-4, 99–101	183.60	3.37	3.62	−59.8	−55.1	−54.5	313.5	N	28.2	26.2
20-4, 124–126	183.85	2.76	2.82	−47.1	−50.2	−49.0	293.5	N	28.0	27.8
20-4, 146–148	184.07	1.65	1.96	+9.3	+17.5	+33.5	302.4	R	27.1	24.0
20-5, 17–19	184.28	2.09	2.45	−23.1	−27.8	−28.9	320.2	N	30.8	26.6
21-1, 24–26	188.05	1.46	1.59	−72.5	−78.1	−80.1	152.4	N	38.6	37.0
21-1, 49–51	188.30	1.01	1.12	−68.7	−71.9	−73.1	280.9	N	33.7	30.5
21-1, 74–76	188.55	1.40	1.57	−52.3	−62.5	−65.2	271.7	N	32.7	29.2
21-1, 99–101	188.80	1.27	1.39	+22.5	−0.4	+42.8	311.5	R	20.5	18.8

Appendix A (continued).

Core, section, interval (cm)	Depth (mbsf)	J NRM (mA/m)	Js NRM (mA/m)	Incl. NRM (deg)	Incl. 20 mT (deg)	Incl. stable (deg)	Decl. stable (deg)	Pol.	MDF (mT)	MDFs (mT)
Hole 689B (Cont.)										
21-1, 124-126	189.05	0.39	0.53	−12.7	−27.5	−47.7	334.0	N	30.0	24.4
21-1, 146-148	189.27	1.38	1.61	−60.2	−66.7	−70.0	346.9	N	33.1	29.3
21-2, 24-26	189.55	1.63	2.10	−59.6	−75.3	−75.2	332.3	N	28.0	22.8
21-2, 49-51	189.80	1.49	1.63	−73.7	−66.0	−70.4	320.4	N	23.0	21.5
21-2, 74-76	190.05	1.46	1.55	−68.6	−55.4	−56.0	317.9	N	12.7	12.2
21-2, 99-101	190.30	1.16	1.42	−11.5	−6.3	−27.1	353.3	N	21.9	23.1
21-2, 124-126	190.55	0.97	1.13	−59.5	−46.2	−47.6	330.8	N	19.6	19.3
21-2, 146-148	190.77	0.48	0.57	+12.4	+11.4	+37.5	359.5	R	14.3	14.8
21-3, 24-26	191.05	0.48	0.53	−47.8	−68.2	−71.2	351.7	N	10.8	9.7
21-3, 49-51	191.30	10.35	10.54	−19.4	−40.5	−47.0	311.1	N	10.2	10.3
21-3, 74-76	191.55	0.19	0.27	−72.1	−71.9	−66.7	7.2	N	25.7	20.0
21-3, 99-101	191.80	0.19	0.20	−71.9	−77.7	−83.4	255.1	N	18.7	18.8
21-3, 124-126	192.05	0.14	0.26	−46.3	−59.0	−81.8	291.6	N	42.3	23.9
22-1, 24-26	197.75	1.60	1.72	−42.3	−57.8	−54.1	140.4	N	14.9	14.7
22-1, 51-53	198.02	1.23	1.28	+76.8	+80.5	+79.2	238.4	R	15.3	15.4
22-1, 75-77	198.26	1.05	1.15	+54.8	+63.1	+68.5	240.3	R	13.9	14.0
22-1, 99-101	198.50	1.76	1.90	+77.8	+79.4	+81.3	318.0	R	14.5	13.3
22-1, 140-142	198.91	1.12	1.28	+25.7	+43.2	+59.8	239.3	R	13.3	13.5
22-2, 24-26	199.25	0.69	0.84	+55.4	+83.0	+85.1	174.3	R	30.8	17.0
22-2, 51-53	199.52	0.76	1.42	−21.9	+19.3	+28.2	257.0	R	43.9	24.3
22-2, 75-77	199.76	1.01	1.39	−42.7	−18.6	+28.1	200.6	R	13.4	17.2
22-2, 99-101	200.00	1.06	1.37	+4.3	+27.0	+35.5	243.1	R	13.0	13.7
22-3, 2-4	200.53	0.67	0.93	+16.8	+44.0	+40.9	254.0	R	9.5	12.2
22-3, 51-53	201.02	3.35	4.25	−53.6	+53.0	+47.5	266.6	R	7.6	8.7
22-3, 86-88	201.37	1.29	2.18	−54.5	−6.0	no	no		9.8	11.8
22-4, 57-59	202.58	0.85	1.05	+40.4	+72.5	+76.3	279.0	R	8.6	8.4
22-4, 87-89	202.88	1.91	4.49	−62.7	+72.2	+68.9	228.1	R	8.2	8.8
22-4, 110-112	203.11	1.37	2.26	−39.5	+48.2	+44.8	242.2	R	9.9	8.9
22-5, 25-27	203.76	1.34	1.65	−0.9	+34.9	+29.4	271.5	R	19.6	14.5
22-5, 99-101	204.50	0.59	1.31	+10.2	+48.8	+42.5	263.2	R	43.8	24.7
22-5, 121-123	204.72	5.81	5.89	+26.4	+25.3	+30.6	261.4	R	19.1	19.0
22-5, 146-148	204.97	2.77	3.22	+3.5	−16.7	−20.2	293.7	N	27.3	22.1
22-6, 12-14	205.13	1.86	2.00	+30.2	+43.7	+44.6	252.9	R	24.5	22.7
23-2, 24-26	208.95	1.61	2.02	−1.0	+41.2	+41.3	240.2	R	8.7	9.1
23-2, 49-51	209.20	0.74	1.58	−12.7	+40.1	+63.1	213.0	R	38.0	18.9
23-2, 74-76	209.45	43.55	43.75	−39.0	−36.4	−25.1	305.4	N	9.0	9.0
23-2, 99-101	209.70	3.72	5.75	+20.1	+27.4	+30.4	252.7	R	7.4	7.6
23-2, 120-122	209.91	1.08	1.82	−32.8	+43.8	+47.6	251.5	R	24.7	10.3
23-2, 144-146	210.15	1.22	1.89	+17.9	+58.9	+58.5	209.8	R	34.0	18.4
23-3, 32-34	210.53	2.40	3.34	+22.9	+59.6	+54.6	250.9	R	25.6	17.5
23-3, 63-70	210.89	3.89	4.19	−12.9	−5.8	+32.3	281.5	R	9.2	9.3
23-3, 97-99	211.18	69.90	71.20	−21.1	−16.1	+56.9	338.0	R	11.8	11.7
23-3, 146-148	211.67	1.69	2.01	+72.2	+84.0	+82.9	309.2	R	26.5	22.4
23-4, 22-24	211.93	1.19	1.65	+55.5	+75.1	+73.4	236.0	R	34.1	25.8
23-4, 46-48	212.17	2.20	3.24	−19.2	+81.9	+77.8	231.8	R	7.1	7.8
23-4, 86-88	212.57	0.98	12.60	−2.3	+77.9	+77.6	190.1	R	29.9	10.7
24-1, 41-43	217.32	0.84	1.11	+5.4	+2.4	no	no		7.4	9.1
24-1, 96-98	217.87	0.69	1.51	−27.0	+39.9	+41.1	20.5	R	29.5	11.1
24-C, 30-32	218.87	77.94	78.14	−46.0	−46.1	−52.0	155.3	N	9.5	9.5

APPENDIX B

Paleomagnetic results for 822 samples of Hole 690B. Explanation same as Appendix A.

Core, section, interval (cm)	Depth (mbsf)	J NRM (mA/m)	Js NRM (mA/m)	Incl. NRM (deg)	Incl. 20 mT (deg)	Incl. stable (deg)	Decl. stable (deg)	Pol.	MDF (mT)	MDFs (mT)
Hole 690B										
1-1, 48–50	0.49	7.56	11.97	−77.4	+6.2	−55.6	318.0	N	4.0	4.7
1-1, 73–75	0.74	3.32	7.87	−73.6	−60.5	−65.2	321.0	N	37.9	23.8
1-1, 98–100	0.99	6.99	7.55	−58.8	−60.7	−61.3	298.5	N	22.2	19.7
1-1, 123–125	1.24	6.81	7.23	−66.8	−58.9	−59.7	310.3	N	26.6	25.1
1-2, 8–10	1.59	4.81	5.47	−46.0	−51.9	−56.0	305.0	N	28.7	24.3
1-2, 32–34	1.83	5.19	5.96	−71.2	−61.7	−64.5	313.8	N	30.3	24.7
1-2, 56–58	2.07	1.60	2.30	−17.5	−13.8	no	no		30.3	25.0
2-1, 24–26	2.35	10.90	11.39	+59.8	+75.5	+76.2	292.3	R	4.0	4.0
2-1, 49–51	2.60	13.46	15.47	+21.6	+34.7	+42.1	312.8	R	3.9	4.3
2-1, 74–76	2.85	1.84	3.14	+29.5	+46.5	+46.9	304.0	R	18.4	16.9
2-1, 99–101	3.10	2.44	3.66	+69.8	+61.0	+62.0	331.3	R	37.4	28.1
2-1, 124–126	3.35	2.20	6.54	+30.2	+33.8	+47.8	266.7	R		38.6
2-1, 145–147	3.56	5.44	7.35	−45.3	−33.1	−60.2	27.5	N	25.3	27.8
2-2, 24–26	3.85	8.41	9.29	−5.9	+26.9	+38.2	286.5	R	4.2	4.3
2-2, 49–51	4.10	4.93	8.47	−54.2	+1.6	+45.9	297.3	R	4.3	3.9
2-2, 74–76	4.35	10.38	12.14	+64.5	−11.7	+51.1	81.7	R	3.4	3.9
2-2, 99–101	4.60	1.64	3.08	+22.6	+28.7	+33.8	3.8	R	46.4	26.4
2-2, 124–126	4.85	1.16	2.76	−71.7	−43.6	no	no		38.3	31.1
2-2, 145–147	5.06	2.05	2.83	−77.5	−73.9	−70.3	310.8	N	32.4	24.5
2-3, 24–26	5.35	2.96	3.30	−10.1	−9.0	no	no		28.4	26.2
2-3, 49–51	5.60	4.13	4.33	−82.4	−78.3	−78.4	315.4	N	25.9	25.6
2-3, 74–76	5.85	4.84	5.56	−86.5	−85.0	−84.3	355.0	N	23.9	25.1
2-3, 99–101	6.10	3.47	3.71	−69.0	−75.6	−77.7	245.5	N	26.1	25.6
2-3, 124–126	6.35	4.35	5.07	−81.0	−86.8	−87.7	277.0	N	25.5	26.5
2-3, 145–147	6.56	1.21	2.25	−85.9	−55.9	−57.3	334.4	N	36.9	23.5
2-4, 24–26	6.85	0.98	1.42	+41.1	+44.4	+52.1	306.3	R	34.0	27.2
2-4, 49–51	7.10	0.74	1.32	−75.7	−68.6	−77.1	326.2	N	31.2	17.3
2-4, 74–76	7.35	1.37	1.74	+37.1	+36.0	+47.1	285.7	R	29.6	26.5
2-4, 99–101	7.60	1.95	2.38	+78.8	+81.6	+82.2	299.5	R	32.3	32.1
2-4, 124–126	7.85	1.90	2.21	+51.4	+48.2	+50.0	317.6	R	32.1	29.3
2-4, 145–147	8.06	2.92	3.23	+64.4	+61.8	+62.6	297.9	R	31.5	29.5
2-5, 24–26	8.35	1.73	2.14	+63.7	+60.4	+60.9	304.8	R	32.2	29.2
2-5, 49–51	8.60	2.55	3.12	+88.1	+79.6	+78.3	330.0	R	33.9	31.0
2-5, 74–76	8.85	4.93	5.48	+77.8	+73.5	+74.3	303.1	R	31.3	29.1
2-5, 99–101	9.10	3.14	3.67	+71.8	+70.5	+71.5	304.7	R	34.1	30.8
2-5, 124–126	9.35	1.21	1.43	+56.8	+53.9	+55.4	326.0	R	38.5	36.1
2-5, 145–147	9.56	0.55	0.97	+69.0	+58.7	+58.0	10.6	R	37.2	46.9
2-6, 24–26	9.85	0.12	0.21	+38.4	+73.7	+70.2	55.5	R	38.5	27.2
2-6, 49–51	10.10	1.22	1.61	+53.5	+64.2	+62.7	66.5	R	33.2	27.7
2-6, 74–76	10.35	1.47	2.60	−55.0	−31.0	−56.9	356.8	N	33.1	24.7
2-6, 99–101	10.60	4.05	5.23	+57.0	+54.0	+56.8	293.7	R	34.4	29.0
2-6, 124–126	10.85	5.99	9.77	+6.9	+64.1	+71.8	288.7	R	16.2	3.6
2-6, 145–147	11.06	2.54	3.05	+61.9	+57.6	+57.9	279.5	R	31.7	27.8
2-7, 24–26	11.35	2.16	2.28	−38.2	−39.7	−38.3	267.0	N	28.1	26.9
2-7, 49–51	11.60	2.73	3.07	−50.9	−48.5	−49.3	34.8	N	34.0	31.5
3-1, 24–26	11.95	1.14	4.78	−13.8	+13.4	+71.6	339.9	R	37.6	29.1
3-1, 49–51	12.20	3.36	6.46	−33.9	+21.3	+59.3	320.1	R	24.6	12.7
3-1, 74–76	12.45	5.46	6.58	−6.6	+24.4	+40.5	337.1	R	15.8	16.1
3-1, 99–101	12.70	2.71	6.02	−25.2	+50.0	+65.3	320.2	R	32.2	10.6
3-1, 125–127	12.96	5.00	6.95	−59.5	−29.7	+42.7	322.8	R	10.6	16.3
3-1, 146–148	13.17	2.52	3.38	+44.7	+60.7	+61.6	305.0	R	29.6	23.5
3-2, 24–26	13.45	2.50	3.11	+7.4	+18.1	+63.9	291.7	R	24.0	23.2
3-2, 49–51	13.70	2.12	3.23	−13.3	+32.8	+56.0	348.2	R	8.8	16.5
3-2, 74–76	13.95	2.96	4.60	−39.9	+22.9	+65.3	288.2	R	18.2	10.7
3-2, 99–101	14.20	2.71	3.25	+41.0	+34.2	+60.3	298.6	R	28.3	25.1
3-2, 125–127	14.46	2.08	3.41	−9.2	+9.0	+62.6	300.1	R	19.7	21.1
3-2, 146–148	14.67	1.34	3.17	+42.6	+64.1	+71.3	292.7	R		31.6
3-3, 24–26	14.95	1.02	1.55	+54.7	+65.4	+66.1	306.6	R		42.4
3-3, 49–51	15.20	2.94	3.67	+74.2	+74.2	+75.4	267.8	R	29.1	36.6
3-3, 73–75	15.44	1.72	3.08	+36.2	+62.1	+68.1	309.2	R	49.4	29.7
3-3, 98–100	15.69	3.08	3.37	+51.2	+55.2	+61.7	295.6	R	27.1	26.4
3-3, 125–127	15.96	2.67	3.29	+66.8	+68.2	+68.7	312.1	R	39.7	39.8
3-3, 146–148	16.17	3.58	5.17	+51.0	+66.2	+66.0	303.2	R		33.3
3-4, 23–25	16.44	3.90	5.02	+75.5	+75.4	+74.7	264.3	R		37.4
3-4, 48–50	16.69	1.97	3.61	+68.4	+73.3	+69.2	318.6	R		35.2
3-4, 73–75	16.94	1.96	3.22	+74.8	+77.2	+71.0	330.4	R		35.6
3-4, 98–100	17.19	4.23	5.79	+11.5	+36.9	+51.5	268.7	R	30.2	22.7
3-5, 23–25	17.94	0.66	1.56	+11.7	+20.9	+51.8	294.9	R		27.1
3-5, 48–50	18.19	1.51	2.50	−52.4	−28.8	+51.9	339.5	R	14.9	28.0
3-5, 73–75	18.44	2.53	4.73	−44.7	−24.4	−67.7	247.1	N	17.5	31.8
3-5, 99–101	18.70	5.59	8.08	−51.6	−11.9	+68.2	279.3	R	8.5	9.2
3-5, 125–127	18.96	4.14	6.28	−45.8	−35.2	−65.4	317.4	N	15.2	15.6
3-5, 147–149	19.18	7.36	7.57	−46.9	−48.6	−51.1	292.9	N	9.7	9.7
3-6, 23–25	19.44	3.60	7.01	−37.2	−56.6	−56.0	283.7	N	28.7	16.0

Appendix B (continued).

Core, section, interval (cm)	Depth (mbsf)	J NRM (mA/m)	Js NRM (mA/m)	Incl. NRM (deg)	Incl. 20 mT (deg)	Incl. stable (deg)	Decl. stable (deg)	Pol.	MDF (mT)	MDFs (mT)
Hole 690B (Cont.)										
3-6, 48-50	19.69	6.64	8.96	−78.4	−46.9	−53.4	285.7	N	11.1	14.8
3-6, 73-75	19.94	9.26	10.86	−54.2	−29.0	−57.6	279.8	N	5.0	6.8
3-6, 99-101	20.20	7.80	10.29	−61.6	−12.1	+41.5	248.8	R	5.3	7.7
3-6, 125-127	20.46	6.10	7.55	−23.9	−5.3	+21.2	288.1	R	8.4	12.5
3-6, 145-147	20.66	3.42	5.52	−48.2	−4.4	+25.3	279.5	R	21.2	18.8
3-7, 23-25	20.94	4.03	4.92	−37.9	−1.0	+42.3	194.1	R	9.0	8.6
3-7, 48-50	21.19	5.81	6.76	−43.2	−21.5	−56.6	280.7	N	10.6	12.4
3-7, 68-70	21.39	13.85	14.33	−66.5	−65.3	−65.5	288.1	N	25.1	24.4
4-1, 24-26	21.65	2.58	3.45	−54.6	−6.2	no	no		4.7	5.9
4-1, 49-51	21.90	2.69	5.64	−49.4	−54.9	−61.8	291.3	N	12.3	24.3
4-1, 74-76	22.15	3.92	4.98	−56.7	−67.5	−62.2	325.6	N	14.4	14.2
4-1, 99-101	22.40	3.26	3.93	−57.8	−66.9	−66.1	341.8	N	17.7	18.8
4-1, 124-126	22.65	2.87	3.15	−14.2	+6.0	+70.9	348.6	R	15.0	14.0
4-1, 145-147	22.86	5.24	5.57	−68.8	−60.8	−63.2	317.4	N	14.5	12.8
4-2, 24-26	23.15	3.06	4.07	−69.3	−54.9	−58.4	283.8	N	19.5	19.0
4-2, 49-51	23.40	5.43	5.66	−72.0	−66.7	−67.7	259.5	N	17.7	16.6
4-2, 74-76	23.65	2.68	3.40	−56.6	−46.3	−50.4	294.2	N	17.8	17.6
4-2, 99-101	23.90	4.85	5.44	−76.7	−74.9	−73.2	320.4	N	24.6	26.4
4-2, 124-126	24.15	5.59	5.79	−82.1	−82.6	−83.1	320.0	N	25.4	25.9
4-2, 145-147	24.36	3.61	4.39	−72.2	−64.9	−70.8	270.7	N	17.5	17.7
4-3, 24-26	24.65	2.61	3.11	−54.6	−52.9	−58.6	291.1	N	5.5	6.7
4-3, 49-51	24.90	3.71	4.27	−67.2	−85.2	−83.9	22.9	N	18.1	14.8
4-3, 74-76	25.15	3.55	4.07	−68.4	−84.9	−84.0	5.3	N	17.8	15.0
4-3, 99-101	25.40	1.98	2.26	−87.4	−82.6	−83.4	267.9	N	22.4	21.3
4-3, 124-126	25.65	2.34	2.97	−78.5	−86.0	−84.9	108.7	N	19.5	22.7
4-3, 143-145	25.84	0.96	1.33	−78.4	−81.0	−82.2	230.3	N	22.7	23.0
4-4, 23-25	26.14	0.67	1.57	−58.5	−75.7	−76.9	259.7	N	24.2	12.2
4-4, 49-51	26.40	0.64	0.91	−14.9	−36.9	−57.0	278.3	N	6.7	4.5
4-4, 74-76	26.65	0.64	0.95	−47.1	−69.1	−70.1	266.4	N	12.9	12.1
4-4, 99-101	26.90	0.31	0.54	−62.5	−64.9	−68.0	219.3	N	7.1	8.2
4-4, 124-126	27.15	0.49	0.82	−27.7	−28.4	−67.7	316.3	N	21.8	14.7
4-4, 143-145	27.34	0.98	1.20	−8.9	−13.5	−51.8	275.9	N	5.0	5.8
4-5, 24-26	27.65	7.12	7.61	−6.1	−67.2	−65.7	231.6	N	3.4	3.5
4-5, 49-51	27.90	0.93	1.19	−36.2	+8.4	−69.0	348.2	N	3.3	4.1
4-5, 74-76	28.15	0.59	0.92	+46.0	+56.6	+67.3	260.9	R	4.5	7.4
4-5, 99-101	28.40	0.27	0.50	+38.9	+62.4	+68.7	244.3	R	35.5	15.3
4-5, 124-126	28.65	0.47	0.68	+34.4	+68.1	+67.8	222.1	R	2.8	4.0
4-5, 143-145	28.84	1.18	1.79	+49.2	+35.0	+35.5	231.7	R	2.9	3.5
4-6, 24-26	29.15	0.68	1.35	−57.0	+29.7	+47.1	197.8	R	17.1	4.2
4-6, 49-51	29.40	2.44	3.06	+46.4	+40.3	+56.9	176.1	R	2.9	3.4
4-6, 74-76	29.65	0.50	0.84	−19.3	−2.5	−44.5	226.8	N	3.8	4.5
4-6, 99-101	29.90	0.31	0.70	−23.6	+42.6	+44.0	298.7	R	32.7	16.6
4-6, 124-126	30.15	2.88	3.38	−20.3	+62.5	+66.9	232.2	R	3.4	3.9
5-1, 25-27	31.36	0.84	1.28	+5.4	−15.3	no	no		28.5	19.5
5-1, 49-51	31.60	2.22	3.46	+59.8	+60.1	+68.8	275.5	R	16.7	4.2
5-1, 74-76	31.85	2.19	2.37	−71.2	−60.3	−69.8	319.9	N	4.2	4.4
5-1, 98-100	32.09	0.95	1.30	−73.1	−26.4	−77.6	197.5	N	9.2	8.7
5-1, 124-126	32.35	1.44	1.62	−68.7	−48.5	−38.2	257.7	N	3.7	4.1
5-1, 144-146	32.55	0.32	1.06	−16.4	−1.4	+56.3	227.7	R	37.2	9.8
5-2, 24-26	32.85	1.04	1.41	+40.3	+67.9	+72.9	246.7	R	22.7	15.4
5-2, 49-51	33.10	0.41	1.20	+37.4	+60.4	+62.0	240.6	R	32.8	14.8
5-2, 74-76	33.35	1.27	2.29	+47.1	+24.7	+30.9	239.1	R	12.1	9.5
5-2, 99-101	33.60	1.38	1.82	−74.7	−60.0	−60.4	283.5	N	21.7	16.7
5-2, 124-126	33.85	5.06	6.92	−40.0	−61.4	−61.0	285.1	N	11.9	4.9
5-2, 144-146	34.05	2.29	3.28	−35.9	−19.4	+54.0	274.7	R	18.1	16.5
5-3, 25-27	34.36	2.51	5.48	−23.2	+53.0	+62.1	275.9	R	23.6	10.4
5-3, 49-51	34.60	1.52	4.14	−36.8	+46.6	+51.8	266.1	R	30.8	9.4
5-3, 74-76	34.85	10.65	12.41	−2.8	+53.4	+62.7	296.0	R	3.1	3.6
5-3, 99-101	35.10	4.04	5.94	−69.3	+38.5	+67.0	237.3	R	3.9	4.6
5-3, 124-126	35.35	5.29	8.48	+12.5	+59.1	+66.8	298.1	R	3.8	3.9
5-3, 144-146	35.55	2.61	4.72	+0.9	+55.7	+61.1	240.8	R	23.3	7.3
5-4, 24-26	35.85	3.91	4.51	−36.2	−0.8	+39.5	338.7	R	8.9	9.1
5-4, 49-51	36.10	2.56	5.99	−20.6	+2.8	+37.8	55.7	R	13.4	4.7
5-4, 74-76	36.35	7.75	12.17	−25.3	−2.7	no	no		4.1	4.1
5-4, 99-101	36.60	6.13	7.64	−69.0	−19.0	−76.3	275.6	N	5.7	6.7
5-4, 124-126	36.85	7.40	11.07	+12.9	−27.5	−56.4	268.4	N	5.8	4.1
5-4, 144-146	37.05	2.33	4.46	−34.0	+3.8	+36.5	4.3	R	21.6	13.9
5-5, 24-26	37.35	3.86	4.11	−58.3	−30.9	−44.8	259.2	N	8.5	8.4
5-5, 49-51	37.60	4.11	5.26	−28.2	−31.7	−76.1	267.9	N	6.1	4.9
5-5, 74-76	37.85	7.24	7.84	−74.1	−30.2	−50.2	269.3	N	4.0	4.0
5-5, 99-101	38.10	4.09	6.47	−5.7	+37.9	+47.3	292.0	R	3.5	3.9
5-5, 124-126	38.35	2.08	4.82	−1.9	+31.7	+34.9	280.7	R	18.3	4.6
5-5, 144-146	38.55	1.59	4.47	−25.3	+34.0	+42.8	256.6	R	29.0	4.8
5-6, 24-26	38.85	3.13	8.15	−2.1	+85.1	+82.3	343.7	R	32.8	9.1
5-6, 49-51	39.10	7.82	10.32	−79.2	−22.6	−77.7	256.6	N	3.6	4.0
5-6, 74-76	39.35	4.02	4.34	−73.0	−62.7	−65.6	318.6	N	10.9	10.2

Appendix B (continued).

Core, section, interval (cm)	Depth (mbsf)	J NRM (mA/m)	Js NRM (mA/m)	Incl. NRM (deg)	Incl. 20 mT (deg)	Incl. stable (deg)	Decl. stable (deg)	Pol.	MDF (mT)	MDFs (mT)
Hole 690B (Cont.)										
5-6, 99-101	39.60	3.28	3.43	−74.6	−70.9	−69.4	296.0	N	22.4	21.4
5-6, 124-126	39.85	2.76	3.00	−49.4	−31.0	−47.5	267.0	N	12.9	11.2
5-6, 144-146	40.05	1.51	2.76	−64.2	+38.9	+50.0	263.1	R	12.0	4.3
5-7, 24-26	40.35	4.49	4.62	−72.5	−63.3	−61.6	291.4	N	9.7	9.5
6-1, 24-26	41.05	3.69	3.75	−73.8	−77.2	−80.0	342.2	N	13.5	13.5
6-1, 50-52	41.31	0.42	0.93	−73.9	−10.2	−68.9	236.1	N	19.6	6.4
6-1, 74-76	41.55	3.69	4.03	−72.0	−81.9	−81.9	340.1	N	15.7	15.3
6-1, 99-101	41.80	2.56	5.13	−57.2	+84.7	+82.1	209.2	R	3.3	7.3
6-1, 124-126	42.05	2.72	3.59	−53.8	+52.9	+55.5	249.3	R	4.0	5.2
6-1, 145-147	42.26	3.58	4.14	−77.1	−41.7	−59.2	307.5	N	4.7	5.8
6-2, 24-26	42.55	3.13	4.19	−49.9	+41.3	+60.8	230.4	R	4.3	5.9
6-2, 49-51	42.80	2.67	4.42	−70.3	+71.4	+69.4	215.5	R	3.1	5.0
6-2, 74-76	43.05	1.95	4.99	−52.7	+75.9	+74.9	269.9	R	3.2	9.0
6-2, 99-101	43.30	3.71	6.27	−75.8	+16.6	no	no		4.0	8.3
6-2, 124-126	43.55	2.29	4.92	+21.0	+83.1	+84.0	217.6	R	33.3	10.0
6-2, 145-147	43.76	5.20	5.98	−86.8	−71.4	−75.6	321.3	N	8.4	9.6
6-3, 24-26	44.05	1.98	2.34	−71.7	−81.7	−81.4	351.9	N	6.0	7.2
6-3, 49-51	44.30	5.75	5.89	−83.5	−88.9	−87.5	103.8	N	17.4	17.1
6-3, 74-76	44.55	5.07	5.33	−73.2	−81.8	−81.1	97.5	N	17.0	16.5
6-3, 99-101	44.80	1.67	2.55	−56.7	+55.6	+51.0	264.7	R	4.4	7.7
6-3, 124-126	45.05	1.25	1.67	−69.7	+28.8	+40.0	208.0	R	4.2	5.5
6-3, 145-147	45.26	0.38	1.77	−20.3	+59.8	+57.2	237.9	R		11.3
6-4, 24-26	45.55	2.04	2.43	−59.2	−62.2	−65.5	288.7	N	11.0	12.8
6-4, 49-51	45.80	0.79	2.31	+21.4	+83.9	+86.5	330.3	R	38.7	20.2
6-4, 74-76	46.05	3.20	3.83	+80.4	+81.4	+81.4	96.7	R	29.7	26.2
6-4, 99-101	46.30	1.24	2.95	−21.3	+65.9	+67.3	315.9	R	28.1	9.9
6-5, 24-26	47.05	3.70	4.13	−66.6	−75.1	−74.9	339.0	N	17.6	17.4
6-5, 49-51	47.30	4.61	5.04	−62.5	−68.9	−68.8	357.9	N	9.5	10.3
6-5, 74-76	47.55	5.74	6.27	−66.3	−75.3	−75.4	353.7	N	11.7	12.0
6-5, 99-101	47.80	6.62	6.77	−74.0		−77.7	355.8	N	23.3	22.7
6-5, 124-126	48.05	4.44	4.85	−70.9	−79.8	−78.1	3.1	N	17.3	17.1
6-5, 145-147	48.26	5.93	6.24	−70.7	−79.4	−78.0	4.4	N	18.7	18.0
6-6, 24-26	48.55	7.54	7.76	−75.0	−79.4	−77.6	10.5	N	15.8	16.2
6-6, 49-51	48.80	11.09	11.31	−67.6	−67.5	−67.6	31.9	N	13.1	13.3
6-6, 74-76	49.05	10.27	10.68	−72.4	−79.2	−77.5	10.4	N	13.4	13.6
6-6, 99-101	49.30	10.56	11.13	−66.9	−77.9	−76.4	16.6	N	9.6	9.8
6-6, 124-126	49.55	6.14	6.75	−63.7	−65.2	−68.2	18.9	N	8.6	9.3
6-6, 145-147	49.76	2.59	2.98	−64.8	−74.9	−72.9	12.6	N	11.1	12.9
6-7, 24-26	50.05	2.35	3.24	−42.4	+37.3	no	no		5.0	8.1
7-1, 24-26	50.65	4.67	5.77	−59.3	−67.7	−77.7	263.0	N	4.5	5.7
7-1, 49-51	50.90	5.81	6.68	−83.8	−44.0	−83.7	52.8	N	4.9	6.0
7-1, 74-76	51.15	3.56	4.01	−80.8	−71.1	−72.9	84.8	N	6.3	7.3
7-1, 99-101	51.40	2.56	3.61	−77.2	+88.4	+72.8	59.4	R	3.3	4.6
7-1, 124-126	51.65	0.88	1.90	−68.3	+83.0	+76.7	46.2	R	3.0	5.9
7-1, 144-146	51.85	1.59	3.04	−73.7	+79.3	+76.7	1.9	R	2.7	4.8
7-2, 24-26	52.15	1.52	2.78	−74.2	+82.6	+86.2	334.1	R	3.0	4.4
7-2, 49-51	52.40	0.69	2.39	−12.8	+84.1	+80.8	70.5	R	38.3	9.3
7-2, 74-76	52.65	1.38	2.04	−49.1	+72.6	+78.5	358.0	R	3.5	5.0
7-2, 99-101	52.90	0.50	1.77	−11.3	+85.7	+84.2	337.2	R	41.6	9.2
7-2, 124-126	53.15	1.79	2.13	−60.9	+30.5	+32.5	256.0	R	4.6	5.7
7-2, 144-146	53.35	3.90	3.93	−71.9	−76.0	−74.9	315.2	N	9.8	9.8
7-3, 24-26	53.65	3.39	3.45	−84.4	−82.6	−84.0	300.0	N	6.1	6.3
7-3, 49-51	53.90	3.38	3.42	−79.8	−84.8	−84.0	278.3	N	17.1	16.9
7-3, 74-76	54.15	3.90	3.93	−77.1	−80.2	−81.1	308.9	N	11.8	11.7
7-3, 99-101	54.40	1.45	1.49	−66.3	−76.8	−73.6	256.0	N	8.3	8.3
7-3, 124-126	54.65	4.72	4.77	−76.8	−82.8	−80.9	279.7	N	15.5	15.2
7-3, 144-146	54.85	0.38	1.68	−8.2	+81.5	+82.8	89.5	R	43.1	9.4
7-4, 24-26	55.15	4.87	4.89	−73.8	−74.6	−74.3	301.3	N	8.4	8.4
7-4, 49-51	55.40	3.14	3.16	−81.7	−79.5	−78.9	306.7	N	15.5	15.4
7-4, 74-76	55.65	3.52	3.62	−72.8	−80.2	−80.8	322.9	N	15.5	14.8
7-4, 99-101	55.90	6.10	6.20	−75.5	−81.0	−80.7	296.1	N	18.5	18.1
7-4, 124-126	56.15	5.97	6.97	−69.4	−80.9	−80.0	313.1	N	13.0	9.4
7-4, 144-146	56.35	5.29	5.32	−70.2	−73.4	−71.8	319.2	N	16.5	16.4
7-5, 24-26	56.65	8.42	9.17	−80.6	−79.8	−80.4	303.8	N	9.5	8.4
7-5, 49-51	56.90	5.03	5.38	−65.2	−76.2	−75.6	296.6	N	16.2	14.6
7-5, 74-76	57.15	2.49	2.56	−72.8	−71.3	−75.5	345.6	N	7.0	7.2
7-5, 99-101	57.40	3.34	3.36	−75.7	−75.6	−76.5	310.6	N	18.6	18.5
7-5, 124-126	57.65	3.85	4.00	−67.0	−73.4	−70.2	307.3	N	13.9	13.3
7-5, 146-148	57.87	4.10	4.13	−74.2	−73.5	−73.5	310.6	N	16.8	16.7
7-6, 24-26	58.15	3.84	4.62	−50.2	−77.7	−76.4	296.9	N	9.8	6.9
7-6, 49-51	58.40	5.63	5.82	−64.8	−76.1	−74.1	285.8	N	4.6	4.7
7-6, 74-76	58.65	3.11	3.17	−73.6	−74.2	−74.6	304.6	N	14.2	14.3
7-6, 99-101	58.90	4.27	4.36	−71.2	−73.9	−73.5	308.4	N	10.2	10.3
7-6, 124-126	59.15	3.45	3.58	−72.0	−73.6	−73.9	316.1	N	17.5	16.8
7-6, 145-147	59.36	2.98	3.06	−79.4	−71.7	−73.6	319.8	N	11.3	11.4
7-7, 24-26	59.65	1.61	2.93	+20.3	−65.9	−62.8	327.9	N	9.1	4.1

Appendix B (continued).

Core, section, interval (cm)	Depth (mbsf)	J NRM (mA/m)	Js NRM (mA/m)	Incl. NRM (deg)	Incl. 20 mT (deg)	Incl. stable (deg)	Decl. stable (deg)	Pol.	MDF (mT)	MDFs (mT)
Hole 690B (Cont.)										
7-7, 49-51	59.90	10.29	10.59	−2.3	−44.8	−45.4	279.5	N	3.4	3.5
7-C, 14-16	60.32	0.54	1.00	−64.5	+74.8	+74.7	326.9	R	3.6	7.2
8-1, 24-26	60.35	2.32	3.08	+75.8	+86.0	+83.3	45.0	R	30.8	26.7
8-1, 49-51	60.60	1.77	2.39	+81.9	+82.7	+84.1	334.3	R	24.5	25.6
8-1, 77-79	60.88	0.43	1.75	−3.5	+84.9	+76.4	39.9	R	49.8	12.0
8-1, 99-101	61.10	1.42	1.71	−40.1	−54.6	−59.9	219.1	N	6.2	6.2
8-1, 124-126	61.35	2.36	4.74	−67.3	−76.7	−81.2	197.8	N	22.2	9.2
8-1, 145-147	61.56	3.49	3.71	−60.9	−74.7	−74.5	234.6	N	8.0	7.9
8-2, 24-26	61.85	3.82	7.51	−70.2	−75.4	−77.9	243.4	N	9.9	6.7
8-2, 49-51	62.10	3.77	7.69	−71.1	−77.2	−78.5	225.4	N	16.2	11.0
8-2, 74-76	62.35	3.37	3.47	−76.3	−84.9	−84.3	213.5	N	13.1	12.8
8-2, 99-101	62.60	3.51	3.69	−73.6	−79.4	−81.8	212.7	N	15.5	14.6
8-2, 124-126	62.85	4.45	4.63	−71.7	−78.1	−79.0	199.7	N	17.6	16.8
8-2, 145-147	63.06	4.48	8.45	−83.9	−81.5	−81.5	210.2	N	17.3	7.6
8-3, 24-26	63.35	2.88	3.01	−86.7	−79.4	−79.1	229.7	N	12.8	12.6
8-3, 49-51	63.60	5.66	5.71	−82.6	−81.5	−82.9	192.9	N	9.0	9.0
8-3, 74-76	63.85	5.94	6.03	−72.3	−79.6	−82.0	214.8	N	9.0	8.9
8-3, 99-101	64.10	7.65	7.80	−76.3	−86.0	−85.4	164.6	N	11.1	10.7
8-3, 124-126	64.35	11.71	11.83	−72.5	−76.3	−78.0	208.0	N	10.3	10.3
8-3, 145-147	64.56	10.51	10.62	−77.1	−78.9	−79.8	200.9	N	13.7	13.5
8-4, 24-26	64.85	3.66	3.84	−78.4	−68.3	−76.2	247.2	N	4.4	4.6
8-4, 49-51	65.10	7.95	8.49	−78.6	−78.6	−78.7	184.0	N	16.3	16.8
8-4, 74-76	65.35	7.35	7.55	−77.6	−83.0	−83.4	181.4	N	18.9	18.4
8-4, 99-101	65.60	2.79	2.86	−73.3	−80.5	−81.9	183.7	N	8.9	8.8
8-4, 124-126	65.85	5.80	7.52	−73.1	−81.6	−81.8	179.2	N	14.3	9.3
8-4, 145-147	66.06	4.81	4.85	−78.6	−78.8	−79.5	178.2	N	17.7	17.7
8-5, 24-26	66.35	5.64	5.98	−69.9	−80.3	−81.4	228.2	N	12.1	10.7
8-5, 49-51	66.60	4.98	5.27	−66.1	−76.5	−79.1	243.0	N	13.5	12.4
8-5, 74-76	66.85	6.27	6.44	−74.3	−80.1	−82.9	237.5	N	15.0	14.5
8-5, 99-101	67.10	5.62	5.83	−75.7	−82.7	−84.1	210.4	N	20.9	20.0
8-5, 124-126	67.35	4.93	5.09	−79.8	−82.9	−83.9	178.5	N	17.7	17.0
8-5, 145-147	67.56	5.46	5.53	−66.9	−75.9	−75.8	229.6	N	11.3	11.0
8-6, 24-26	67.85	4.24	4.42	−75.2	−82.8	−83.0	229.1	N	14.7	13.8
8-6, 49-51	68.10	1.31	2.14	−42.1	+79.2	+81.9	237.7	R	3.3	4.9
8-6, 74-76	68.35	3.86	4.02	−67.9	−82.8	−76.1	217.7	N	6.2	6.2
8-6, 99-101	68.60	1.09	1.84	−25.9	+78.5	+78.5	251.6	R	3.7	5.6
8-6, 124-126	68.85	1.25	2.67	+53.1	+82.3	+80.9	20.2	R	36.3	19.9
8-6, 145-147	69.06	0.73	2.68	+46.8	+80.2	+78.5	358.5	R	45.5	17.4
8-7, 24-26	69.35	1.55	3.68	+66.4	+84.4	+84.2	31.6	R	38.2	20.8
8-7, 49-51	69.60	0.74	2.37	+47.5	+80.2	+81.6	10.4	R	41.2	17.8
9-1, 24-26	70.05	0.99	1.24	+45.7	+27.1	+34.5	287.8	R	15.6	13.6
8-C, 13-15	70.10	1.22	2.32	+56.6	+76.3	+75.5	24.8	R	35.2	19.4
9-1, 52-54	70.33	1.58	2.73	−66.9	+63.6	+65.0	303.8	R	3.3	4.6
9-1, 74-76	70.55	0.93	4.13	+44.0	+84.4	+82.6	63.4	R	44.2	14.4
9-1, 99-101	70.80	2.13	4.33	+69.6	+81.7	+82.1	65.1	R	37.6	22.7
9-1, 124-126	71.05	1.94	2.26	+86.4	+77.5	+75.7	72.3	R	29.2	26.4
9-1, 144-146	71.25	1.06	2.67	+54.9	+86.5	+85.7	18.6	R	39.8	18.4
9-2, 24-26	71.55	1.03	2.74	+66.7	+80.2	+78.5	64.9	R	39.5	19.3
9-2, 49-51	71.80	0.77	1.73	−52.8	+81.5	+81.3	221.0	R	3.7	4.9
9-2, 74-76	72.05	1.94	2.21	−44.1	−17.2	+19.0	312.8	R	4.7	5.6
9-2, 99-101	72.30	4.06	4.13	−68.1	−76.1	−76.3	279.7	N	10.5	10.1
9-2, 124-126	72.55	2.62	2.72	−57.5	−66.4	−66.2	278.5	N	9.4	9.4
9-2, 144-146	72.75	4.04	4.06	−77.9	−77.8	−78.0	282.3	N	8.9	8.9
9-3, 24-26	73.05	5.36	5.44	−76.8	−80.5	−79.3	271.4	N	15.0	15.1
9-3, 49-51	73.30	5.57	5.93	−64.4	−77.3	−79.1	267.3	N	17.0	15.3
9-3, 74-76	73.55	5.89	6.13	−68.3	−79.8	−81.8	284.5	N	13.9	13.1
9-3, 99-101	73.80	6.64	6.86	−63.7	−75.2	−77.6	279.1	N	11.5	10.7
9-3, 124-126	74.05	1.69	3.34	−55.0	+82.1	+89.2	108.2	R	3.4	4.8
9-3, 144-146	74.25	0.54	3.27	+50.6	+83.7	+83.1	51.4	R		16.0
9-4, 24-26	74.55	2.05	2.88	+76.5	+81.1	+81.4	78.1	R	34.8	27.3
9-4, 48-50	74.79	2.98	5.48	+72.4	+84.8	+83.2	84.9	R	35.3	22.3
9-4, 74-76	75.05	2.04	4.42	+77.7	+82.8	+81.3	93.4	R	38.0	22.1
9-4, 99-101	75.30	5.78	9.52	+63.7	+82.5	+82.0	87.1	R	30.7	19.8
9-4, 118-120	75.49	1.23	2.48	+56.0	+83.1	+82.7	63.7	R	34.4	18.6
9-5, 2-4	75.83	2.58	6.32	+52.0	+76.8	+75.2	79.5	R	37.1	17.5
9-5, 24-26	76.05	2.28	3.42	+62.5	+81.5	+78.8	57.8	R	28.8	19.9
9-5, 49-51	76.30	3.11	5.04	+75.6	+82.6	+81.6	64.5	R	34.2	23.9
9-5, 74-76	76.55	1.61	3.67	+20.4	+82.9	+81.1	37.7	R	31.4	9.9
9-5, 99-101	76.80	1.37	4.26	+71.6	+80.7	+79.8	67.7	R	39.6	19.4
9-5, 124-126	77.05	0.95	1.97	+18.4	+79.4	+75.9	24.2	R	30.1	8.8
9-5, 144-146	77.25	0.97	2.39	+41.8	+83.9	+84.1	135.6	R	38.0	16.1
9-6, 24-26	77.55	1.40	2.08	+45.5	+75.2	+72.8	9.0	R	24.5	13.0
9-6, 49-51	77.80	1.65	2.60	−46.2	+62.6	+61.5	276.4	R	3.6	4.7
9-6, 74-76	78.05	1.92	3.91	+49.4	+83.8	+83.0	54.4	R	33.7	16.8
9-6, 99-101	78.30	0.94	1.88	−17.4	+79.1	+80.8	343.7	R	23.2	5.3
9-6, 124-126	78.55	1.97	3.24	−20.9	+63.6	+67.8	297.5	R	4.8	5.2

Appendix B (continued).

Core, section, interval (cm)	Depth (mbsf)	J NRM (mA/m)	Js NRM (mA/m)	Incl. NRM (deg)	Incl. 20 mT (deg)	Incl. stable (deg)	Decl. stable (deg)	Pol.	MDF (mT)	MDFs (mT)
Hole 690B (Cont.)										
9-6, 144–146	78.75	1.16	2.22	+22.0	+73.6	+76.3	330.2	R	29.5	15.6
9-7, 24–26	79.05	1.31	2.62	+11.5	+67.7	+68.3	325.1	R	30.7	11.7
9-7, 49–51	79.30	0.94	2.45	−4.0	+72.3	+75.7	348.3	R	33.9	8.3
10-1, 30–32	79.71	6.66	8.37	+4.8	+5.2	+20.4	275.0	R	3.6	3.8
10-1, 49–51	79.90	0.96	2.93	+34.0	+65.5	+68.7	300.4	R	36.4	12.5
10-1, 74–76	80.15	3.47	4.71	−62.3	−20.7	−23.4	298.4	N	4.7	4.9
10-1, 99–101	80.40	3.10	4.83	−37.8	+48.7	+52.6	301.5	R	4.0	3.9
10-1, 124–126	80.65	0.87	2.93	−56.3	+52.0	+54.6	306.4	R	35.6	5.5
10-1, 145–147	80.86	2.97	3.39	−63.0	−69.1	−74.5	334.9	N	8.6	7.5
10-2, 24–26	81.15	8.26	8.81	−73.6	−60.0	−64.0	324.5	N	4.7	4.6
10-2, 49–51	81.40	3.45	4.32	−81.1	−33.7	−51.1	300.7	N	7.4	6.3
10-2, 74–76	81.65	9.48	10.14	−74.5	−43.8	−48.9	309.9	N	6.6	6.3
10-2, 99–101	81.90	4.48	5.30	−87.6	−58.3	−61.1	316.4	N	16.3	12.9
10-2, 124–126	82.15	6.83	7.98	−69.3	−55.8	−58.5	314.1	N	20.0	16.2
10-2, 147–149	82.38	8.20	8.77	−62.2	−52.8	−54.3	309.9	N	10.8	9.6
10-3, 24–26	82.65	12.31	18.44	+40.2	−54.6	−55.9	293.3	N	3.1	3.5
10-3, 49–51	82.90	8.15	8.53	−61.3	−42.7	−48.2	294.0	N	5.1	5.7
10-3, 74–76	83.15	2.43	3.76	−36.1	−56.5	−60.3	292.3	N	15.7	7.8
10-3, 99–101	83.40	2.83	2.95	−68.2	−71.8	−73.6	13.6	N	9.5	9.1
10-3, 124–126	83.65	3.14	3.34	−62.3	−81.4	−81.4	44.7	N	8.2	7.5
10-3, 147–149	83.88	2.69	2.74	−72.3	−71.7	−73.3	345.9	N	5.9	5.9
10-4, 24–26	84.15	2.33	2.45	−53.0	−14.9	+34.2	256.9	R	3.5	3.7
10-4, 49–51	84.40	1.61	2.22	−29.7	+63.3	+65.4	308.4	R	3.8	3.9
10-4, 74–76	84.65	1.38	2.35	−10.9	+58.7	+58.0	295.7	R	4.1	4.9
10-4, 99–101	86.90	1.21	6.35	−8.9	+81.7	+79.6	337.1	R	43.9	8.3
10-4, 124–126	86.15	1.51	3.88	−52.2	+69.2	+67.2	300.4	R	4.6	5.5
10-4, 147–149	85.38	5.67	7.57	−16.8	+64.1	+65.7	289.7	R	3.0	3.6
10-5, 24–26	85.65	2.04	5.68	−59.0	+72.3	+73.3	278.5	R	32.7	5.4
10-5, 49–51	85.90	1.32	5.52	−64.5	+75.4	+74.5	270.6	R	42.0	6.6
10-5, 74–76	86.15	2.48	6.29	+2.1	+66.7	+64.8	299.0	R	37.2	13.6
10-5, 99–101	86.40	1.12	6.30	−15.9	+76.5	+75.7	285.5	R	46.4	9.2
10-5, 124–126	86.65	1.35	4.78	−15.0	+77.8	+75.8	266.0	R	37.9	7.4
10-5, 147–149	86.88	2.72	4.51	−59.6	+68.6	+70.0	274.4	R	7.6	6.8
10-6, 24–26	87.15	5.73	8.10	−22.0	+67.8	+66.5	273.2	R	3.1	3.8
10-6, 49–51	87.40	1.85	2.87	+59.1	+70.7	+72.1	284.2	R	30.6	20.7
10-6, 74–76	87.65	1.59	3.58	+44.9	+73.5	+74.3	267.5	R	36.5	20.6
10-6, 99–101	87.90	1.80	3.18	+75.0	+76.2	+76.0	274.3	R	40.6	31.0
10-6, 124–126	88.15	2.62	4.70	+66.3	+76.4	+76.7	268.0	R	35.8	24.2
10-6, 147–149	88.38	3.97	5.50	−10.9	+28.6	+31.4	281.3	R	24.8	15.3
10-7, 24–26	88.65	0.88	5.36	−12.5	+71.6	+72.2	271.4	R	48.3	9.7
10-7, 49–51	88.90	3.06	3.61	+55.1	+71.4	+72.1	272.3	R	28.7	24.9
10-7, 74–76	89.15	1.47	4.10	+18.0	+76.3	+75.0	281.1	R	38.6	15.9
11-1, 24–26	89.35	2.18	3.00	−17.3	+15.0	+16.1	301.1	R	13.8	5.9
11-1, 46–48	89.57	2.73	3.65	+53.2	+84.3	+83.2	332.5	R	22.9	13.5
11-1, 72–74	89.83	2.55	4.70	+51.3	+81.4	+80.8	341.3	R	34.7	21.3
11-1, 96–98	90.07	0.40	5.22	−40.9	+83.4	+83.6	354.1	R		8.9
11-1, 122–124	90.33	2.61	5.29	−38.8	+73.7	+71.0	310.2	R	3.8	4.8
11-1, 146–148	90.57	2.01	2.47	+78.4	+77.4	+74.8	327.5	R	29.3	25.2
11-2, 24–26	90.85	1.57	2.26	+34.8	+67.6	+65.1	318.1	R	30.4	21.8
11-2, 46–48	91.07	1.86	3.19	+10.4	+69.6	+70.2	286.0	R	23.1	8.8
11-2, 72–74	91.33	2.52	3.16	−65.4	+13.7	+31.5	305.8	R	4.3	4.9
11-2, 96–98	91.57	0.85	1.20	−46.4	−8.1	no	no		9.7	8.6
11-2, 122–124	91.83	2.85	3.10	−41.1	−14.5	−50.2	283.3	N	6.1	6.4
11-2, 146–148	92.07	4.32	5.27	+1.8	+48.1	+46.0	290.7	R	4.6	6.1
11-3, 24–26	92.35	13.44	13.75	−79.4	−66.6	−67.3	263.3	N	8.7	8.5
11-3, 46–48	92.57	3.08	3.82	−66.3	−72.0	−72.9	260.5	N	20.7	15.6
11-3, 72–74	92.83	7.18	7.19	−72.5	−73.1	−73.2	240.4	N	23.8	23.8
11-3, 96–98	93.07	5.90	5.99	−66.2	−72.1	−71.4	236.1	N	12.8	12.7
11-3, 122–124	93.33	3.84	3.92	−80.2	−78.6	−79.8	223.8	N	18.1	17.6
11-3, 147–149	93.58	4.26	4.33	−85.3	−81.8	−80.1	266.3	N	13.4	13.6
11-4, 24–26	93.85	4.16	4.22	−75.3	−77.7	−77.6	236.7	N	20.7	20.4
11-4, 46–48	94.07	4.11	4.14	−75.9	−74.2	−74.3	231.6	N	20.6	20.6
11-4, 72–74	94.33	3.17	3.22	−71.9	−74.5	−74.2	258.8	N	18.3	18.1
11-4, 96–98	94.55	4.01	4.09	−71.3	−74.7	−74.5	250.7	N	14.3	13.9
11-4, 122–124	94.83	4.32	4.35	−71.4	−73.4	−72.9	253.6	N	15.2	15.1
11-4, 147–149	95.08	4.21	4.31	−60.9	−67.5	−65.5	245.7	N	14.5	14.0
11-5, 24–26	95.35	6.23	6.29	−82.5	−78.6	−78.3	238.9	N	16.4	16.1
11-5, 46–48	95.57	6.55	6.63	−80.2	−74.1	−73.6	264.0	N	18.2	17.9
11-5, 72–74	95.83	1.30	2.98	−63.7	+42.2	+41.2	278.8	N	20.6	7.7
11-5, 96–98	96.07	2.75	7.90	no	+3.6	no	no		4.0	8.9
11-5, 122–124	96.33	1.16	2.62	−13.8	+69.5	+67.9	288.8	R	30.8	7.2
11-5, 146–148	96.57	2.74	3.04	no	−19.1	no	no		4.2	4.5
11-6, 24–26	96.85	3.94	4.02	−68.0	−64.0	−63.9	247.4	N	15.8	16.3
11-6, 46–48	97.07	6.38	6.56	−81.8	−72.7	−72.1	233.5	N	12.7	12.5
11-6, 72–74	97.33	4.13	4.27	−61.9	−68.5	−70.2	247.6	N	16.0	15.3
11-6, 96–98	97.57	3.29	3.47	−77.7	−73.8	−73.5	240.6	N	19.0	17.7

Appendix B (continued).

Core, section, interval (cm)	Depth (mbsf)	J NRM (mA/m)	Js NRM (mA/m)	Incl. NRM (deg)	Incl. 20 mT (deg)	Incl. stable (deg)	Decl. stable (deg)	Pol.	MDF (mT)	MDFs (mT)
Hole 690B (Cont.)										
11-6, 122–124	97.83	1.94	1.97	−64.6	−65.3	−67.1	258.4	N	8.2	8.1
11-6, 147–149	98.08	2.47	2.68	−60.3	−70.8	−72.9	229.2	N	19.1	17.0
11-7, 25–27	98.36	4.36	4.57	−73.1	−63.9	−65.2	264.2	N	12.7	11.5
11-7, 46–48	98.57	3.89	3.96	−73.8	−74.4	−73.7	252.9	N	19.9	20.1
11-7, 67–69	98.78	5.93	6.20	−69.5	−77.0	−78.0	254.4	N	19.9	18.9
12-1, 48–50	99.29	3.34	6.83	+42.2	+32.7	+40.8	193.4	R	9.0	6.3
12-1, 48–50	99.29	3.34	6.83	+42.2	+32.7	+40.8	193.4	R	9.0	6.3
12-1, 72–74	99.53	1.61	1.98	−87.9	−67.6	−69.6	246.4	N	7.9	8.7
12-1, 103–105	99.84	14.42	16.11	+62.1	−65.2	−65.7	231.2	N	3.1	3.5
12-1, 122–124	100.03	3.06	3.13	−78.6	−82.5	−82.4	266.9	N	11.1	11.4
12-1, 146–148	100.27	4.43	4.45	−59.9	−57.3	−57.8	248.9	N	7.9	7.9
12-2, 24–26	100.55	2.45	2.69	−51.2	−48.9	−51.6	256.9	N	16.3	16.9
12-2, 48–50	100.79	16.84	21.28	+19.6	−64.3	−64.0	251.3	N	2.9	3.4
12-2, 72–74	101.03	7.72	7.81	−65.4	−65.2	−65.9	215.6	N	9.0	9.1
12-2, 99–101	101.30	6.45	6.62	−59.6	−66.6	−65.8	267.4	N	9.7	9.4
12-2, 122–124	101.53	1.20	3.27	−35.3	+62.1	+57.9	354.0	R	34.5	7.3
12-2, 146–148	101.77	4.05	4.59	−72.6	+13.7	+30.9	278.9	R	3.7	4.1
12-3, 24–26	102.05	5.87	6.38	−42.8	−25.3	−29.9	230.6	N	7.7	7.2
12-3, 48–50	102.29	29.34	35.34	+51.4	−66.2	−67.3	246.2	N	2.9	3.4
12-3, 72–74	102.53	7.37	7.54	−66.0	−72.0	−70.7	265.7	N	13.6	13.3
12-3, 99–101	102.80	4.87	4.93	−72.3	−67.2	−68.2	282.9	N	18.3	18.1
12-3, 122–124	103.03	7.83	8.00	−68.1	−68.5	−69.1	280.4	N	10.9	10.6
12-3, 146–148	103.27	8.29	8.39	−69.7	−64.0	−64.9	263.6	N	10.3	10.1
12-4, 24–26	103.55	3.78	4.03	−62.2	−63.7	−66.0	214.8	N	18.0	16.7
12-4, 48–50	103.79	6.22	6.70	−59.8	−70.7	−71.6	253.8	N	13.2	11.9
12-4, 72–74	104.03	9.28	9.55	−75.0	−73.9	−76.6	223.6	N	9.9	9.7
12-4, 99–101	104.30	5.18	5.23	−71.1	−70.1	−70.4	227.5	N	15.2	15.0
12-4, 122–124	104.53	3.09	3.51	−58.9	−60.6	−60.6	182.2	N	24.2	20.2
12-4, 146–148	104.77	6.35	6.44	−77.4	−78.8	−80.9	198.9	N	7.5	7.7
12-5, 24–26	105.05	2.90	3.68	−63.7	−49.1	−49.6	220.8	N	14.3	9.5
12-5, 48–50	105.29	3.06	3.22	−69.0	−57.5	−65.4	207.5	N	3.8	3.9
12-5, 72–74	105.53	2.86	3.86	+37.8	−20.5	−59.9	235.3	N	3.1	3.1
12-5, 96–98	105.77	1.02	1.38	−37.5	+38.4	+35.6	224.9	R	7.1	6.9
12-5, 118–120	105.99	0.93	2.03	−45.3	+76.0	+71.7	228.9	R	25.4	4.9
12-6, 24–26	106.55	5.51	6.12	−75.8	−65.5	−68.8	239.7	N	12.7	9.8
12-6, 48–50	106.79	4.94	5.17	−71.1	−64.6	−65.2	272.5	N	16.4	15.5
12-6, 72–74	107.03	7.77	8.19	−68.5	−76.2	−77.6	278.0	N	10.2	9.4
12-6, 99–101	107.30	5.85	5.88	−69.7	−65.5	−66.5	262.4	N	8.8	8.9
12-6, 122–124	107.53	8.51	8.70	−65.3	−62.3	−63.8	278.6	N	6.6	6.5
12-6, 146–148	107.77	5.71	5.83	−64.7	−59.5	−59.8	275.1	N	7.6	7.6
12-7, 24–26	108.05	6.17	6.23	−64.3	−63.9	−66.2	267.4	N	6.1	6.3
12-7, 48–50	108.29	4.99	5.17	−58.3	−67.7	−67.9	254.0	N	10.2	9.7
13-1, 24–26	108.75	1.58	2.70	−37.1	−50.0	−48.9	305.1	N	32.8	17.9
13-1, 49–51	109.00	3.09	3.77	−51.4	−73.1	−73.5	342.8	N	11.1	9.2
13-1, 74–76	109.25	3.29	3.63	−67.7	−81.7	−79.2	309.8	N	8.8	7.8
13-1, 98–100	109.49	7.91	7.94	−79.3	−82.2	−81.1	54.6	N	6.6	6.6
13-1, 124–126	109.75	3.75	4.17	−66.9	−85.8	−87.0	318.0	N	9.1	8.0
13-1, 146–148	109.97	3.57	4.20	−54.6	−76.3	−74.8	333.9	N	9.1	7.5
13-2, 24–26	110.25	6.36	10.79	−83.3	−81.2	−81.7	323.7	N	5.2	29.9
13-2, 49–51	110.50	120.31	121.16	−31.3	−64.2	−84.6	29.2	N	6.3	6.3
13-2, 74–76	110.75	4.28	4.55	−64.1	−76.7	−73.8	350.5	N	4.8	5.0
13-2, 99–101	111.00	15.56	16.66	−25.3	−84.2	−86.1	108.7	N	3.2	3.3
13-2, 124–126	111.25	3.42	3.65	−74.0	−82.7	−79.8	7.4	N	9.2	8.9
13-2, 148–150	111.49	7.09	7.29	−69.7	−80.7	−82.1	74.8	N	5.7	5.3
13-3, 24–26	111.75	5.61	5.64	−80.0	−78.4	−78.7	14.0	N	7.3	7.3
13-3, 49–51	112.00	5.93	6.41	−59.0	−81.1	−81.5	312.0	N	4.3	4.2
13-3, 74–76	112.25	6.14	6.23	−80.7	−74.7	−75.8	325.8	N	7.0	7.0
13-3, 99–101	112.50	6.25	6.31	−76.7	−79.7	−80.3	73.6	N	8.7	8.6
13-3, 124–126	112.75	3.95	4.02	−85.0	−82.5	−85.1	41.5	N	9.4	9.3
13-3, 148–150	112.99	3.49	4.08	−63.9	−75.0	−77.4	339.1	N	8.7	7.2
13-4, 24–26	113.25	5.16	5.30	−75.6	−86.3	−87.7	223.0	N	9.9	9.6
13-4, 49–51	113.50	3.40	4.09	−58.6	−76.2	−76.5	49.1	N	19.9	13.6
13-4, 74–76	113.75	7.65	7.81	−86.1	−77.6	−79.5	87.5	N	9.3	8.9
13-4, 99–101	114.00	4.43	5.12	−59.8	−77.5	−77.2	68.8	N	17.8	13.1
13-4, 124–126	114.25	6.21	6.33	−76.7	−85.3	−83.8	351.3	N	6.7	6.5
13-4, 148–150	114.49	3.01	3.34	−79.0	−84.3	−85.0	29.5	N	17.7	15.4
13-5, 24–26	114.75	4.62	5.06	−67.3	−77.9	−78.2	347.4	N	4.4	4.6
13-5, 49–51	115.00	5.11	5.44	−73.5	−87.7	−87.4	287.5	N	8.3	7.7
13-5, 74–76	115.25	5.11	6.50	−45.6	−76.2	−77.6	330.8	N	7.1	4.6
13-5, 99–101	115.50	3.19	3.67	−62.9	−75.9	−75.0	327.8	N	13.9	10.2
13-5, 124–126	115.75	4.91	4.97	−85.9	−81.7	−85.5	279.3	N	4.9	4.9
13-5, 148–150	115.99	2.16	2.50	−71.4	−82.0	−83.8	280.7	N	12.9	10.1
13-6, 24–26	116.25	4.63	4.71	−72.5	−64.0	−65.4	275.2	N	4.6	4.7
13-6, 49–51	116.50	3.94	4.03	−79.6	−73.8	−76.4	238.2	N	4.9	4.9
13-6, 74–76	116.75	3.29	3.72	−67.3	−84.8	−84.1	40.8	N	12.9	9.9
13-6, 99–101	117.00	5.95	6.10	−74.2	−87.6	−87.9	131.0	N	5.9	5.8

Appendix B (continued).

Core, section, interval (cm)	Depth (mbsf)	J NRM (mA/m)	Js NRM (mA/m)	Incl. NRM (deg)	Incl. 20 mT (deg)	Incl. stable (deg)	Decl. stable (deg)	Pol.	MDF (mT)	MDFs (mT)
Hole 690B (Cont.)										
13-6, 124–126	117.25	4.75	4.93	−78.5	−86.9	−86.3	320.3	N	4.9	4.9
13-6, 148–150	117.49	2.74	3.19	−64.3	−80.7	−81.5	125.0	N	9.2	7.6
13-7, 24–26	117.75	4.44	4.50	−87.8	−84.7	−85.7	166.0	N	4.9	4.9
13-7, 49–51	118.00	4.06	4.17	−83.0	−83.0	−82.3	284.0	N	9.7	9.5
13-C, 15–17	118.46	3.94	3.97	+80.5	+83.0	+81.2	340.3	R	4.7	4.7
14-1, 25–27	118.76	6.37	8.24	+64.1	−5.9	no	no		4.1	3.7
14-1, 50–52	119.01	3.18	3.93	−42.7	−63.0	−64.2	336.6	N	19.8	14.0
14-1, 74–76	119.25	6.65	6.79	−65.2	−64.0	−63.4	317.5	N	4.7	4.7
14-1, 99–101	119.50	4.07	4.23	−63.5	−54.7	−56.2	327.7	N	6.1	6.0
14-1, 124–126	119.75	8.04	8.57	−78.8	−57.5	−60.3	315.9	N	5.4	5.2
14-1, 146–148	119.97	3.31	3.52	−74.7	−61.6	−65.5	323.3	N	18.2	16.8
14-2, 25–27	120.26	3.17	3.45	−78.6	−71.7	−70.0	317.7	N	15.1	13.2
14-2, 50–52	120.51	7.13	7.21	−84.0	−78.1	−79.4	317.9	N	6.8	6.7
14-2, 74–76	120.75	6.07	6.17	−64.1	−60.9	−61.5	307.4	N	6.9	6.8
14-2, 99–101	121.00	2.80	2.87	−67.2	−65.0	−64.3	349.4	N	9.9	10.0
14-2, 124–126	121.25	4.44	5.01	−78.8	−68.1	−68.1	284.8	N	14.1	11.0
14-2, 146–148	121.47	5.24	5.27	−77.1	−73.2	−73.7	316.7	N	5.9	6.0
14-3, 25–27	121.76	7.05	7.47	−45.8	−62.2	−59.2	330.0	N	4.1	4.2
14-3, 50–52	122.01	5.12	5.40	−88.4	−74.8	−76.7	335.2	N	8.5	7.8
14-3, 74–76	122.25	4.89	4.98	−57.9	−63.6	−61.6	310.5	N	6.1	6.0
14-3, 99–101	122.50	3.32	3.39	−75.7	−67.1	−67.7	329.1	N	9.7	9.6
14-3, 124–126	122.75	6.09	6.39	−85.0	−68.9	−70.0	299.6	N	5.1	5.3
14-3, 146–148	122.97	3.04	3.11	−79.3	−66.4	−66.4	327.1	N	6.0	5.9
14-4, 24–26	123.25	2.13	3.41	−61.6	−71.5	−74.8	290.4	N	24.1	12.1
14-4, 50–52	123.51	1.95	2.20	−75.0	−53.9	−54.5	301.7	N	13.2	11.0
14-4, 74–76	123.75	2.44	3.08	−82.5	+10.7	+31.0	255.3	R	3.9	4.2
14-4, 99–101	124.00	2.18	2.37	−53.2	−25.2	+21.1	262.5	R	4.6	4.9
14-4, 124–126	124.25	3.61	4.68	−79.1	+70.5	+73.7	265.5	R	2.9	3.7
14-4, 146–148	124.47	1.82	2.54	−57.1	+18.4	+24.4	256.8	R	6.5	6.1
14-5, 24–26	124.75	1.08	1.89	−50.5	+18.8	+19.3	260.2	R	7.0	4.7
14-5, 50–52	125.01	1.63	2.64	−25.0	+48.5	+48.7	282.4	R	4.7	5.5
14-5, 74–76	125.25	3.14	3.50	−68.2	+5.6	+32.0	269.9	R	3.6	3.8
14-5, 99–101	125.50	1.80	2.43	−48.7	+15.4	+24.5	274.4	R	10.1	8.9
14-5, 124–126	125.75	3.53	7.25	−71.7	−7.2	+29.1	264.3	R	6.5	5.2
14-5, 146–148	125.97	1.77	3.06	−46.3	+64.6	+65.4	287.5	R	3.9	5.6
14-6, 24–26	126.25	2.09	2.35	−67.7	+2.6	no	no		4.2	4.3
14-6, 50–52	126.51	1.24	3.92	−3.3	+64.7	+65.4	268.4	R	39.5	9.3
14-6, 74–76	126.75	1.12	2.93	+21.0	+72.5	+71.6	288.3	R	35.1	12.8
14-6, 99–101	127.00	1.50	3.64	−60.8	+62.2	+63.3	273.7	R	22.0	4.9
14-6, 124–126	127.25	0.40	3.27	−55.3	+53.7	+51.7	278.9	R		9.4
14-6, 146–148	127.47	1.15	5.18	+53.7	+77.5	+78.0	298.1	R	47.8	15.9
14-7, 25–27	127.76	1.47	4.40	−18.2	+74.4	+77.6	281.5	R	31.9	6.9
14-7, 50–52	128.01	1.88	3.58	+45.8	+71.1	+70.0	271.6	R	31.9	19.1
15-1, 24–26	128.35	2.66	3.15	−51.3	−17.6	+47.1	269.2	R	4.6	4.9
14-C, 24–26	128.60	1.20	2.17	−47.1	+30.2	+57.6	283.1	R	16.9	7.6
15-1, 49–51	128.60	1.12	2.41	+37.4	+25.7	+51.5	278.1	R	26.7	10.7
15-1, 74–76	128.85	2.28	3.11	−16.3	+15.1	+60.2	287.7	R	5.9	5.1
15-1, 99–101	129.10	4.58	5.22	−60.4	−54.2	+32.0	247.2	R	4.2	4.2
15-1, 124–126	129.35	2.86	4.23	−30.3	+47.5	+53.4	257.6	R	6.8	4.9
15-1, 144–146	129.55	3.19	4.81	+29.3	+47.0	+53.7	261.6	R	13.9	6.0
15-2, 24–26	129.85	2.90	4.05	−23.0	+46.0	+63.0	286.3	R	4.1	4.6
15-2, 49–51	130.10	5.99	6.99	−77.9	−19.2	+10.5	263.3	R	4.4	4.3
15-2, 64–66	130.25	3.26	3.75	−63.6	+3.9	+52.1	72.2	R	4.1	4.7
15-2, 74–76	130.35	5.06	5.78	−64.1	−5.2	+46.0	267.2	R	4.4	4.6
15-2, 99–101	130.60	3.11	6.76	−7.3	−14.5	−41.7	296.4	N	23.4	5.0
15-2, 107–109	130.68	4.12	4.42	−66.5	+9.1	+63.9	240.9	R	4.0	4.3
15-2, 124–126	130.85	4.31	4.77	−43.6	−12.4	−45.5	276.1	N	12.2	10.8
15-2, 144–146	131.05	7.83	9.36	−77.7	−1.4	+16.0	271.4	R	4.1	4.1
15-3, 6–8	131.17	3.37	3.53	−66.7	−40.7	−61.5	301.0	N	6.0	6.3
15-3, 24–26	131.35	3.25	4.05	−37.3	−25.4	−46.4	278.6	N	22.1	16.7
15-3, 49–51	131.60	6.36	7.55	−72.1	−38.0	−57.9	286.2	N	4.3	4.1
15-3, 74–76	131.85	5.46	5.96	−51.1	−20.1	−42.5	286.0	N	7.8	7.5
15-3, 88–90	131.99	4.74	4.89	−49.9	−27.7	−65.3	340.1	N	4.5	4.6
15-3, 99–101	132.10	4.73	5.53	−83.8	−30.7	−66.5	285.8	N	6.7	5.8
15-3, 124–126	132.35	4.94	6.22	−56.7	+8.2	+26.4	251.9	R	5.6	5.9
15-3, 144–146	132.55	6.58	7.66	−41.6	+15.6	+64.2	243.4	R	4.5	4.8
15-4, 24–26	132.85	6.09	6.74	−62.1	−19.9	−50.0	288.3	N	4.9	4.8
15-4, 32–34	132.93	3.98	4.17	−42.3	−26.4	−30.3	314.0	N	4.6	4.6
15-4, 49–51	133.10	2.71	2.83	−55.4	−39.7	−46.0	272.1	N	8.1	8.1
15-4, 64–66	133.25	2.37	3.10	−37.4	+59.2	+60.5	65.6	R	4.5	6.3
15-4, 74–76	133.35	3.18	4.09	−38.9	+14.2	+41.7	266.9	R	8.2	7.1
15-4, 99–101	133.60	3.08	3.65	−58.0	+8.9	+34.3	237.4	R	6.4	7.0
15-4, 124–126	133.85	1.73	3.13	−6.2	+51.6	+55.9	238.3	R	27.3	11.0
15-4, 144–146	134.05	3.60	4.03	−21.6	+7.9	+37.9	278.4	R	13.5	12.6
15-5, 24–26	134.35	2.72	4.35	−42.2	+44.5	+55.4	254.4	R	8.5	7.3
15-5, 49–51	134.60	0.60	2.52	−13.3	+78.4	+72.9	143.3	R		9.7

Appendix B (continued).

Core, section, interval (cm)	Depth (mbsf)	J NRM (mA/m)	Js NRM (mA/m)	Incl. NRM (deg)	Incl. 20 mT (deg)	Incl. stable (deg)	Decl. stable (deg)	Pol.	MDF (mT)	MDFs (mT)
Hole 690B (Cont.)										
15-5, 74–76	134.85	6.47	8.88	−66.5	+66.3	+64.8	269.3	R	5.3	7.1
15-5, 99–101	135.10	2.96	4.13	−15.2	+37.3	+42.3	245.1	R	4.4	6.1
15-5, 124–126	135.35	2.63	3.98	+49.4	+60.6	+64.7	237.3	R	42.0	26.8
15-5, 144–146	135.55	1.80	2.15	+50.8	+50.5	+51.3	251.5	R	44.2	37.6
15-6, 24–26	135.85	4.76	7.20	+35.1	+69.8	+68.4	226.4	R	33.7	19.2
15-6, 49–51	136.10	1.58	3.57	+41.8	+60.7	+62.1	265.1	R		23.7
15-6, 74–76	136.35	1.71	2.85	+6.1	+44.0	+53.5	270.2	R	45.7	21.7
15-6, 99–101	136.60	2.43	2.71	−5.6	+20.3	+26.1	279.9		14.4	13.5
15-6, 124–126	136.85	3.00	3.62	no	+5.2	no	no	R	13.3	13.1
15-6, 144–146	137.05	3.57	4.54	−62.0	−14.9	+38.2	271.4	R	8.4	8.1
15-7, 24–26	137.35	3.45	5.62	no	+7.7	no	no		8.7	8.6
15-7, 49–51	137.60	4.87	5.14	−68.6	−48.6	−49.0	277.9	N	11.8	11.3
16-1, 24–26	138.05	5.47	10.95	−65.3	−27.6	−45.7	296.1	N	8.2	11.6
16-1, 49–51	138.30	4.95	5.33	−52.0	−34.2	−41.0	327.9	N	14.0	13.4
16-1, 74–76	138.55	11.09	11.78	−70.2	−58.1	−63.8	351.5	N	11.9	11.6
16-1, 99–101	138.80	6.98	7.20	−65.2	−61.0	−64.2	310.0	N	14.5	14.6
16-1, 124–126	139.05	1.26	3.00	+8.8	+23.6	+39.6	320.0	R	41.8	23.4
16-1, 144–146	139.25	2.27	4.01	−40.5	−2.8	−57.3	309.3	N	14.2	20.9
16-2, 24–26	139.55	1.78	3.23	−38.5	−12.0	−86.3	289.8	N	47.9	31.3
16-2, 49–51	139.80	1.42	2.79	+78.4	+77.0	+74.9	278.4	R		31.5
16-2, 74–76	140.05	0.81	2.60	−57.1	+44.5	+44.0	312.3	R		14.1
16-2, 99–101	140.30	1.13	2.75	−16.5	+35.5	+46.2	299.0	R		22.9
16-2, 124–126	140.55	2.44	3.28	−64.3	−12.5	−87.6	255.7	N	15.0	13.0
16-2, 144–146	140.75	1.32	1.65	+19.6	+32.1	+40.7	310.7	R	47.5	37.9
16-3, 24–26	141.05	2.41	3.63	+68.1	+59.6	+59.7	283.7	R		34.9
16-3, 49–51	141.30	3.42	4.22	+80.2	+72.9	+72.4	272.3	R	46.2	36.2
16-3, 74–76	141.55	2.61	3.82	+70.2	+65.9	+66.1	282.7	R		35.7
16-3, 99–101	141.80	3.03	3.51	+58.1	+58.2	+55.9	303.5	R	38.1	31.7
16-3, 124–126	142.05	3.53	4.50	+68.7	+65.4	+65.9	281.6	R	41.9	33.0
16-3, 144–146	142.25	5.37	6.44	+75.5	+74.8	+74.4	293.9	R	37.3	30.6
16-4, 24–26	142.55	2.70	4.83	+30.8	+57.8	+50.9	292.4	R	45.5	25.2
16-4, 49–51	142.80	2.65	4.26	+56.8	+60.6	+62.7	294.7	R	40.5	28.5
16-4, 74–76	143.05	1.74	3.55	+16.1	+51.3	+47.3	289.9	R	36.9	25.6
16-4, 99–101	143.30	0.98	2.44	+40.8	+56.6	+46.3	314.4	R		26.9
16-5, 24–26	144.05	1.68	3.46	−8.0	+6.6	no	no			38.9
16-5, 49–51	144.30	0.59	1.31	+37.8	+45.0	+59.2	303.7	R		41.3
16-5, 74–76	144.55	2.93	3.33	−70.1	−62.1	−60.7	334.9	N	36.4	29.4
16-5, 99–101	144.80	4.30	4.41	−69.1	−63.3	−65.0	319.2	N	39.0	37.7
16-5, 124–126	145.05	4.03	4.33	−72.9	−66.5	−67.8	297.5	N	47.0	37.2
16-5, 144–146	145.25	3.05	3.37	−55.8	−42.7	−47.1	319.4	N	31.9	26.3
16-6, 24–26	145.55	2.07	3.04	−83.3	−50.7	−67.4	320.2	N	16.3	18.4
16-6, 49–51	145.80	1.39	2.07	−20.5	+9.9	+18.5	270.4	R	43.3	34.3
16-6, 74–76	146.05	0.25	1.14	−31.6	+18.7	+54.4	311.0	R		30.1
16-6, 99–101	146.30	2.50	2.69	−73.0	−70.2	−69.2	309.8	N	39.6	36.1
16-6, 124–126	146.55	3.99	4.16	−71.0	−70.3	−68.5	335.8	N	31.7	31.5
16-6, 144–146	146.75	1.62	2.85	−73.0	−38.4	−47.8	42.9	N	13.3	20.0
16-7, 24–26	147.05	2.29	2.79	−76.1	−60.8	−66.7	302.5	N	23.4	22.1
16-7, 49–51	147.30	3.00	3.30	−83.2	−74.9	−74.7	291.3	N	35.7	29.8
17-1, 24–26	147.75	3.52	5.17	−2.0	+10.2	+19.5	272.4	R	43.2	31.7
17-1, 49–51	148.00	4.56	5.66	−70.4	−12.2	+48.0	306.5	R	9.7	11.0
17-1, 74–76	148.25	5.10	6.48	−78.7	−58.8	−80.2	185.2	N	9.5	12.4
17-1, 99–101	148.50	5.55	5.95	−70.2	−56.9	+42.4	294.7	R	10.1	10.4
17-1, 124–126	148.75	6.80	8.31	−61.4	−6.8	+49.7	322.0	R	8.8	9.4
17-1, 144–146	148.95	51.01	52.38	−57.0	−56.7	−61.9	279.8	N	6.3	6.4
17-2, 24–26	149.25	3.63	5.25	−71.4	−41.5	−50.3	282.5	N	19.7	15.4
17-2, 49–51	149.50	8.58	9.43	−74.9	−59.0	−63.7	255.0	N	8.8	8.6
17-2, 74–76	149.75	5.66	6.51	−51.0	−27.8	−33.8	287.4	N	9.8	10.6
17-2, 99–101	150.00	3.62	4.71	−73.3	−25.5	+34.2	300.6	R	9.0	9.1
17-2, 124–126	150.25	3.68	4.77	−58.5	−29.8	+16.5	314.2	R	9.4	11.8
17-2, 144–146	150.45	4.11	4.77	−54.3	−75.6	−59.6	11.7	N	8.6	8.5
17-3, 24–26	150.75	6.56	9.08	−68.6	−24.0	−54.8	229.4	N	11.6	12.7
17-3, 49–51	151.00	3.54	5.94	−13.1	−58.8	−67.4	337.0	N	3.9	9.2
17-3, 74–76	151.25	13.57	14.64	−74.6	−54.8	−50.5	289.1	N	9.6	9.9
17-3, 99–101	151.50	10.55	11.63	−84.4	−57.1	−57.4	295.7	N	11.3	9.9
17-3, 124–126	151.75	6.26	7.11	−30.1	−10.7	−40.2	264.6	N	13.7	13.9
17-3, 144–146	151.95	6.57	8.25	−62.0	−48.3	−62.6	234.4	N	19.6	16.8
17-4, 24–26	152.25	13.06	14.33	−71.2	−47.2	−56.7	253.4	N	8.3	8.3
17-4, 49–51	152.50	8.15	8.89	−39.3	−23.5	−40.4	246.5	N	9.3	9.8
17-4, 74–76	152.75	12.17	13.39	−83.9	−46.9	−68.3	271.1	N	7.6	7.9
17-4, 99–101	153.00	13.53	14.70	−79.6	−53.7	−70.2	267.3	N	8.7	8.9
17-4, 124–126	153.25	8.16	9.32	−74.3	−49.1	+24.3	311.9	R	12.6	13.1
17-4, 144–146	153.45	8.02	8.85	−76.7	−49.7	−74.1	248.1	N	9.6	9.8
17-5, 24–26	153.75	10.98	12.10	−66.9	−40.6	−69.4	313.1	N	6.3	6.7
17-5, 49–51	154.00	7.78	8.97	−75.0	−55.6	−81.0	237.7	N	9.5	9.2
17-5, 74–76	154.25	12.64	13.63	−69.0	−49.2	−69.8	326.5	N	7.2	7.2
17-5, 99–101	154.50	10.29	10.82	−78.4	−60.9	−64.6	311.6	N	9.5	9.7

Appendix B (continued).

Core, section, interval (cm)	Depth (mbsf)	J NRM (mA/m)	Js NRM (mA/m)	Incl. NRM (deg)	Incl. 20 mT (deg)	Incl. stable (deg)	Decl. stable (deg)	Pol.	MDF (mT)	MDFs (mT)
Hole 690B (Cont.)										
17-5, 124–126	154.75	5.39	8.98	−73.1		+29.7	326.7	R	4.8	6.6
17-5, 144–146	154.95	7.84	13.07	+40.6	+55.4	+52.6	291.2	R	25.3	10.3
17-6, 24–26	155.25	18.52	19.84	+46.5	+31.4	+33.5	311.6	R	7.4	7.4
17-6, 49–51	155.50	2.45	8.84	−34.0	+61.5	+58.8	307.7	R	32.7	9.2
17-6, 74–76	155.75	0.47	5.54	−49.8	+52.0	+50.1	298.0	R	67.4	8.9
17-6, 99–101	156.00	47.05	47.32	+70.8	+66.8	+66.2	310.9	R	5.8	5.8
17-6, 124–126	156.25	3.45	9.24	+83.7	+74.2	+70.9	313.8	R	37.2	19.2
17-6, 144–146	156.45	5.43	7.08	+60.5	+64.8	+62.3	301.2	R	26.9	21.9
17-7, 24–26	156.75	1.83	5.34	+11.2	+63.4	+53.1	291.2	R	38.1	14.8
17-7, 49–51	157.00	2.22	11.75	+43.4	+73.2	+71.9	289.3	R	47.2	15.1
18-1, 24–26	157.45	6.23	13.25	−8.7	+64.4	+59.6	299.2	R	27.8	7.7
18-1, 49–51	157.70	6.42	6.89	+50.0	+61.0	+58.0	305.5	R	13.9	12.5
18-1, 74–76	157.95	4.20	6.85	+4.7	+54.3	+43.6	312.3	R	18.8	9.1
18-1, 99–101	158.20	3.52	6.24	+14.4	+50.3	+50.4	313.3	R	24.6	10.6
18-1, 124–126	158.45	5.94	8.83	−14.1	+53.7	+45.7	286.4	R	12.4	7.1
18-1, 144–146	158.65	31.16	34.81	−51.6	+67.1	+61.0	272.3	R	4.6	5.2
18-2, 24–26	158.95	2.36	4.30	−78.5	+16.5	no	no		4.2	4.6
18-2, 49–51	159.20	3.15	5.34	+23.5	+51.2	+49.7	303.5	R	19.8	10.8
18-2, 74–76	159.45	5.95	6.23	−43.2	−32.7	−45.5	283.6	N	7.3	7.4
18-2, 99–101	159.70	2.52	5.29	+30.8	+59.6	+56.7	292.5	R	30.1	15.1
18-2, 124–126	159.95	4.60	4.92	+22.7	+1.9	−28.8	259.4	N	9.3	9.6
18-2, 144–146	160.15	3.12	5.13	−68.6	−12.9	−22.7	278.3	N	22.6	8.4
18-3, 24–26	160.45	6.56	9.12	+73.0	+61.3	+54.6	283.7	R	22.7	14.5
18-3, 49–51	160.70	2.06	5.17	+34.0	+27.7	+31.5	267.6	N	37.3	16.1
18-3, 74–76	160.95	4.66	6.63	−27.6	+18.2	+21.0	301.4	R	14.8	8.7
18-3, 99–101	161.20	2.87	2.90	+71.9	+68.4	+67.6	271.0	R	20.2	20.1
18-3, 124–126	161.45	4.79	6.60	+23.9	+46.7	+44.6	249.8	R	20.1	12.8
18-3, 144–146	161.65	3.35	8.77	−2.9	+64.1	+58.2	262.4	R	33.2	8.8
18-4, 24–26	161.95	1.78	3.24	−26.1	+65.4	+69.2	302.0	R	4.3	6.9
18-4, 49–51	162.20	0.93	2.00	−46.3	+41.6	+52.6	263.6	R	23.9	5.0
18-4, 74–76	162.45	0.55	0.85	−33.3	+43.6	+72.0	254.2	R	6.3	6.7
18-4, 99–101	162.70	0.83	1.42	−22.7	+34.4	+54.3	308.8	R	17.7	7.5
18-4, 124–126	162.95	0.09	0.18	+79.6	+70.7	+65.9	211.2	R		20.8
18-4, 144–146	163.15	0.07	0.13	+59.4		+87.3	163.9	R		14.9
18-5, 24–26	163.45	1.52	1.88	−60.1	+39.1	+43.8	284.7	R	3.6	4.4
18-5, 49–51	163.70	0.23	0.52	−24.5	+78.6	+85.9	347.8	R	3.6	8.4
18-5, 74–76	163.95	0.13	0.24	+57.4	+82.7	+84.5	235.2	R		16.5
18-5, 99–101	164.20	5.03	6.09	+15.7	+43.2	+40.0	298.3	R	11.3	9.3
18-5, 124–126	164.45	0.70	2.57	−23.4	+34.3	+34.2	305.5	R	27.9	5.4
18-5, 144–146	164.65	101.17	101.70	+9.7	+16.6	+81.8	332.0	R	10.0	10.0
18-6, 24–26	164.95	3.72	7.16	−51.5	+63.8	+60.4	314.3	R	4.2	5.0
18-6, 49–51	165.20	1.38	4.02	+27.0	+72.8	+71.7	311.0	R	36.0	12.6
18-6, 74–76	165.45	0.28	0.96	+51.2	+59.0	+68.8	271.6	R	38.9	9.8
18-6, 99–101	165.70	2.46	4.50	+23.7	+51.4	+50.1	287.3	R	30.4	19.2
18-6, 124–126	165.95	0.09	0.16	+50.9	+59.7	+65.5	1.6	R		13.3
18-6, 144–146	166.15	0.58	0.67	+63.6	+81.4	+76.4	143.3	R	4.8	6.1
19-1, 24–26	167.15	0.04	0.04	+20.9		no	no			
19-1, 49–51	167.40	0.54	0.59	−59.1	−23.9	−70.4	206.8	N	3.5	3.8
19-1, 74–76	167.65	0.01	0.08	+28.3	−1.1	no	no			8.3
19-1, 99–101	167.90	0.04	0.06	−76.7	−69.0	−67.7	197.5	N	14.6	12.2
19-1, 124–126	168.15	0.02	0.20	−49.9	+39.9	no	no		46.6	14.9
19-1, 144–146	168.35	0.04	0.11	−6.0	+20.5	no	no		17.0	11.8
19-2, 24–26	168.65	0.01	0.01	+71.1		no	no			
19-2, 49–51	168.90	0.02	0.02	no		no	no		4.5	3.8
19-2, 74–76	169.15	0.05	0.05	+57.7		no	no			
19-2, 99–101	169.40	0.64	2.59	−51.5	+74.6	+77.3	209.5	R	39.4	8.3
19-2, 124–126	169.65	3.45	3.84	+39.9	+63.4	+58.3	226.3	R	4.6	5.3
19-2, 144–146	169.85	2.77	3.54	−29.8	−5.3	no	no		12.2	13.5
19-3, 24–26	170.15	5.44	9.66	+51.4	+76.0	+81.0	219.2	R	27.6	17.6
19-3, 49–51	170.40	4.32	7.51	+43.2	+55.9	+55.3	240.9	R	19.8	14.8
19-3, 74–76	170.65	2.66	5.43	−56.8	−1.3	−56.4	201.6	N	19.0	9.3
19-3, 99–101	170.90	4.13	8.20	+68.1	+73.9	+69.9	229.5	R	26.7	16.7
19-3, 124–126	171.15	2.42	3.04	−25.1	−15.7	−49.6	228.6	N	8.2	8.7
19-3, 144–146	171.35	2.35	5.96	−24.5	+56.4	+52.2	259.9	R	21.9	8.1
19-4, 24–26	171.65	1.69	4.42	−2.7	+41.2	+38.6	203.5	R	27.7	11.0
19-4, 49–51	171.90	5.99	6.54	+51.4	+56.3	+55.2	242.7	R	11.7	11.6
19-4, 74–76	172.15	2.86	4.17	+8.9	+54.6	+52.2	223.2	R	15.2	9.2
19-4, 99–101	172.40	2.50	5.63	+2.5	+43.1	+50.4	245.4	R	18.7	9.1
19-5, 24–26	173.15	4.34	9.16	+26.6	+66.0	+64.8	222.3	R	29.3	16.3
19-5, 49–51	173.40	5.58	5.98	+78.1	+68.2	+68.7	266.2	R	12.4	12.1
19-5, 74–76	173.65	8.40	9.93	+34.2	+61.7	+58.9	280.8	R	15.2	12.7
19-5, 99–101	173.90	6.12	8.64	+17.1	+55.9	+52.6	240.8	R	14.8	12.7
20-1, 24–26	174.55	5.70	6.48	−78.9	−54.0	−76.5	320.1	N	8.6	8.3
20-1, 49–51	174.80	3.02	3.87	+35.7	+26.8	+30.9	263.2	R	18.9	14.8
20-1, 74–76	175.05	5.53	11.07	−35.7	+86.0	+81.3	304.4	R	7.3	8.7
20-1, 99–101	175.30	2.04	3.86	−18.4	+56.3	+47.0	285.1	R	20.9	10.0

Appendix B (continued).

Core, section, interval (cm)	Depth (mbsf)	J NRM (mA/m)	Js NRM (mA/m)	Incl. NRM (deg)	Incl. 20 mT (deg)	Incl. stable (deg)	Decl. stable (deg)	Pol.	MDF (mT)	MDFs (mT)
Hole 690B (Cont.)										
20-1, 124–126	175.55	2.73	5.73	−51.4	+63.1	+60.1	248.0	R	9.2	8.6
20-1, 145–147	175.76	4.22	7.70	+10.6	+67.3	+60.6	285.1	R	24.9	12.9
20-2, 24–26	176.05	2.40	7.63	+6.1	+74.2	+69.5	263.6	R	36.1	9.9
20-2, 49–51	176.30	0.61	5.24	−9.0	+56.4	+43.9	271.3	R	49.8	9.1
20-2, 74–76	176.55	3.32	7.42	+46.6	+75.8	+68.4	256.8	R	30.2	14.1
20-2, 99–101	176.80	3.38	12.96	+19.2	+77.9	+75.3	262.7	R	39.6	12.8
20-2, 124–126	177.05	3.98	7.40	+2.6	+60.0	+53.1	274.6	R	26.3	13.5
20-2, 145–147	177.26	2.87	11.02	−39.2	+67.9	+61.3	245.1	R	37.7	9.5
20-3, 24–26	177.55	7.61	15.44	−58.3	+70.8	+63.2	263.1	R	4.3	7.8
20-3, 49–51	177.80	4.14	10.39	+6.1	+77.0	+74.8	255.1	R	34.7	9.7
20-3, 74–76	178.05	4.50	8.93	−30.1	+63.5	+59.1	275.5	R	23.5	8.2
20-3, 99–101	178.30	5.28	88.18	+39.4	+73.9	+70.3	249.1	R	18.9	5.5
20-3, 124–126	178.55	2.83	7.49	+8.3	+61.2	+58.7	266.1	R	4.4	8.9
20-3, 145–147	178.76	2.26	6.66	+1.1	+66.2	+64.2	250.5	R	39.4	13.3
20-4, 24–26	179.05	1.77	5.87	+27.5	+58.8	+56.6	250.2	R	47.1	15.5
20-4, 49–51	179.30	4.64	8.13	+10.1	+41.8	+39.1	250.2	R	16.3	15.7
20-4, 74–76	179.55	5.26	6.34	+47.0	+58.3	+55.9	261.1	R	20.9	14.8
20-4, 99–101	179.80	3.33	5.60	+68.5	+57.5	+60.0	228.1	R	22.1	31.2
20-4, 122–124	180.03	3.74	4.65	+51.4	+65.8	+62.7	265.3	R	25.0	20.1
20-C, 15–17	180.44	5.53	5.95	+49.4	+56.9	+54.3	299.9	R	20.3	19.1
21-1, 24–26	180.55	1.96	2.77	+39.6	+52.5	+50.4	300.4	R	28.5	23.4
21-1, 49–51	180.80	4.89	6.06	+57.8	+73.6	+72.2	306.3	R	28.5	23.6
21-1, 74–76	181.05	1.88	3.50	+75.6	+65.3	+65.8	266.5	R	33.4	21.7
21-1, 99–101	181.30	1.64	2.52	+49.5	+52.4	+49.9	280.7	R	33.2	24.6
21-1, 124–126	181.55	3.63	5.70	+52.3	+63.5	+62.5	304.1	R	29.1	20.3
21-1, 144–146	181.75	4.05	5.03	+22.7	+38.8	+34.7	289.2	R	26.2	20.9
21-2, 24–26	182.05	3.89	5.40	+34.3	+57.5	+55.8	289.0	R	24.4	17.6
21-2, 49–51	182.30	4.15	11.33	+85.4	+67.9	+65.8	312.3	R	44.5	20.9
21-2, 74–76	182.55	5.31	6.33	+77.7	+74.0	+73.8	288.8	R	22.2	17.6
21-2, 99–101	182.80	3.46	4.14	+46.2	+47.1	+43.8	271.1	R	22.4	18.5
21-2, 124–126	183.05	3.40	3.99	+78.4	+63.1	+61.7	299.5	R	23.2	21.2
21-2, 144–146	183.25	3.43	5.84	+55.3	+59.0	+58.3	302.2	R	36.8	25.2
21-3, 24–26	183.55	1.79	3.30	+0.5	+46.1	+43.7	281.3	R	25.7	14.0
21-3, 49–51	183.80	2.01	3.71	+32.8	+48.6	+45.4	322.6	R	36.1	22.2
21-3, 144–146	184.75	3.02	3.84	+64.1	+50.3	+51.5	288.6	R	20.3	18.9
21-4, 17–19	184.98	2.37	3.08	+27.5	+17.7	+25.3	284.9	R	11.3	8.7
21-C, 4–6	185.25	2.82	3.98	+47.1	+2.2	+41.6	175.6	R	4.8	5.8
22-1, 49–51	185.70	5.73	6.16	−41.2	−54.8	−53.3	303.1	N	7.4	7.5
22-1, 74–76	185.95	6.55	6.61	−72.0	−67.8	−67.6	298.3	N	10.4	10.3
22-1, 99–101	186.20	6.56	6.84	−80.3	−72.2	−72.4	290.4	N	16.8	15.2
22-1, 124–126	186.45	2.63	2.90	−47.1	−48.3	−46.2	267.5	N	18.4	16.9
22-1, 147–149	186.68	2.36	3.16	−6.8	−44.9	−62.6	272.2	N	14.9	13.9
22-2, 24–26	186.95	6.15	6.54	−38.7	−25.7	−27.3	288.2	N	8.1	8.2
22-2, 49–51	187.20	5.92	6.52	−50.4	−38.4	−40.5	284.7	N	9.9	9.3
22-2, 74–76	187.45	3.33	4.33	−11.7	−47.1	−42.3	307.8	N	24.7	19.8
22-2, 99–101	187.70	5.46	6.17	−67.8	−45.2	−50.1	289.4	N	9.0	8.2
22-2, 124–126	187.95	1.32	2.21	−28.0	−35.0	−57.5	295.9	N	34.7	29.1
22-2, 146–148	188.17	6.28	7.13	−25.3	−44.3	−48.2	291.6	N	24.3	19.8
22-3, 24–26	188.45	3.39	3.90	−50.8	−47.2	−50.6	299.0	N	27.9	22.8
22-3, 49–51	188.70	3.98	5.18	−68.7	−58.8	−65.4	278.4	N	21.9	9.5
22-3, 74–76	188.95	8.92	9.36	−64.3	−62.1	−64.9	286.4	N	20.3	18.7
22-3, 99–101	189.20	3.11	3.81	−48.3	−69.1	−72.4	268.3	N	29.1	23.3
22-4, 24–26	189.95	3.44	4.17	−59.8	−45.5	−46.1	280.7	N	22.9	25.3
22-4, 49–51	190.20	4.42	4.93	−56.6	−61.2	−62.4	291.3	N	23.6	20.9
22-4, 74–76	190.45	4.84	6.98	−52.7	−59.7	−58.1	289.9	N	32.5	24.1
22-4, 99–101	190.70	6.71	6.85	−70.1	−68.6	−69.2	300.3	N	20.2	19.8
22-4, 119–121	190.90	10.69	10.84	−54.5	−55.5	−54.2	294.7	N	18.9	18.8
23-1, 25–27	191.46	2.32	5.58	−78.6	−70.8	−70.7	294.9	N	43.4	23.9
23-1, 46–48	191.67	6.55	7.45	−57.0	−69.0	−67.5	319.2	N	28.6	25.8
23-1, 75–77	191.96	3.10	5.72	−71.8	−84.2	−84.2	326.2	N	37.7	25.1
23-1, 99–101	192.20	6.45	6.55	−62.1	−65.7	−64.4	305.1	N	21.0	20.7
23-1, 124–126	192.45	3.58	4.06	−74.1	−65.6	−68.9	318.6	N	28.7	26.4
23-1, 147–149	192.68	5.07	5.14	−68.5	−71.6	−69.9	340.4	N	17.9	17.7
23-2, 47–49	193.18	0.31	0.88	−33.5	−34.2	−69.4	306.6	N	59.2	38.0
23-2, 75–77	193.46	1.48	1.96	−36.1	−52.3	−73.4	311.5	N	6.7	8.4
23-2, 98–100	193.69	1.54	2.28	−26.1	−24.6	−51.3	341.0	N	32.4	25.6
23-2, 123–125	193.94	3.15	3.33	−31.5	−32.1	−42.4	271.1	N	9.7	10.2
23-2, 146–148	194.17	2.25	2.79	−28.2	−46.6	−48.0	292.9	N	29.7	24.5
23-3, 25–27	194.46	2.81	3.10	−13.4	−19.4	−28.6	287.7	N	20.0	18.2
23-3, 48–50	194.69	1.52	2.29	−37.8	−50.0	−59.0	286.5	N	36.4	24.0
23-3, 75–77	194.96	2.14	2.71	−33.9	−19.3	−39.8	300.6	N	9.4	10.7
23-3, 100–102	195.21	2.45	3.34	+18.3	+4.6	−29.9	316.1	N	9.1	9.9
23-3, 124–126	195.45	1.57	1.95	−32.2	−2.0	−48.7	233.2	N	5.3	6.4
23-3, 148–150	195.69	2.07	2.87	−5.1	+4.0	−32.8	292.9	N	21.5	23.6
23-4, 24–26	195.95	2.74	3.23	+8.6	+16.3	no	no		21.7	19.4
23-4, 48–50	196.19	1.75	2.87	+42.2	+36.7	+40.2	275.1	R	33.1	25.4

Appendix B (continued).

Core, section, interval (cm)	Depth (mbsf)	J NRM (mA/m)	Js NRM (mA/m)	Incl. NRM (deg)	Incl. 20 mT (deg)	Incl. stable (deg)	Decl. stable (deg)	Pol.	MDF (mT)	MDFs (mT)
Hole 690B (Cont.)										
23-4, 75–77	196.46	0.61	2.21	−23.5	+8.1	no	no		45.0	16.7
23-4, 99–101	196.70	2.86	3.46	+50.9	+26.3	+35.3	275.9	R	11.9	12.0
23-4, 124–126	196.95	1.63	2.10	−26.1	+2.9	no	no		23.4	18.6
23-4, 147–149	197.18	11.45	12.91	−45.1	−4.5	no	no		5.5	5.8
23-5, 25–27	197.46	1.20	2.77	−3.5	+26.1	+25.8	254.9	R	35.5	18.0
23-5, 48–50	197.69	0.84	3.85	−37.6	+25.9	+29.6	272.1	R	48.4	14.2
23-5, 75–77	197.96	1.02	2.31	−4.8	+31.2	+30.4	256.0	R	35.0	18.3
24-1, 25–27	198.46	3.15	3.62	−0.4	+27.0	+22.9	283.1	R	14.8	12.0
24-1, 50–52	198.71	2.56	3.06	+55.7	+64.6	+60.5	290.2	R	27.0	22.7
24-1, 75–77	198.96	2.88	3.53	+39.6	+73.6	+72.6	310.8	R	19.1	13.8
24-1, 99–101	199.20	1.93	3.03	−7.6	+38.7	+52.4	316.9	R	4.2	7.2
24-1, 124–126	199.45	3.20	3.57	+73.7	+75.6	+73.4	305.7	R	23.6	22.4
24-1, 147–149	199.68	1.99	2.80	+60.0	+82.6	+78.3	321.9	R	33.1	25.8
24-2, 22–24	199.93	4.01	4.31	+6.3	+14.0	no	no		16.3	15.2
24-2, 50–52	200.21	2.07	2.93	+9.3	+57.0	+53.6	277.0	R	21.5	13.7
24-2, 75–77	200.46	3.86	4.38	+10.3	+19.4	+28.8	280.0	R	14.4	14.6
24-2, 99–101	200.70	0.98	3.00	−58.9	−25.1	−35.2	263.3	N	38.0	9.6
24-2, 124–126	200.95	2.97	3.89	−40.2	+9.7	no	no		12.4	9.8
24-2, 147–149	201.18	2.92	3.13	+30.5	+34.7	+33.7	277.3	R	20.9	20.5
24-3, 25–27	201.46	3.36	3.77	+14.1	+29.1	+27.1	278.4	R	19.3	16.8
24-3, 50–52	201.71	2.62	3.52	−49.9	−8.8	no	no		20.4	12.0
24-3, 75–77	201.96	4.41	4.85	−18.6	−0.3	no	no		12.8	11.8
24-3, 99–101	202.20	5.65	5.90	+2.8	+12.7	+14.8	285.5	R	11.8	11.6
24-3, 124–126	202.45	7.50	7.75	−21.1	−20.8	−27.0	271.0	N	14.8	14.3
24-3, 146–148	202.67	1.83	2.21	+32.6	+17.1	+18.4	276.5	R	21.4	17.0
24-4, 25–27	202.96	5.80	5.94	−30.5	−29.3	−30.6	259.4	N	15.4	15.4
24-4, 50–52	203.21	2.08	2.45	+3.6	−10.2	−15.3	280.9	N	21.5	16.4
24-4, 75–77	203.46	3.03	3.59	+23.7	−16.9	−21.3	261.2	N	12.3	9.7
24-4, 99–101	203.70	2.14	2.46	−16.7	+6.2	+33.7	330.2	R	9.2	9.5
24-4, 123–125	203.94	2.93	3.50	−1.0	+5.5	no	no		15.8	13.7
25-1, 24–26	204.45	0.78	3.14	+2.6	+83.2	+86.4	253.5	R		11.6
25-1, 48–50	204.69	3.27	4.84	+10.3	+46.3	+50.6	312.5	R	24.8	13.7
25-1, 72–74	204.93	1.22	2.25	+83.0	+70.9	+68.0	91.7	R	34.4	22.8
25-1, 99–101	205.20	0.97	1.95	−55.5	+41.5	+64.4	266.3	R	20.5	8.3
25-1, 124–126	205.45	2.22	2.50	−21.7	+16.2	+24.4	251.0	R	9.3	8.9
25-1, 146–148	205.67	1.43	2.07	−40.1	−54.0	−63.0	330.1	N	31.6	19.7
25-2, 24–26	205.95	0.11	0.26	−22.4		+77.8	12.2	R	3.8	4.5
25-2, 48–50	206.19	3.94	6.03	−20.9	+24.8	+39.3	283.8	R	23.4	11.3
25-2, 72–74	206.43	4.23	5.25	+11.5	+38.7	+40.2	296.9	R	24.2	18.0
25-2, 99–101	206.70	2.64	3.35	−18.2	+5.0	+30.7	278.6	R	18.9	16.4
25-2, 124–126	206.95	1.22	1.87	−17.7	+39.4	+75.2	277.2	R	13.7	11.4
25-2, 146–148	207.17	0.05	0.22	−51.9	+67.3	+37.1	314.3	R	9.8	11.3
25-3, 24–26	207.45	0.50	1.96	−23.8	−1.4	+41.6	253.3	R	39.2	16.7
25-3, 48–50	207.69	1.25	1.55	−0.1	−3.1	+48.9	277.5	R	9.7	9.4
25-3, 72–74	207.93	2.36	2.52	−27.6	−22.0	no	no		11.6	11.4
25-3, 99–101	208.20	2.59	3.19	−29.8	−37.7	−40.1	263.5	N	19.9	16.8
25-3, 124–126	208.45	2.12	2.62	−58.6	−18.2	−54.2	302.8	N	12.9	9.1
25-3, 146–148	208.67	1.81	2.24	−17.0	−14.6	+40.1	239.9	R	18.1	14.8
25-4, 24–26	208.95	2.18	3.24	−37.5	+1.3	no	no		15.6	8.6
25-4, 48–50	209.19	2.26	2.39	+51.3	+65.4	+63.1	282.6	R	14.4	14.6
25-4, 72–74	209.43	1.01	1.60	−17.4	+13.3	+60.6	246.3	R	20.5	12.5
25-4, 99–101	209.70	4.38	5.23	−51.8	+1.4	+26.0	280.0	R	7.6	7.6
25-5, 24–26	210.45	3.19	3.73	−28.9	−11.7	no	no		13.6	12.2
25-5, 48–50	210.69	4.86	5.51	−51.6	−58.5	−55.2	273.1	N	28.8	26.4
25-5, 72–74	210.93	7.13	7.64	−67.7	−58.9	−60.4	262.9	N	21.5	19.6
25-5, 99–101	211.20	5.27	5.41	−57.0	−58.3	−56.7	273.4	N	13.5	13.0
25-5, 124–126	211.45	3.41	3.62	−68.1	−63.4	−65.8	275.6	N	27.9	26.8
25-5, 146–148	211.67	2.22	3.91	−9.5	−49.1	−46.7	278.0	N	38.4	20.0
25-6, 24–26	211.95	3.92	4.56	−66.4	−57.5	−55.1	275.6	N	30.8	27.2
25-6, 48–50	212.19	4.62	5.90	−41.2	−56.0	−53.3	261.8	N	21.2	14.0
25-6, 72–74	212.43	3.19	4.82	+55.3	−48.2	−51.6	261.3	N	8.0	7.7
25-6, 99–101	212.70	9.78	9.78	−16.9		no	no			
25-6, 124–126	212.95	5.60	6.04	−30.4	−30.3	−35.3	276.4	N	22.1	20.0
25-6, 146–148	213.17	3.80	4.14	+19.9	+2.7	+33.4	271.5	R	19.9	19.0